AN ELECTROPHYSIOLOGICAL STUDY OF ION TRANSPORT ACROSS THE ISOLATED PERFUSED MALPIGHIAN TUBULE OF *ONYMACRIS PLANA*.

David Willis Fisher

Thesis submitted in fulfilment of the requirements

for the degree Master of Science (Physiology)

1992

University of Cape Town
Department of Physiology
Medical School, Observatory.

Acknowledgements

I wish to express my sincere thanks to the following:

To God Almighty for all his blessings, who without nothing matters.

To Professor Leon Isaacson for his help and encouragement in all and every aspect of this thesis.

To Dr. Sue Nicolson for her endless editing.

To Grace Fisher for timeous grammatical editing.

To all those who in some way contributed to the completion of this thesis.

To my wife, Hayley, who made the effort worth while.

CONTENTS

TABLES

FIGURES

ABSTRACT

AN ELECTROPHYSIOLOGICAL STUDY OF ION TRANSPORT ACROSS THE ISOLATED PERFUSED MALPIGHIAN TUBULE OF *ONYMACRIS PLANA.*

A knowledge of the ionic and electrical gradients across the Malpighian tubules of *Onymacris plana* is fundamental to the understanding of the transport mechanisms of fluid across the basolateral and apical membranes. Until now no one has investigated the isolated perfused Malpighian tubule of *Onymacris plana* and simultaneously measured basolateral potentials.

Malpighian tubule segments (about 1mm length) were dissected out and perfused in vitro according to the method of Burg et. al. (1966), while the basolateral membrane potential (Vbl) was measured by means of an intracellular microelectrode. Using cable analysis, the effects of DNP, chloride free Ringers, $BaCl_2$ (a K^+-channel blocker), low (25 mM) and high (130 mM) potassium Ringers (bathing medium), cyclic-AMP and a corpora cardiaca homogenate (CCH) on the transepithelial resistance and the fractional resistances of the basolateral and apical membranes were investigated.

The large potential jumps across the apical membrane compared with the basolateral membrane, illustrated clearly that the apical membrane was far less permeable than the basolateral membrane. The high K^+ permeability of the basolateral membrane was endorsed by the 3-fold increase in FRBL% in response to $BaCl_2$, thereby also confirming the presence of K^+-specific channels in the basolateral membrane. This view was further supported by the rapid depolarization of the basolateral membrane by increasing the K^+ concentration of the bathing medium. The high K^+-Ringer also hyperpolarised Vo while Va was slightly depolarised.

The introduction of Cl^--free Ringers (CFR) resulted in the immediate hyperpolarization of the intracellular (Vbl) and transepithelial (Vo) potentials. However, although Vbl was stable Vo decreased exponentially, but normally settled at a potential above the control; the change in Vo was therefore as a result of changes at the apical membrane.

CCH elicited a variable response. The fact that Vo, but not Vbl, was affected, alludes to an apical mechanism being responsible for the CCH induced fluid secretion. Cyclic-AMP initially decreased Vo while increasing Vbl. However, after 20 - 30 minutes Vo increases significantly.

DNP caused the rapid depolarization of Vo, Vbl and Va. This response further supported the view that active transport of ions was intimately involved with fluid secretion.

This study endorses the prevalent view that the Malpighian tubule cells of *Onymacris plana* is dependent on the transport of K^+ as a means to drive fluid secretion and also provides

further insight into the mechanisms governing fluid secretion. The current thought is that K^+ transport across the apical membrane into the lumen is driven by the active extrusion of protons into the lumen; these protons subsequently provide the gradient which drives an antiport mechanism for the transport of K^+ into the lumen. Furthermore, measurements of the transepithelial and basolateral potentials made it possible to present an expanded electrical equivalent circuit of the Malpighian tubule.

ABBREVIATIONS	
ABBREVIATIONS AND UNITS	**EXPLANATIONS**
Vo; millivolts (mV)	Proximal transtubular potential
Va; millivolts (mV)	Apical membrane potential
Vbl; millivolts (mV)	Basolateral membrane potential
Vt; millivolts (mV)	Transepithelial potential
λ (lambda); microns (μ)	Length constant; Lambda
Rt; kOhms/cm	Transepithelial resistance
Rc; MOhms/cm	Core/lumen resistance
D; microns (μ)	Luminal diameter
SCCv; μA/cm	Virtual short circuit current
SCC; $\mu A/cm^2$	Short circuit current
Ri; kOhms	Input resistance
FRBl%	Percent fractional resistance of the basolateral membrane
CCH	Corpora cardiaca homogenate
DH	Diuretic hormone
CFR	Chloride free Ringers
DNP	2', 4'-dinitrophenol
c-AMP	cyclic adenosine-3',5'-monophosphate

Table 1: Above are the explanations for the abbreviations used throughout the text.

INTRODUCTION

Insects live in almost every conceivable habitat on land and in fresh water; only the polar regions and the oceans seem to be relatively free from them. Dryness, deserts and absence of water seems to be no barrier to these animals. *Onymacris plana* is one such animal, a beetle, which thrives on the dunes of the harsh Namib desert. The ability of this insect to regulate its water balance within such a harsh environment is therefore intriguing.

As Malpighian tubules are responsible for the formation of the primary excretory fluid of insects, and in isolation can survive for prolonged periods of time, it makes an excellent tissue for the study of many aspects of epithelial transport.

In order to understand more precisely the cellular mechanisms of ion transport in the Malpighian tubule of this desert beetle, *Onymaris plana*, it was necessary to obtain measurements of the potentials and resistances across the transepithelial and basolateral membranes of the tubule cell. In the past various techniques have been used to measure these potentials and resistances which contribute towards the functioning of Malpighian tubules. The most frequently used technique in the literature is the "oil-gap" technique originally designed by Ramsay (1954). Most researchers have employed the "oil-gap" technique in its original form or modified it (O'Donnell and Maddrell, 1984) to obtain the data reported on Malpighian tubules. However, this technique is prone to errors and its validity has been questioned (Aneshansley et. al., 1988; Isaacson and Nicolson, 1989) and is discussed in chapter 2.

These errors can be avoided if the tubules are perfused in vitro (Burg et. al., 1966) (see chapter 2 for an explanation), which is the technique employed by this study. As this useful technique has so far only been employed by three research laboratories to investigate the mechanisms involved in fluid transport across insect Malpighian tubules, information in the literature is quite scarce (Williams and Beyenbach, 1984; Petzel et. al., 1987; Aneshansley et.

al., 1988; Weltens et. al., 1992; Leyssens et. al., 1992)[a]. Furthermore, owing to the fact that individual Malpighian tubule cells of *Onymacris plana* are large and relatively easy to impale with microelectrodes, it was relatively easy to investigate, simultaneously, both the transepithelial and basolateral potentials of the isolated, perfused Malpighian tubule. Isolated perfusion has the added benefit of facilitating the use of cable analysis to measure the resistances across the transepithelial and basolateral membranes. With the use of cable analysis values of the transepithelial resistance, fractional resistances of the basolateral membrane and length constant, among others, are also reported in this study.

It is convenient to use the electrophysiological data, mentioned above, to model the transport of ions across the Malpighian tubule with the aid of an electrical equivalent circuit. Although a simple electrical equivalent circuit of the Malpighian tubule has been presented by Isaacson et. al. (1989), the purpose of this study was to present an expanded electrical equivalent circuit as a model of ionic transport. In addition to this, a model of a Malpighian cell of *Onymacris plana* showing the different modes of ionic transport and fluid movement was constructed.

In this thesis, chapter 1 deals with the Malpighian tubule's transport of fluid and inorganic ions with emphasis on the species *Onymacris plana*, while chapter 2 examine the different electrophysiological methods which were used to investigate the underlying mechanisms involved in Malpighian tubular transport. Chapter 3 reports in detail on the various methods and techniques that were used to obtain the data experimentally. Chapter 4 records all the statistically manipulated data, while in chapter 5 the data are discussed. This is followed by various appendixes (A-E).

[a]Some of the data presented in this thesis has been published by Isaacson, Nicolson and Fisher, 1989.

CHAPTER 1

LITERATURE REVIEW

MALPIGHIAN TUBULES

1.1 Introduction

Insects are small and therefore have a large surface area to volume ratio for passive exchange with the environment. In spite of this, insects can be found in a wide variety of environments: fresh water, sea water marshes and tide pools, alkaline salt lakes, humid terrestrial areas and the harsh environment of deserts (Phillips, 1981). Furthermore, insects ingest a variety of plant and/or animal material which may include toxins and alkaloids. These factors may invariably affect the internal milieu (haemolymph) of insects. Nevertheless, insects are able to regulate the composition of their haemolymph within narrow limits (Edney, 1977; Stobbart and Shaw, 1974). The excretory system is largely responsible for this.

The excretory systems of insects consist of two parts: elongated tubular structures called the Malpighian tubules, which are bathed in haemolymph, and the hindgut consisting of the ileum and rectum. A primary isosmotic urine, containing most small haemolymph solutes (Phillips, 1983), is formed by secretory mechanisms into these tubules. This primary urine then enters the gut at the juncture between the midgut and the hindgut. From here the secreted fluid (primary urine) could flow rostrally into the midgut, or caudally into the hindgut. Here, depending on the insect's needs, fluid and/or solutes within the lumen can

either be reabsorbed across the hindgut and rectal epithelia or be excreted (see fig. 1.1).

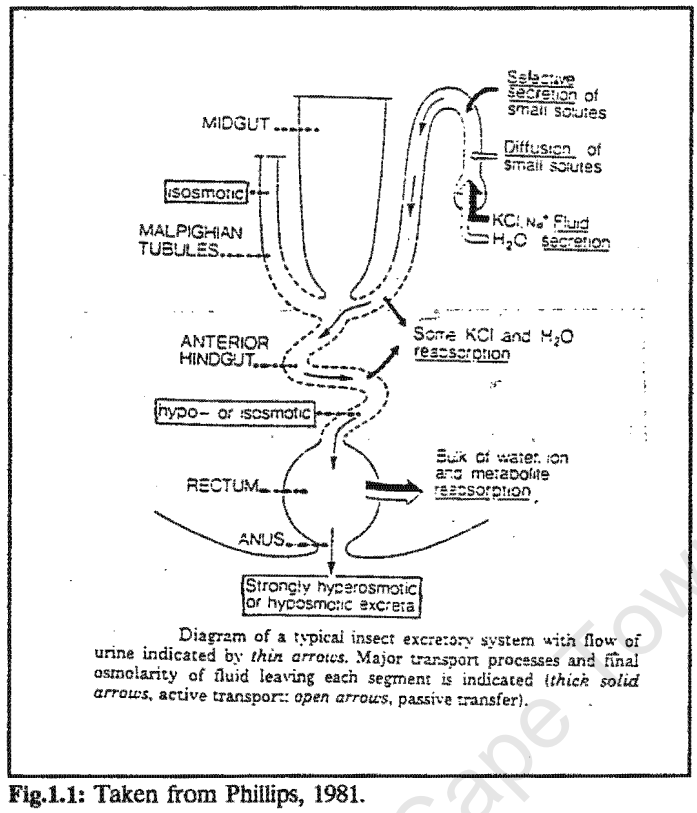

Diagram of a typical insect excretory system with flow of urine indicated by *thin arrows*. Major transport processes and final osmolarity of fluid leaving each segment is indicated (*thick solid arrows*, active transport; *open arrows*, passive transfer).

Fig.1.1: Taken from Phillips, 1981.

1.2 Structure of Malpighian Tubules

One end of each Malpighian tubule is closed (blind-ended) while the other end leads into the alimentary canal. While the blind end of the tubule in most insects are free within the haemocoel, in some insects eg. *Onymacris plana* it is not free, but associated with the rectum to form the rectal complex - this is important for the production of a dry faeces. Tubules are 2-100 mm long and about 100 μm - 200 μm in diameter, while the total number of tubules in insects range from 2 to 250 (Phillips, 1981). Some insects have a network of smooth muscle surrounding the outside of the Malpighian tubule (eg. *Onymacris plana*) (Bradley, 1985; Hanrahan and Nicolson, 1987). This smooth muscle allows the tubules to wave about within the haemocoel and also locally constricts the lumen diameter during contractions

contractions (Isaacson et. al., 1989).

The cells of insect Malpighian tubules, including those of *Onymacris plana* (Hanrahan and Nicolson, 1987), have apical microvilli projecting into the lumen (Bradley, 1985). On the basal, haemolymph-facing side the cells have elaborations of the plasma membrane. It was supposed that these were no more than simple pleating of the cell surface (Phillips, 1981). However, O'Donnell et. al. (1985) produced evidence to show that, in *Rhodnius*, the cells have a complex array of long basal projections which run parallel to the cell surface under the basement membrane. Basal membrane infoldings are also found in *Onymacris plana* (Hanrahan and Nicolson, 1987).

In terms of regional differences in Malpighian tubules, two broad categories can be distinguished: (i) Tubules that show marked regional differences, eg. *Drosophila* (Wessing and Eichelberg, 1969) and *Rhodnius* (Wigglesworth and Salpeter, 1962) and (ii) Tubules that show minimal regional differentiation but are composed of intermingled cell types eg. *Calliphora* (Berridge and Oschman, 1969) and *Onymacris plana* (Hanrahan and Nicolson, 1987). In the latter case cells have been divided into Type I and Type II cells on the basis of their structural differences and their affinity for lead nitrate (Berridge and Oschman, 1969). In the Malpighian tubules of *Onymacris plana* Type II cells are much smaller than the Type I cells and make up only 5% of the tubular cells (Hanrahan and Nicolson, 1987).

1.3 Mechanisms of Fluid Secretion

Fluid secretion across the Malpighian tubules depend upon ion movements, i.e. fluid is

thought to passively follow the active transport of ions (Phillips, 1981). The ions that predominate in the secreted fluid is K^+ and Cl^- in herbivorous insects (although Na^+ and Cl^- are the major ions secreted in blood sucking insects). The rate of fluid secretion by isolated Malpighian tubules is usually proportional to the external potassium concentration and saturation is observed when levels of this cation are high (Phillips, 1981). If all the external potassium is replaced by sodium, fluid secretion is greatly reduced (Phillips, 1981). Elevation of haemolymph potassium automatically leads to greater elimination of this ion by the excretory system by stimulating fluid secretion, because levels of this cation in the secretion usually do not change substantially when fluid secretion increases. For example, in *Onymacris plana*, increases of secretion rate in response to treatment with a diuretic homogenate (made up of brain, corpora cardiaca and prothoracic ganglia), caused no significant change in the concentration of secreted K^+ (187 mM (control) to 186 mM (stimulated); Nicolson and Hanrahan, 1986). Concentrations of potassium in the secreted fluid (100-180 mM) are normally 3 - 30 times higher than those in the haemolymph and do not change much if haemolymph Na^+/K^+ is varied over a wide range (Phillips, 1981). In blood-sucking insects, however, excess NaCl must be eliminated after feeding rather than KCl. In these species fluid secretion could either be driven by Na^+ alone (eg. tsetse fly; Gee, 1976) or by both Na^+ and K^+ transport (eg. *Rhodnius*; Maddrell, 1977).

Basolateral membrane: Throughout the literature various modes of ion transport across the basolateral membrane have been cited, mostly involving the transport of K^+. Firstly, entry of K^+ may occur in exchange for cellular Na^+ by means of a typical Na^+-K^+-ATPase pump in the basal membrane. Although this ATPase does occur in the basolateral membranes of Malpighian tubules, its activities usually do not affect fluid secretion (Maddrell and Overton, 1988). Secondly, K^+ may enter via a Na^+-K^+ exchange (antiport) system in the basolateral

membrane. Maddrell and Overton (1988) demonstrated that these Na^+/K^+ exchange pumps are ouabain sensitive. These two mechanisms at the basolateral membrane has been repeatedly drawn upon to explain the common observation that K^+-driven fluid secretion is stimulated by Na^+ when external concentrations of K^+ are low (Baldrick et. al., 1988). Furthermore, studies on *Rhodnius*, using intracellular microelectrode recording methods, indicated that the basal cell membrane is permeable to K^+ but not to Na^+ or Cl^- (O'Donnell and Maddrell, 1984). This formed the basis for the postulation of a third mechanism of K^+ transport which involves the cotransport of the following ions in the ratio: $Na^+:K^+:2Cl^-$ (O'Donnell and Maddrell, 1984). Similarly, Hegarty et. al. (1991) provided evidence for coupled cation-Cl^- transport during stimulated secretion by Malpighian tubules of *Aedes aegypti*. Earlier, in support of this Williams et. al. (1984) had demonstrated the dependence of Vt on Na^+ in *Aedes aegypti*. In this report the lowering of bath Na^+ concentration (from 159 to 9 mM) caused a prompt drop (-23 ± 6 mV) in Vt in all the tubules. In the ionic transport model for the Malpighian tubule of *Drosophila hydei*, Bertram et. al. (1991) suggested that the basolateral membrane includes both the $Na^+:K^+:2Cl^-$ co-transport mechanism as well as an active K^+-Na^+ pump which pumps K^+ into the cell in exchange for Na^+.

The coupled cation-Cl^- transport has already been mentioned as one mechanism involved in the transport of Cl^- across the basolateral membranes of the Malpighian tubules of several insect species (O'Donnell and Maddrell, 1984; Hegarty et. al., 1991). Furosemide, which inhibits the coupled entry of NaCl into vertebrate epithelial cells (Frizzell et. al, 1979), completely stops fluid secretion by *Rhodnius* tubules (O'Donnell and Maddrell, 1984). In this same species Cl^- is secreted against a large electrical (30 mV lumen negative) and a slight concentration difference while the fluid secretion rate is proportional to Cl^- over a limited

range (0-30mM Cl^-) (Phillips, 1981). Williams et. al. (1984) demonstrated the dependence of Vt on Cl^- in *Aedes aegypti* by reporting that the lowering of bath Cl^- concentration (from 157 mM to 7 mM) caused an increase in Vt (14 ± 5 mV) in most tubules studied. However, Nicolson and Isaacson (1987) found that the basolateral membrane of the unstimulated, non-perfused isolated Malpighian tubule of *Onymacris plana* to possessed an appreciable permeability to Cl^-. Thus, although the main mechanism involving Cl^- transport across the basolateral membrane in most insects appears to be a co-transporting mechanism, other mechanisms may exist.

Fourthly, a very important means of ion movement across the basolateral membrane includes ion-specific channels. For example, Nicolson and Isaacson (1990), using the patch clamp technique, demonstrated the presence of K^+ channels in the basal membrane of *Onymacris plana*. This is consistent with the high K^+ conductance across the basal membrane reported by Nicolson and Isaacson (1987). A high basal permeability to K^+ is also evident in tubules of *Locusta* (Morgan and Mordue, 1983), *Rhodnius* (O'Donnell and Maddrell, 1984) and *Carausius* (Pilcher, 1970).

Other ions that cross the basolateral membrane via channels include sodium. For instance a sodium-selective entry mechanism that is blocked by amiloride (a sodium channel blocker) is reported for tubules of the tsetse fly (Gee, 1976). Amiloride also decreases fluid secretion in 5-HT stimulated tubules of *Rhodnius prolixus* (Maddrell and O'Donnell, 1992).

The apical membrane: The apical membrane has been demonstrated to be the site at which electrogenic transport occurs and the mechanism by which K^+ has been implicated in apical transport has up to now not been clear. Most workers propose that the exit of K^+ from the

cell across the apical membrane into the tubule lumen is an energy-requiring step (Baldrick et. al., 1988). The basis for this postulation is that the unstimulated Malpighian tubule's lumen is usually positive to the haemocoel by 10 to 30 mV while the cell interior is electrically negative to both the haemocoel and the lumen, providing an up-hill electrical gradient for K^+ movement into the lumen (Phillips, 1981)(as is the case of *Onymacris plana* tubules; Nicolson and Isaacson, 1987). Furthermore, using the patch-clamp technique, the intracellular levels of K^+ were estimated to be about 158 mM in *Onymacris plana* (Nicolson and Isaacson, 1990). This estimate is close to the 153 mM recently measured with ion selective electrodes in tubule cells within the rectal complex of *Tenebrio* (O'Donnell and Machin, 1991). These estimates strongly suggest that a chemical gradient exist against which K^+ moves into the lumen across the apical membrane (the concentration of K^+ in the secreted fluid of unstimulated tubules of *Onymacris plana* is 187 mM; Nicolson and Hanrahan, 1986). In certain insects this active transport of K^+ usually requires some external Na^+ for maximum activity. Maddrell (1977) has provided some evidence that Na^+ and K^+ transport in insect Malpighian tubules occurs by a "common pump" which actually has a higher affinity for Na^+ than K^+. Whether this pump transports K^+ and Na^+ depends on intracellular levels of these cations and hence on the relative rates of their entry mechanisms that are present or predominate in their basal membranes. For example, if the basal plasma membrane is made permeable to Na^+ by removing external Ca^{2+}, insect tubules and other insect epithelia switch from K^+ to Na^+ secretion (Maddrell, 1977; Berridge, 1977). The cellular location (apical membrane) of this "K^+ pump" and its insensitivity to ouabain supports the view that the ubiquitous Na^+-K^+-ATPase of vertebrate epithelia is not responsible for fluid secretion in insect Malpighian tubules (Maddrell, 1971, 1977; Phillips, 1981; Maddrell and Overton, 1988).

It now seems certain that the "common pump" consists of two components. Recently, Bertram et. al. (1991) suggested an ionic transport model for the Malpighian tubule of *Drosophila hydei*. Using an antibiotic (a specific inhibitor bafilomycin A_1 which inhibits fluid secretion in the Malpighian tubules of *Drosophila*) they demonstrated the existence of a vacuolar-type H^+-ATPase which led them to proposed a novel mechanism for K^+ secretion across the apical membrane. The mechanism involves protons (H^+) which are actively pumped into the lumen, establishing a proton gradient from the lumen into the cell. This proton gradient in turn drives the K^+ secretion via a K^+-H^+ antiport mechanism in the apical membrane. If the antiport specificity for K^+ or Na^+ depends on their intracellular levels then the mechanism further provides an explanation for the switch in the secretion from K^+ to Na^+ in tubules that have a higher basal membrane permeability to Na^+ (Maddrell, 1977; Berridge, 1977). Bafilomycin A_1 also stops fluid secretion in the tubules of *Onymacris rugatipennis* (Nicolson, unpublished) as well as in *Formica polyctena* (Weltens et. al., 1992). In *Rhodnius proxilus*, using another vacuolar-ATPase inhibitor (NBDCl) fluid secretion was inhibited (Maddrell and O'Donnell, 1992). This provides evidence that the same mechanism for K^+ secretion in *Drosophila* probably exist in many insects.

In 1987 Wright and Beyenbach indicated that in *Aedes aegypti* Na^+ and K^+ ions are thought to be secreted across the apical membrane by active transport (which we probably now know to be the "proton pump - cation-H^+ antiport complex) while Cl^-, as a balancing anion, is secreted by a passive process. At this stage they demonstrated that chloride channels are present in the apical membrane of the mosquito (*Aedes aegypti*; Wright and Beyenbach, 1987). Bertram et. al. (1991) endorsed this view by postulating an apical Cl^- specific channel to allow for passive chloride fluxes. It follows, therefore, that Cl^- exits the cell down a favourable electrical gradient, i.e. the internal environment of the Malpighian cell is always

negative relative to the lumen.

1.4 Hormonal control of diuresis in insects

Due to their diverse habitats and feeding habits some insects need to conserve water (eg. the Namib desert beetle *Onymacris plana*), while other insects need to rid themselves of the excess body weight (eg. the mosquito *Aedes aegypti* which can consume a blood meal twice its body weight within 5 minutes). In the latter case diuresis begins soon after the commencement of feeding (Spring, 1990). This diuretic function in insects like the mosquito is understandable as the increase in body weight after feeding would perilously compromise flying; however, in a desert beetle excretory loss of water would seriously dehydrate the insect (*Onymacris plana* can survive without water for long periods and its diet is mostly dry plant material). However, in every species which has been studied hormones which affect diuresis have been reported to act upon Malpighian tubules (Phillips, 1981; Spring, 1990). Nicolson and Hanrahan (1986) were in fact very surprised to find diuresis in a desert insect. However, the function of diuresis in the Malpighian tubules of these desert insects is not to eliminate fluid, but rather as a mechanism for the rapid removal of metabolic waste from the haemolymph (Nicolson, 1991). Thus, when an insect needs to conserve water, the fluid entering the gut is reabsorbed leaving behind the unwanted waste products from the haemolymph and the gut's undigested contents (in *Onymacris plana* dry faeces are excreted). It follows therefore, that hormones could control the rate of secretion and reabsorption by acting mainly on two epithelial sites, i.e. either the Malpighian tubule or the hindgut and rectum (Spring, 1990).

Ordinarily, fluid secretion into Malpighian tubules occurs at a low rate; however, in *in vitro*

preparations, extracts from insect nervous tissue result in increases in fluid secretion in many species. For example, treating isolated Malpighian tubules from *Onymacris plana* with homogenised neural tissue results in a substantial increase in fluid secretion (Nicolson and Hanrahan, 1986). Periodical diuresis is thus under endocrine control.

The application of very sensitive techniques such as high performance liquid chromatography (HPLC) to the study of insect diuretic hormones has indicated that they are widely distributed throughout the central nervous system of insects; however, the most concentrated source, and presumably the main site of release, is the corpus cardiacum (Phillips, 1983). Diuretic peptides have recently been isolated and characterised. Most of these peptides are quite large and are composed of between 30 and 46 amino acids (Kay et. al., 1992). The considerable sequence homology between diuretic peptides of different insects has led to the categorization of these peptides into family groups.

HPLC techniques have also revealed that some insect species contain more than one diuretic hormone, possibly acting via different second messenger systems and exerting differing effects on the Malpighian tubules (Petzel et. al., 1985, 1987).

Diuretic activity has been demonstrated in the prothoracic ganglion, the brain and the corpora cardiaca of *Onymacris plana*. Preliminary work on the biochemistry of this insect showed that diuretic activity was surprisingly maintained after incubation with pronase (Nicolson, 1991). The diuretic activity was also stable to boiling (Nicolson, 1991). However, the exposure to the haemolymph resulted in the inactivation of diuretic activity (Nicolson and Hanrahan, 1986; Nicolson, 1991). Furthermore, the Malpighian tubules of *Onymacris rugatipennis* (which showed no significant difference as from those of *Onymacris plana*;

Nicolson, 1991) were not affected by several biogenic amines, with the exception of 5-HT, which significantly decreased fluid secretion. HPLC work revealed only 2 fractions increased the rate of secretion and found no evidence for antidiuretic activity.

1.5 Diuresis in *Onymacris plana*

Onymacris plana is a beetle that lives on the sand dunes in the Namib desert, and therefore water conservation would be expected to dominate its excretory physiology. It's isolated Malpighian tubules, secrete fluid at a rate of 3.3 nl/min under control conditions (Nicolson and Hanrahan, 1986). However, when stimulated by a diuretic homogenate (DH; made up of brain, corpora cardiaca and prothoracic ganglion) it was initially surprising to find a 20-25 fold increase in fluid secretion (Nicolson and Hanrahan, 1986). Exogenous cyclic-AMP (1 mM) also increased fluid secretion but its effects were smaller and took a longer time to come into effect (Nicolson and Hanrahan, 1986).

The cation composition of the secreted fluid contained a high K^+ concentration (187 mM) and a low Na^+ concentration (22 mM). Stimulation with DH led to the doubling of the Na^+ concentration but no significant change in the K^+ concentration (Nicolson and Hanrahan, 1986).

Further electrophysiological studies on isolated non-perfused tubules shed some light on the mechanisms whereby DH and c-AMP brought about an increase fluid secretion. DH resulted in a decrease in the transepithelial potential (Vt) whereas c-AMP caused and increase in Vt. However, both DH and c-AMP did not significantly effect the basolateral potential (Vbl) (Nicolson and Isaacson, 1987). It thus appears that the changes in Vt accompanying

stimulation are a reflection of potential changes across the apical membrane.

Initial experiments on isolated perfused segments of tubules showed that although a homogenate of the corpora cardiaca (CCH) produced a varied effect on Vt the mean result was a decrease in Vt (Isaacson et. al., 1989). The authors suggested that although CCH has diuretic activity the homogenate might also contain other unknown chemical factors. These experiments also showed that both CCH and c-AMP decreased the transepithelial resistance (Rt). However, whether this decrease in Rt is ascribed to changes at the basolateral and apical membranes and/or across the shunt remains unknown. Isaacson et. al. (1989) also showed that the effects of CCH and c-AMP were not additive. After Vt had increased as a result of c-AMP treatment, addition of CCH resulted in a significant decrease.

1.6 Conclusion

Mechanisms that control the movement of ions and water across the Malpighian epithelium appear to be complex and governed by a number of factors. Secretion and reabsorption of fluid appear to be mainly under the short term control of peptide hormones.

Although electrophysiological methods have played a major role in the elucidation of some of the transport mechanisms across the Malpighian tubule, other methods and bioassays has and will have to in the future complement each other if the overall, integrated picture of the regulation of insect excretion is to be understood. Hormone purification techniques that have

recently been employed to isolate and elucidate the structure of hormones will play a major role in clarifying hormonal function in Malpighian tubules.

Diuresis, roughly divides insect excretion mechanisms into two broad categories: those insects which employ diuresis as a mechanism to rid themselves of body weight after a feeding session, eg. the mosquito; and those insects in which diuresis occurs in the Malpighian tubules and reabsorption in the hindgut and rectum, promoting the clearance of metabolic waste from the haemolymph, but not a nett loss of body fluid, eg. the desert beetle, *Onymacris plana*.

CHAPTER 2

ELECTROPHYSIOLOGY

2.1 Introduction

Determination of the transmembrane and transepithelial potential differences is essential to the understanding of the mechanisms of ionic transport in epithelia. Epithelial transport of ions results in the generation of a transepithelial voltage (Vt) and the transported ions in turn affect the transport of fluid across epithelia. The measurement of the electrophysiological parameters is therefore of obvious interest.

Insect physiologists have generally used one of three methods to measure Vt. These methods are summarized below.

2.2 Electrophysiological methods

2.2.1 METHOD 1: The "Oil-gap" Method:

The technique designed by Ramsay (1954) has been the undisputed method for the study of the transport functions of Malpighian tubules. It has since been modified and used extensively for the measurement of Vt (O'Donnell and Maddrell, 1984). Berridge and Prince

(1972) had modified Ramsay's design to consist essentially of positioning the dissected tubule across three compartments: a central one filled with oil and two lateral ones containing Ringer's solution. The purpose of the central oil-filled chamber is to electrically insulate the two lateral electrode containing chambers. Generally, the lateral bath containing the longer part of the tubule (or the end of the tubule that is sealed) is called the peritubular bath and houses the ground electrode; the lateral bath containing the shorter, lumen-open end of the tubule is called the luminal bath and houses the electrode that senses the luminal voltage.

The validity of the "oil-gap" method assumes that: the tubule is electrically homogeneous along its length; the insulated portion between the two baths is electrically silent; the values of length constant and core resistance are immaterial; and the resistance of the open end of the tubule is so low as to effectively short-circuit such transtubular potentials as may be present in the luminal bath.

Aneshansley et. al. (1988) showed that the "Vt" measured by the Ramsay method may be positive or negative depending on the magnitude of current leaks via the peritubular water film of the oil bathed tubule segment. Their circuit analysis also predicted that lumen diameter would also affect Vt; i.e if the lumen resistance was allowed to change while all the other resistances remained constant and the lateral cell-to-cell voltage was zero, then as lumen diameter increases (i.e. core resistance drops) the measured Vt as measured by the "oil-gap" method approaches the real Vt. Isaacson and Nicolson (1989) showed that the length of tubule in the lumen bath was critical to the resultant Vt, i.e. the longer the tubule in the lumen bath the smaller the recorded Vt and vice versa. They also showed that the tubule segment within the central oil chamber showed appreciable electrical activity, and that

this would be shunted, in each bath, by the core resistances of the electrically active or inactive tubule segment in series with the resistance at the tubule orifice; therefore the longer the tubule segment, the greater the core resistance, and so the larger the potential generated of the tubule in that particular bath.

2.2.2 METHOD 2: Microelectrode transepithelial voltage

The microelectrode transepithelial voltage method could be seen as an addition to the "oil-gap" method described above. Here the tubule lumen is punctured with a microelectrode to measure the voltage between the lumen and the bath. However, Morgan and Morgue (1983) performed this method by pinning the ends of a short segment of Malpighian tubule to the floor of a bath perfused with a Ringer solution (no oil was used in this experimental technique). Three electrodes are used in this arrangement: an earth electrode in contact with the bath Ringers, a recording microelectrode impaled across the basolateral membrane (measuring the intracellular potential) or impaled across the tubule epithelium in contact with the fluid within the lumen (measuring Vt); and a second reference electrode (to provide a differential recording). Aneshansley et. al. (1988) showed that the transepithelial potential (Vt) measured in this way was much closer, but lower (in the oil-gap method) than those measured by perfusion method. The lower Vt appeared to be as a result of the current flow through the oil-bathed tubule segment.

2.2.3 METHOD 3: The Isolated perfusion Method

In this method the lumen to bath voltage, Vt, is measured in isolated perfused tubules in the following manner. Using suction, one end of the isolated segment of tubule is pulled into the mouth of the glass holding pipette and a perfusion pipette inside the holding pipette is advanced into the lumen of the segment. The other end of the segment is pulled into the mouth of a third pipette, the collecting pipette, into which the perfusion fluid emerges (Burg et. al., 1966). The transepithelial voltage (Vt) of isolated tubule segments can easily be measured by incorporating electrodes into the chamber containing the bathing fluid and into the holding assembly of the inner perfusion pipet. The electrodes contacting the solutions are salt-agar bridges connected to calomel half cells, from which the signal is passed to a recorder (Lapointe et. al, 1984).

One important aspect of electrical measurements in isolated perfused tubule segments is that the voltage-measuring electrode in the lumen is the perfusing pipet itself. The transepithelial voltage (Vo) recorded is, therefore, that existing between the tip of the perfusing pipet and the bathing solution (Lapointe et. al., 1984). It is therefore important to note that Vt is synonymous with Vo as measured in the *in vitro* perfusion experiments.

2.3.1 Measurement of Transepithelial Resistance

Transepithelial resistance can be measured by passing a constant current pulse across the tubular epithelium and observing the resultant change in the transepithelial voltage (Helman, 1972). Various pipet arrangements have been used to accommodate the dual functions of

passing current and measuring voltage at the perfusing pipet. The most common method involves the use of a single electrode, the inner perfusion pipet, which is used to inject (pass) current into the lumen and measure the transepithelial potential (Vt) concurrently (Burg et. al., 1968).

The problem presented by the resistance of the perfusion pipet glassware during current injection is overcome using a Wheatstone bridge circuit (Helman et. al., 1971). This electric bridge nulling circuit is used to initially null the voltage deflection to zero in the absence of a tubule, i.e., to "balance out" the voltage changes due to the resistance of the perfusion pipette, so that only the voltage deflection due to the tubule is recorded (Helman et. al., 1977). An alternative method for measuring the transtubular resistance by-passes the use of a Wheatstone bridge in that the current pulsing electrode is placed within the perfusion pipette (Greger and Schlatter, 1983). In the latter case double perfusion pipettes are used, one of which is used for current injection while the other is used for the recording of the transepithelial potential. This set-up prevents any electrical coupling between the current injection and voltage recording channel. An added advantage is that the design enables the immediate changing (<1 second) of the

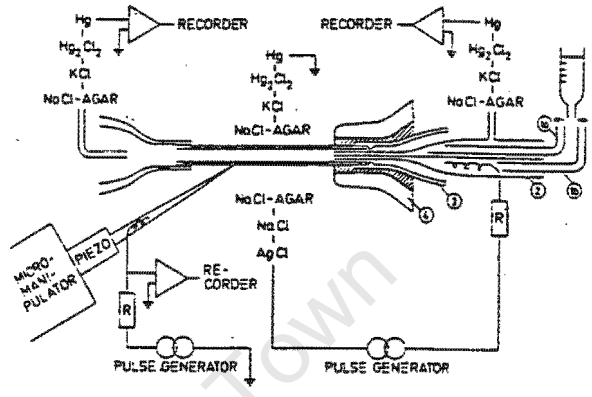

Fig. 1. Schematic view of the methods to record transepithelial and transmembrane *PDs*, as well as the transepithelial resistance and the voltage divider ratio in isolated perfused cTAL segments. The cTAL segment is perfused from right to left through a dual channel perfusion pipette *2*. The active channel is determined by the position of a three-way-valve. The composition of the perfusate in the two channels of the perfusion pipette can be varied through 2 fluid exchange pipettes *1a* and *1b*. The tubule is held by the perfusion holding pipette *3* and by the collection pipette. For optimal insulation an outer sylgard pipette *4* is used. The transepithelial *PD* is measured at the perfusion and on the collection side via NaCl-Agar bridges (sol. 1, Table 2 + 50 g agar-agar $\cdot l^{-1}$) and calomel half cells via the grounded bath. The transepithelial resistance is determined by constant current pulses, produced by a current generator and a resistor (*R*), injected through channel *2b* of the perfusion pipette. The current loop is closed by a separate NaCl-Agar bridge and by a stimulation isolation unit, such that the current loop is off ground. Individual cells are impaled through the basolateral membrane using microelectrodes mounted on a piezo stepping element [11]. The position of the electrode is controlled by a micromanipulator. The *PD* across the basolateral membrane is recorded via Ag/AgCl half cell, and is referenced to the grounded bath. The resistance of the microelectrode is monitored by the injection of current pulses through a second current injection loop

Fig. 2.1: Taken from Greger and Schlatter (1983).

lumen perfusate (see fig. 1.2).

2.3.2 Cable Analysis

In the case of tubular epithelia, interpretation of electrical measurements (eg. transepithelial resistance) is complicated by the geometry of the tubule. However, these problems have been overcome through the use of **cable analysis** (Helman et. al., 1971). Helman et al. (1971) applied standard cable equations (Taylor, 1963) to the particular case presented by the tubule, i.e. a cylinder of finite length, L, having a presumably homogeneous wall and luminal cross-sectional area. Thus cable analysis considers the Malpighian tubule as a cylindrical tube of constant cross-sectional area and uniform electrical properties. The analysis yields a tubule length constant (λ), a radial resistance (transtubular resistance), and a tubule axial resistance (core resistance).

When the current pulse is passed at one end of the tubule, i.e. from the perfusion pipet, the resultant voltage is maximal at the perfusion end of the tubular segment and is attenuated with distance away from this point, due to the current flow across the tubular epithelium.

For transepithelial resistance measurements in segments of tubular epithelium, the following equations are used:

$$\frac{L}{\lambda} = \cosh^{-1}(V_o/V_L) \quad (1)$$

$$R_c = \frac{V_o \tanh(L/\lambda)}{I_o \lambda} \quad (2)$$

$$R_t = \frac{2\pi r V_o \lambda \tanh(L/\lambda)}{I_o} \quad (3)$$

where Rc is the resistance of the luminal solution ($M\Omega.cm^{-1}$), Rt is the epithelial resistance ($k\Omega.cm^2$), Io is the current passed, L is the tubule length, Lambda (λ) is the length constant, and Vo and VL are the recorded voltages at the perfusing and collecting ends of the segment, respectively.

However, the use of **cable analysis** in measuring transepithelial resistances becomes invalid if there is cell-to-cell coupling via the gap junctions. This diverts too much of the injected current into neighbouring cells (Frömter, 1986). If cell-to-cell coupling does exist, the fractional resistance along the length of the tubule would be different from each other and vice versa. Therefore, to test for cell-to-cell coupling, intracellular recordings from three or more sites along the length of the tubule are made. If the fractional resistance along the basolateral membrane differs appreciably then the results obtained by cable analysis are invalid.

2.4 Electrical Equivalent Circuits

In order to understand more precisely the cellular mechanisms of ion transport, it is

necessary to obtain measurements of the driving forces and membrane conductances for

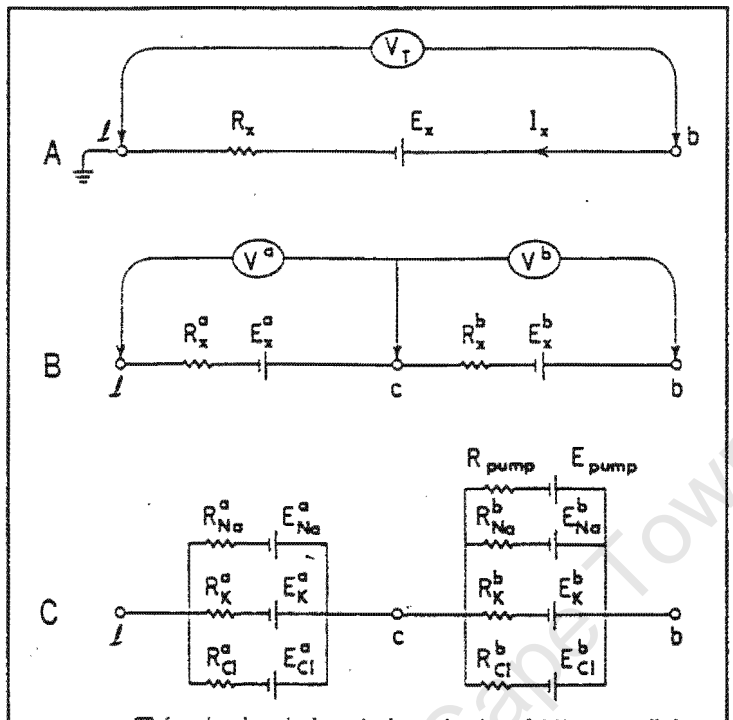

Thévenin electrical equivalent circuits of (*A*) transcellular pathway, (*B*) apical and basolateral membranes, and (*C*) individual pathways across apical and basolateral membranes that, for this example, are assumed to be separate for Na, K, and Cl. The intracellular compartment is isopotential, as indicated by node c.

Fig 2.2: See text for further explanation. The above is taken from Helman and Thompson (1982).

ion movement across both the apical and basolateral membranes, as well as through the paracellular pathways (shunts) of an epithelium. Physiologists commonly employ electrical terms, symbols and circuits when describing epithelia. The simplest electrical equivalent circuit of the transepithelial pathway is given by an electromotive force (emf), Ex, and a resistance, Rx, which simply implies that a relation exist between the transepithelial potential (Vt) and the current flow (Ix) (see figure 2.2). In Malpighian tubules the existence of two membranes in series forming the transcellular pathway is recognized, i.e. the apical and

basolateral membranes. It follows, therefore, to model each membrane with its Thévenin equivalent E^a, E^b, R^a and R^b, where the a and b refers to the apical and basolateral membranes respectively. Indeed, voltages and conductances are readily measured in epithelial systems that have complex parallel and series routes of ion transport. It is, therefore, appropriate to model the behaviour of epithelia with **electrical equivalent circuits** (Helman and Thompson, 1982). The ultimate aim of this technique, taken with other data, is to provide an electrical model from which an understanding of the relationship between the specific forces and the resultant ionic fluxes which occurs at each membrane (barrier) in transepithelial transport. Figure 2.2 gives examples of a few electrical equivalent circuits.

2.5 CONCLUSION

With the need for reliable measurements of transepithelial voltage it is clear that method 1 ("oil-gap" method) is prone to artifacts and at best avoided. Method 2 (microelectrode transepithelial voltage method) offers more reliable results but also suffers from the experimental design defects. It is therefore clear that while method 3 (isolated perfusion method) requires a great deal more skill and equipment to perform an experiment it does have a number of advantages: much more reliable voltage recordings; cable analysis is facilitated by the experimental design; measurements of secretion can easily be carried out, i.e. volume, rate of secretion and ion concentration measurements can be carried out with ease while simultaneously monitoring the electrophysiological parameters of the tubule. One of the outstanding advantages of method 3 as opposed to the other methods is the easy changing of the perfusate composition.

CHAPTER 3

METHODS AND MATERIALS

3.1 Preparation of Tubules

Tubules were obtained from adult female beetles (*Onymacris plana*) supplied by the Desert Ecological Research Unit at Gobabeb, Namibia, and maintained in the laboratory as described previously (Nicolson and Hanrahan, 1986).

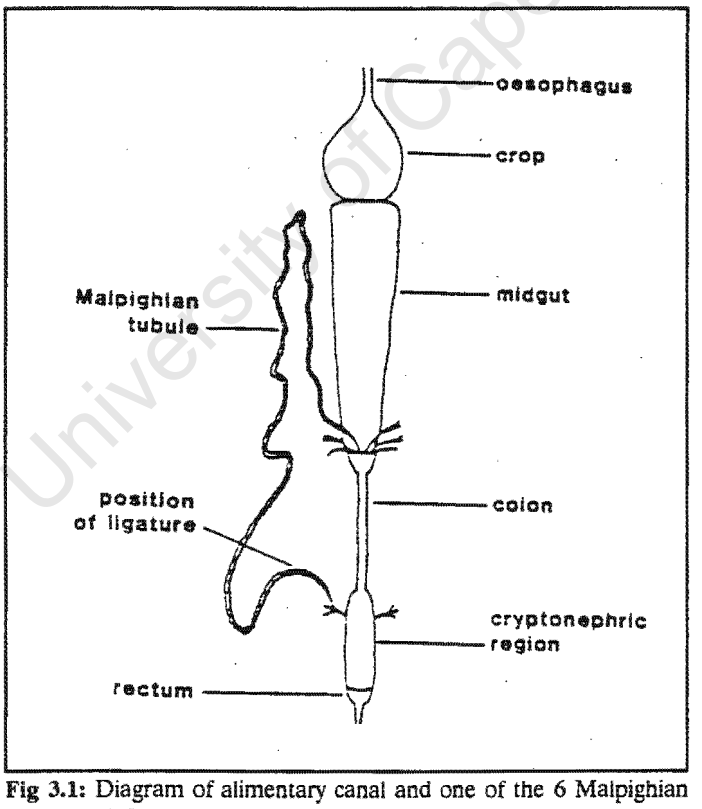

Fig 3.1: Diagram of alimentary canal and one of the 6 Malpighian tubules of *Onymacris plana*.

As the tubules of *Onymacris plana* are structurally homogeneous along most of the length of the free segment (Hanrahan and Nicolson, 1987), a segment of the mid-portion of one

of the more accessible dorsal or lateral tubules was dissected out. Usually only one tubule segment was used from any one beetle (see fig. 3.1). The isolated segment was perfused *in vitro* as described by Burg et. al., (1966) (see chapter 2 for more details) (see fig. 3.2). As the transepithelial potential was found to be independent of the rate of perfusion, the height of the reservoir of perfusion fluid was held constant at some 12 cm above the bath throughout the experiments reported here. The actual rate of perfusion was not measured routinely, but was noted to be 40 to 60 nl/min in a few unstimulated tubules. All experiments were carried out at room temperature (21-23°C); most were of 2-5 hour duration. Changes in stimulant, inhibitor or solute concentrations of the bathing fluid were effected by three-fold washout of the bath (2 ml) with the new solution.

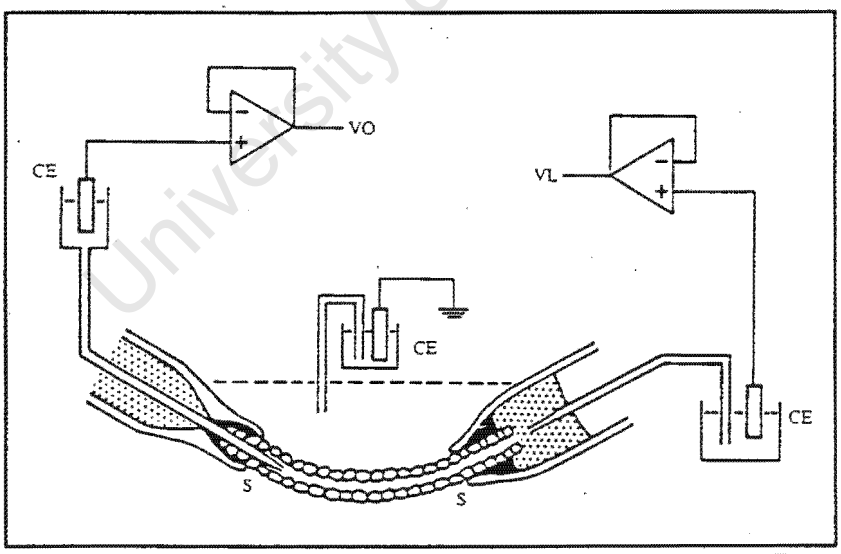

Fig.3.2: Perfusion arrangement for basolateral cell membrane impalement. Taken from Isaacson and Nicolson, 1989.

3.2 Mounting of tubules

In those experiments in which cable analysis was to be performed, care was taken to ensure that only short lengths (0.5-1 mm) of tubule were exposed to the bath solution; this minimised errors in measurement of the current-induced voltage jumps at the distal end of the tubule (Lapointe et. al., 1984). A layer of unpolymerised Sylgard (Dow Corning) within the orifices of both the holding and collecting pipettes ensured electrical isolation of the tubule from the bath.

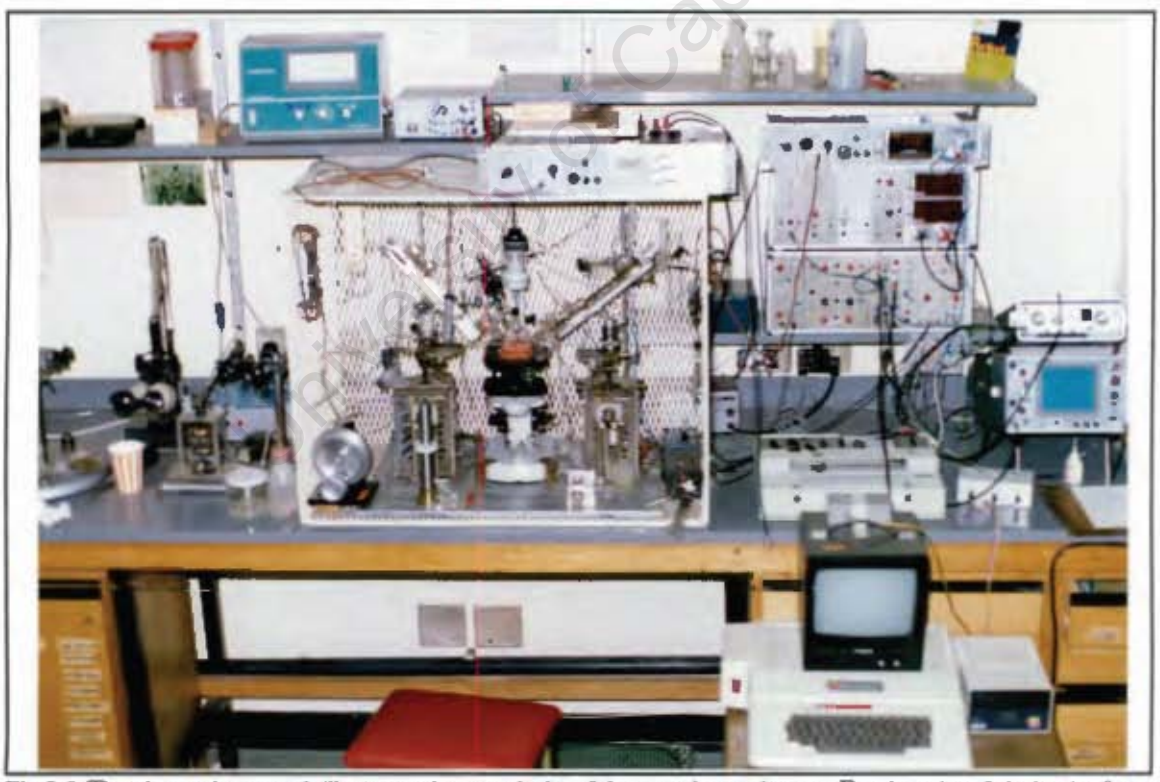

Fig.3.6: The above photograph illustrates the complexity of the experimental setup. For the sake of clarity the front screen of the Faraday cage was removed. The 3 DPM's (right of cage) read out Vo, Vl and I.

3.3 Electrical Measurements

Capacitive coupling between the power (AC) and the microelectrode input circuit is responsible for most of the interference problems in transepithelial and especially intracellular recordings because of the high impedance of the input circuit. The interfering signal is transmitted from the source "aerial" (eg. alternating mains voltage) through the dielectric medium of the air with the high impedance part of the input circuit acting as a "receiving aerial" (Purves, 1981). To alleviate this problem the experimental set-up was housed within a metal mesh enclosure (i.e. Faraday cage) with five sides. The front of the Faraday cage had a sliding door (sixth side) which covered the front of the cage while recording was in progress. However, experience showed that it mattered little whether or not the door was closed.

The bath was held at ground potential by a saturated KCI calomel electrode immersed in bath fluid and joined to the bath by a short wide-bore (5 mm ID) 3% agar saturated--KCI bridge (see fig. 3.2); the dimensions of this bridge were dictated by the need to ensure a non-detectable (< 0.5 mV) potential drop at this point during passage of current through the tubule.

Similar electrodes detected the transtubular electrical potential differences at both the proximal (Vo) and distal (Vl) ends of the tubule. The electrode at the proximal end was placed within the perfusion reservoir while that at the distal end, bathed in perfusion fluid, was joined to the luminal fluid within the collecting pipette by a thin 3% agar saturated-KCI bridge. Both Vo and Vl are expressed relative to the bathing solution.

Possible inter-electrode drift was checked by occasionally joining the latter electrodes to the bath by still other 3% agar saturated-KCI bridges; this was found to be a necessary precaution in view of the sometimes small (< 5 mV) voltage jumps detected at the far end of the tubule on current injection.

The calomel electrodes, sensing Vo and Vl, were joined to high input impedance (> 10^{12} Ohms) unity-gain voltage followers, which at the proximal end (Model P1, Bio-electric Instruments, U.S.A.) incorporated a bridge circuit, thus permitting measurement of the jump in proximal transtubular potential upon injecting current into the tubule via the perfusion pipette. As the resistance of the perfusion pipette was some 5 to 6 megohms, and the tubule input resistance only a few hundred kilohms (see chapter 4: Results and Appendix B), it was found advantageous to replace the single-turn bridge-balance potentiometer originally provided in the Model PI by a 20-turn potentiometer; this permitted precise and reproducible balancing of the bridge. Small changes in bath temperature (1-2°C) were found to cause significant bridge imbalance (presumably by altering both the conductivity of the fluids within the bath, and the dimensions of the tip of the perfusion pipette).

A perspex glass shield was designed in order to alleviate temperature changes in the bath caused by air currents. The shield was supported in an upright position by a metal base. The dimensions of the shield are shown in figure 3.4. The shield was designed so that the eye-pieces of the microscope protruded through it; this allowed the un-interrupted viewing of the perfused isolated tubule.

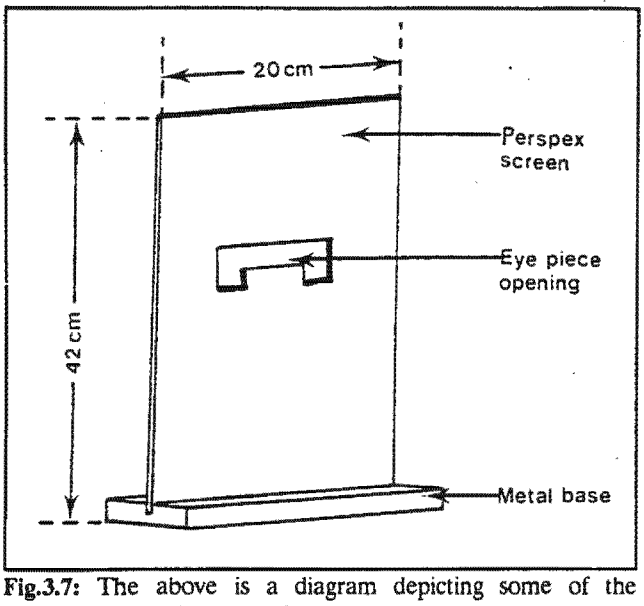

Fig.3.7: The above is a diagram depicting some of the dimensions and features of the transparent perspex screen.

The current-induced transtubular voltages, the temporal excursions of which were monitored on an oscilloscope, did not exhibit polarisation potentials (Helman et. al., 1971), i.e. they were of constant amplitude in the last two thirds of the 600 msec current pulse; only these latter voltages were recorded. In any given tubule, at any given time, the amplitude of this current-induced voltage was found to be linearly proportional to the amount of current injected, and symmetrical about zero (see fig. 3.5); this relationship was occasionally found useful in checking the bridge balance during prolonged experiments, i.e. if the bridge was balanced (before mounting a tubule), and a current pulse is passed through the perfusion setup, the current profile, as seen on the oscilloscope, will have hardly deviated from the zero base line.

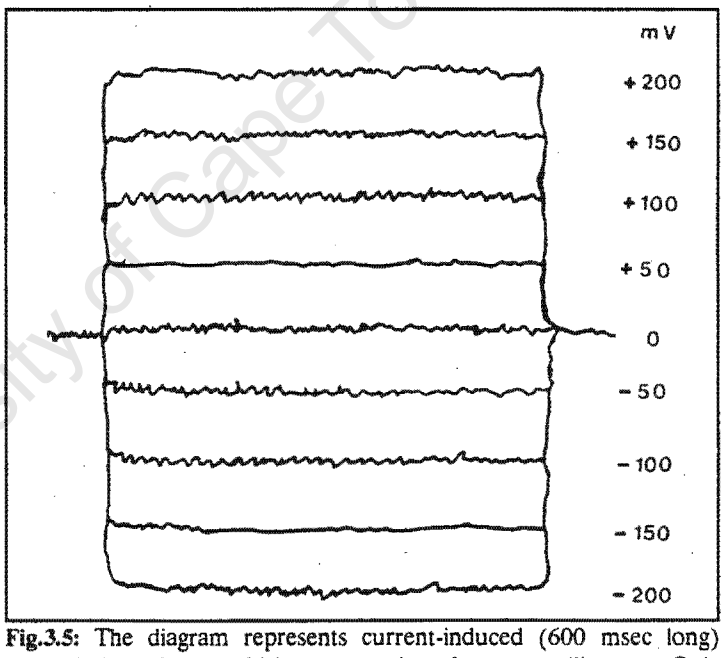

Fig.3.5: The diagram represents current-induced (600 msec long) transtubular voltages, which were monitored on an oscilloscope. Only voltages in the latter 500 ms were recorded. (n=12).

Vo was displayed on a digital millivoltmeter, of 0.1 mV maximal resolution, and recorded

continuously on a millivolt chart recorder. The tubule was subjected to hyperpolarising current pulses, of 600 msec duration and 200 nano-amps maximum amplitude, at short intervals (usually 5-10 min) throughout each experiment. Where transient changes in Vo of only a few minutes duration were encountered, as for example immediately after addition of diuretic homogenate (CCH) (see section 3.6 for details) to the bath, this interval was as short as 1 min.

The values of Vo and Vl, as accessed repeatedly (3x) immediately before and then during the last half of each 600 msec current pulse, were captured on an Apple II micro-computer (for program notes see Appendix A), equipped with an 8-bit multi-channel A/D converter (Mountain Hardware, U.S.A.); maximal resolution was 0.5 mV (see Appendix B).

The Malpighian tubule of *Onymacris plana*, as described previously (Nicolson and Isaacson, 1987), frequently displays small and regular oscillations in transtubular potential, each voltage excursion being accompanied by a localised contraction of the muscle associated with the tubule wall. Care was taken to inject intra-luminal current pulses only between contractions except when the effects of these contractions upon the tubule's cable parameters were being investigated.

In those experiments in which the effects of changes in perfusate composition (altered ionic composition, or addition of inhibitors) on Vo were studied, it was found convenient to perfuse longer (2-3 mm) tubule segments with their distal ends left open to the bath. As shown below, the length constant of *Onymacris plana* tubules is but a small fraction

of a millimeter. Thus shortening these long tubule segments by 0.5 mm to 1 mm, or advancing the perfusion pipette 200-300 μm down the length of the tubule, was found to be without effect on Vo.

The tubule outer diameter and the distance between the Sylgard seals at its ends, were measured with an ocular micrometer. Specific resistance of the perfusate, measured with a laboratory conductivity meter, was 61.5 Ohm.cm. These values, in conjunction with the changes induced in Vo and Vl by current injection, were employed to calculate by cable analysis, the tubule's input resistance, length constant, transepithelial and core resistances as well as the lumen diameter. The relevant equations have been described (Helman et. al., 1971), and their use commented upon repeatedly and are accordingly not reproduced here (see appendix C for a summary of cable equations). However, the measurement of the length (L) deserves some comment ('L' in the cable equations; see chapter 2). There was a relative uncertainty of about 10 % regarding the absolute measurement of the mounted tubule segment. The uncertainty, which was compounded by observing the tubule from below, arose due to the curved nature of the mounted tubule. Further uncertainty existed as to the precise beginning or end of the tubule, that is, where it encounters the Sylgard. However, the observable curved length of the tubule may be estimated by using trigonometry and assuming that the perfusing pipette angle holds for the tubule as well. It should be noted that although an error in 'L' will lead to an over- or under-estimation of the absolute value of Rt, it will not influence the comparison of the relative values of Rt between two experimental situations using the same tubule arrangement.

The short-circuit current, a measure of active transport pump activity, may be calculated either corrected for surface area (SCC; $\mu A/cm^2$; see equation 4) or as the 'virtual' short-circuit current (SCCv; $\mu A/cm$; see equation 5).

$$SCC = \frac{Vo}{Rt \times \pi \times D} \quad (4)$$

$$SCCv = \frac{Vo}{Rt} \quad (5)$$

[Rt = transepithelial resistance; D = lumen diameter]

As SCC is a function of both pump activity and of surface area, and as changes in lumen diameter (and so of surface area) featured in most of the experiments reported below (see Results), short-circuit current is reported here as SCCv rather than as SCC (other than in tables 4.1 and 4.2, where both measures are listed, by way of illustration). See appendix C for a summary of all the formulae and equations used in this work.

3.4 Measurement of Intracellular Potentials (Vbl):

Cells were impaled across the basolateral cell membrane with microelectrodes that were filled with 3 M KCl by back-injection. The electrodes were made with filamented borosilicate glass capillaries (1.2 mm (OD), Clark Electromedical Instruments), and the tips fabricated on a vertical microelectrode puller (David Kopf). Microelectrodes made on this puller had shanks approximately 1-1.5 cm long and resistances of 35-60 MΩ when filled with 3 M KCl.

In order to impale the tubule cells the microelectrode was introduced into the bath from the front of the chamber and positioned with a hydraulic-drive remote-controlled micromanipulator (MO-102, Narishige). The tip of the microelectrode was placed on the basement membrane of the tubule at a 30-40° angle and advanced into the cell by tapping lightly on the micromanipulator control box. Although cells along the entire length of the tubule could be impaled, all stable impalements were obtained within a distance of 200 μm from the tip of the perfusion pipette, with the majority of stable impalements being obtained within a distance of 50 μm from the perfusion pipette tip. The inability to obtain stable impalements at distances greater than 200 μm from the perfusion pipette probably reflects the fact that the middle portion of the tubule tended to twist and vibrate during the process of microelectrode advancement (i.e., tapping on the micromanipulator control box). In contrast, movements of the tubule were minimized near the perfusion pipette. To reduce further vibration of the preparation, the entire perfusion apparatus was supported on a metal platform which rested on a number of squash balls (Dunlop, yellow dot).

The fractional resistance of the basolateral membrane (FRBL) is defined as the voltage divider ratio; it is the ratio of the basolateral membrane resistance over the total transcellular resistance according to the equation (equation 6) below where the ΔVbl and ΔVo are, respectively, the basolateral membrane voltage deflection and the transepithelial voltage deflection consequent to the current pulse injected into the tubular lumen via the perfusion pipette, and where Rbl and Ra are, respectively, the basolateral and apical membrane resistances (Petzel et. al., 1987).

$$FRBL = \frac{\Delta V_{bl}}{\Delta V_t} = \frac{\Delta V_{bl}}{\Delta V_a + \Delta V_{bl}} = \frac{R_{bl}}{R_a + R_{bl}}$$

For the purpose of this study FRBL was expressed as a percentage (FRBL%). The fractional resistance of the apical membrane (FRa%) was determined as follows:

$$FRa\% = 100 - FRBL\%$$

3.5 Solutions

The control bath solution, based upon the haemolymph composition of *Onymacris plana* (Nicolson and Hanrahan, 1986), was very similar to that used previously on unperfused tubules (Nicolson and Isaacson, 1987). It contained (mM): 125 NaCl, 15 KCl, 5 $MgCl_2$, 2 $CaCl_2$, 6 $KHCO_3$, 4 KH_2PO_4, 10 glycine, 10 proline, 10 serine, 10 histidine, 10 glutamine and 50 glucose (see appendix E). The control perfusate contained 20 mM NaCl and 130 mM KCl but was otherwise identical to the control bath solution; this solution was also used as the bath solution in those experiments in which the tubules were to be exposed to a high ambient K concentration. The high-K, low-Na perfusion fluid was intended to approximate the **in vivo** situation and previous experiments on unperfused tubules. The basal membrane of *Onymacris plana* tubules, although highly permeable to K^+, is apparently impermeable to Na^+ (Nicolson and Isaacson, 1987), so that the simultaneous change in bath Na^+ concentration is irrelevant.

Bath solutions of zero Cl^- concentration were made by replacing NaCl by sodium isothionate, KCl by potassium gluconate, $MgCl_2$ and $CaCl_2$ by the respective sulphates, and adding extra glucose to maintain the normal osmolality (385 mOsm/kg water).

The solution in which the tubules were dissected was identical to that of the control bath except that additional glucose was substituted for the amino acids. Routine addition of traces of phenol red to all solutions provided a check that the pH was maintained at about 7.0. All solutions, which were stored frozen, were allowed to equilibrate to room temperature before use. See appendix E for tables containing the various stock concentrations for the above solutions.

3.6 Drugs and CCH

Where indicated, the following were administered dissolved in either the bath solution or the perfusate: c-AMP (1 mM; Na salt, Sigma); 2', 4'-dinitrophenol (DNP; 1 mM; British Drug Houses). The corpora cardiaca were carefully dissected from the head of *Onymacris plana* using a dissecting-microscope and a set of fine jewellers forceps. The corpora cardiaca were clearly distinguishable from the surrounding neural and fatty tissue by its bluish colour and its triangular shape. Diuretic hormone extract (CCH) was prepared by homogenising the corpora cardiaca of the donor beetle in 5 μL of control bath solution.

3.7 Statistics

All results are presented as means ± standard deviation unless stated otherwise. Paired and independent sample t-tests were used to assess the significance of differences between means. P values of less than 0.05 were regarded as significant.

CHAPTER 4

RESULTS

4.1.1 Dimensions of the tubules

The Malpighian tubules of *Onymacris plana* have an irregular, knobby external appearance. The cells are usually so heavily pigmented as to render virtually impossible the visualisation of the lumen. In a few tubules with relatively little pigment (fig 4.1) the luminal cross section was seen to be markedly irregular. The maximum outer diameter of perfused, non-stimulated and non-contracting tubules was about 138 μm (range 110-184 μm; n=121).

Fig. 4.9: Isolated perfused Malpighian tubule of *O.plana*. This particular tubule is unusually transparent, so that in this instance the lumen is visible as is also the tip of the perfusing pipette within it.

4.1.2 Equilibration time

The transtubular potentials recorded at the proximal and distal ends of the tubule were almost never identical. At the start of perfusion Vo was always positive. Vl was smaller

than Vo and sometimes even a few millivolts negative to the bath (when Vo was low) (cf. Appendix D). During the first half-hour of perfusion Vo usually fell, more or less steeply (fig. 4.2), while Vl decreased to a lesser extent. Throughout the 2-5 hour period of perfusion Vl was always markedly (on average, 10 mV) less than Vo. Changes induced in Vo by any experimental procedure were accompanied by a parallel, but smaller, change in Vl. It is of interest to note once most of the cable parameters settled down they remained consistent in any particular tubule. The data suggests that an equilibrium period ±20 to 40 minutes was adequate.

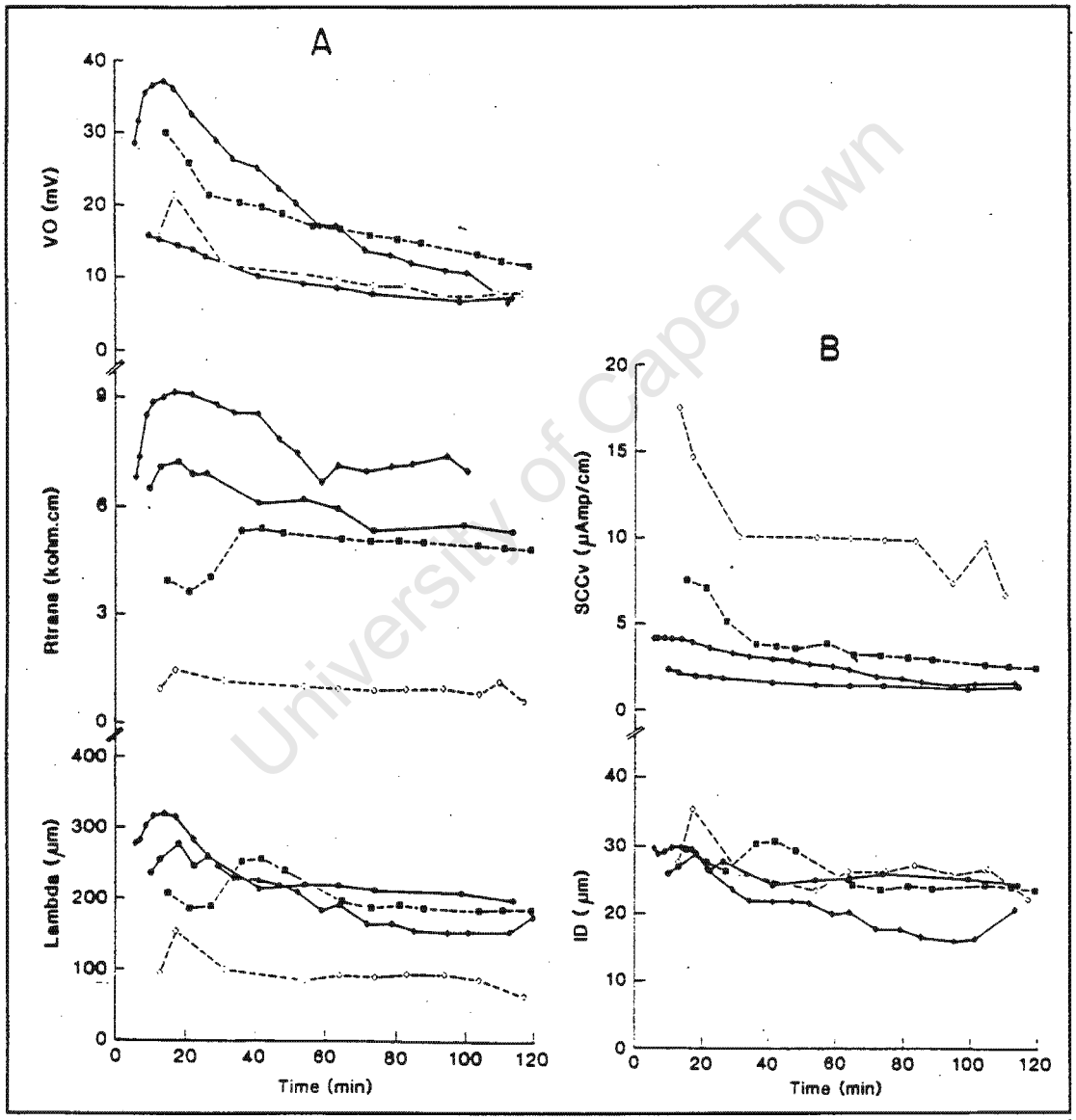

Fig. 4.2: V_o and cable parameters measured repeatedly in 4 Malpighian tubule segments during 120 min of perfusion. Tubules are identified by different symbols.

4.1.3 Normal Cable Parameters

Sampling for control cable analysis data began about 31 minutes (± 21 min) after mounting the tubule. All the following control values relate to this starting time of the experiment and were calculated from 32 tubules; these normal values are all presented as mean ± S.D. (see table 4.1).

The control Vo had a mean of 18.5 ± 8.8 mV. The input resistance (i.e. the potential change at the proximal end of the tubule divided by the injected current) had a mean value of 241 ± 212.9 kOhms. The average values for the length constant, the transtubular resistance, the core resistance, the diameter of the lumen and the fractional resistance of the basolateral membrane were calculated using cable analysis (see chapter 3 for an explanation). The fractional resistance of the basolateral membrane percent (FRBL%), as determined by intracellular puncture and cable analysis, had a mean of 14.01% ± 12.04%. The true SCC had a much higher value (497.2 ± 50.9 $\mu A/cm^2$) than the virtual SCC (4.6 ± 4.3 $\mu A/cm$); SCC is reported here as the "virtual" SCC (SCCv), i.e. not corrected for surface area (see equations 7 and 8 in appendix C). For a summary of the above normal values and their standard deviations see table 4.1.

VARIABLE	N	MEAN	S.D.
Vo (mV)	32	18.5	8.8
R_i (kOhms)	32	241.3	212.9
Lambda (microns)	32	325.4	191.7
R_t (kOhms.cm)	32	6.21	3.9
R_c (MOhms/cm)	32	15.3	29.6
Lumen Diameter (microns)	32	39.1	21.8
SCCv ($\mu A/cm$)	32	4.6	4.3
SCC ($\mu A/cm^2$)	32	497.2	495.7
FRbl%	32	14.01	12.04

Table 4.1: The above summarize the control values for the various cable parameters. See table 1 for cable abbreviations.

4.1.4 Tubular contractions

Contractions of the tubule often commenced within a few minutes of starting perfusion, and were sometimes as frequent as one or two per minute. They appeared to be localised constrictions rather than longitudinally peristaltic and, for no apparent reason came and went for prolonged periods. They were abolished on adding 120 mM potassium or DNP and sometimes CCH (diuretic homogenate/hormone) to the bath. Table 4.2 lists the values of Vo and of the various cable parameters during and between three successive contractions as found in a single tubule (with 1 mM c-AMP in the bath). In this case the contractions occurred at 1 minute intervals.

During successive intervening relaxed periods Vo and the various cable parameters were little changed. During contractions the calculated diameter fell markedly with corresponding changes in Vo, input resistance, length constant, SCC, and the core resistance, whereas the transtubular resistance and the virtual SCC essentially remained constant.

PARAMETERS	relaxed	contracted	relaxed	contracted	relaxed	contracted
Time, min	100	101	101.5	102	102.5	103
Vo, mV	41	51	45	52	48	56
Rinput, kOhm	152	372	165	382	175	356
λ, μm	270	105	277	119	269	135
Rtrans,kOhm.cm	4.01	3.93	4.45	4.55	4.60	4.80
SCCv, μA/cm	10.3	13.0	10.1	11.4	10.5	11.7
SCC, μA/cm^2	869	2,776	874	2,328	951	2,152
Rcore, MOhm/cm	5.51	35.40	5.80	32.11	6.37	26.38
D, μm	38	15	37	16	35	17

Table 4.2: Vo and cable parameters were recorded over a 3-minute period during and between muscle contractions. Tubule had been perfused for a 100 min and exposed to cAMP. See table 1 for abbreviation explanations.

4.2 Microelectrode Impalement Potentials

4.2.1 Controls

Upon impaling the tubule two voltage stages were always observed. The first voltage stage was less than the second with a mean potential of -9.6 ± 2.1 mV. Whenever the microelectrode was advanced further, mostly by the gentle tapping of the micromanipulator, a clear-cut, steady second stage potential (mean ± S.D. = -23.96 ± 6.4 mV) was observed (see fig. 4.3). The first stage potential was possibly due to the electrode tip being situated between the basement membrane and the tubular epithelium; therefore, on further advancement of the micro-electrode, the Malpighian tubular cell was impaled and thus the observed second stage potential. It is easy for the novice to mistake the first stage potential as that of a tubule epithelial cell as this potential is steady and mimics most changes across the basolateral membrane (although these changes are smaller; see chapter 5 for discussion).

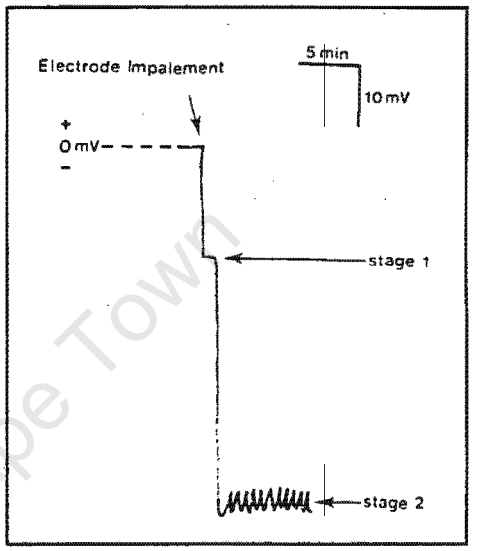

Fig 4.3: The potential profile across the basolateral membrane upon impalement.

4.2.2 Control Vo, Vbl and Va

The average control values for the transepithelial (Vo), basolateral (Vbl) and apical (Va) membrane potentials were 18.5±8.8 mV, -21.1±6.8 and 39.6±10.6 mV, respectively (N=32).

4.2.3 Fractional Resistance of the basolateral membrane along tubule length.

Validation of cable analysis depends on the demonstration that there is no change in the

fractional resistance (FRBl) along the length of the tubule (c.f. Frömter, 1986).

The fractional resistance of the basolateral membrane (expressed as a percentage) was measured at three sites along the length of the tubule with the impalement sites approximately 100, 200 and 300 μm distal to the tip of the perfusion pipette. The FRBl% of site 1 was statistically compared to site 2 and site 3 in all five tubules. Site 1 (FRBL%=17.4±3.0) was not significantly different from site 2 (16.9±2.4) or site 3 (17.6±3.5%) (P>0.995).

4.2.4 The Apical Versus Basolateral Resistances

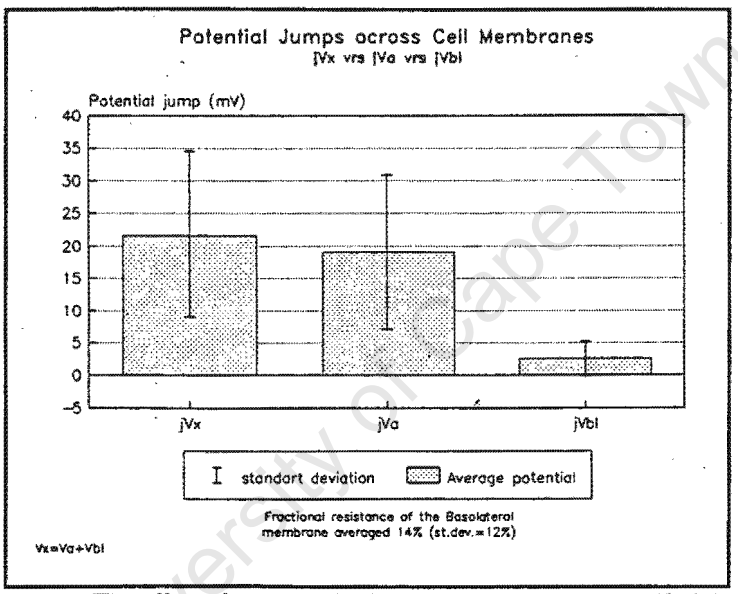

Fig 4.4: The effect of current injection into the tubule lumen. jV_x, jV_{bl} and jV_a are the potential jumps across the tubule epithelium, basolateral and apical membrane.

In 32 tubules the mean voltage jump across the basolateral membrane (jV_{bl}) was 2.6±2.7 mV, while the voltage jump across the tubule wall at the site of impalement (i.e. jV_{tx} as calculated from cable equation 9: see appendix C) was 21.63±12.75 mV. Using the equation $jV_a=jV_{tx}-jV_{bl}$, the potential jump across the apical membrane (jV_a) was calculated to be 19.06±11.9 mV. The potential 'jumps' across the apical and basolateral membranes are proportional to the resistances across them; the fractional resistance of the apical membrane was always much larger (86%) than the fractional resistance of the basolateral membrane (FRBL%=14.01±12.04%; P<0.00001) (see fig 4.4).

4.3 Changes Induced In Vo, Vbl And Cable Parameters

4.3.1 Effects of DNP

The effects of DNP on the transepithelial (Vo) and basolateral membrane (Vbl) potential are illustrated in figure 4.5 and summarized in table 4.4. Under control conditions Vbl and the apical membrane potential (Va) were -25.2±10.7 mV and 37.34±11.63 mV respectively while Vo was 11.62±13.2 mV (N=10). The addition of DNP to the bathing medium caused the immediate depolarization of all potentials. In the presence of DNP Vbl was depolarized to -12±11.43 mV ($P<0.02$), Va to 14.7±5.34 mV ($P<0.05$) and Vo to 2.7±3.64 mV ($P<0.05$). On the replacement of DNP Ringers with control bath Ringers, Vo, Vbl and Va never completely recovered and returned to control values (4.9±3.94 mV, -14.1±11.35 mV and 19±8.9 mV respectively). Means were all significantly different from each other at $P<0.05$.

Table 4.3 summarises the effects of DNP on the cable parameters. Ten in a total of 11 experiments summarized in table 4.5 involved intracellular puncture. The addition of DNP to the bath resulted in a significant (0.05) drop in the short circuit current (SCCv) from 2.05±1.8 μA/cm to -0.58±1.3 μA/cm (n=11; $P<0.5$). However, the other cable parameters measured in table 4.3 underwent no significant changes ($P>0.05$).

Although DNP depolarized both Vo, Va and Vbl, the overlaying muscle oscillations on Vbl were not abolished (fig 4.5 A).

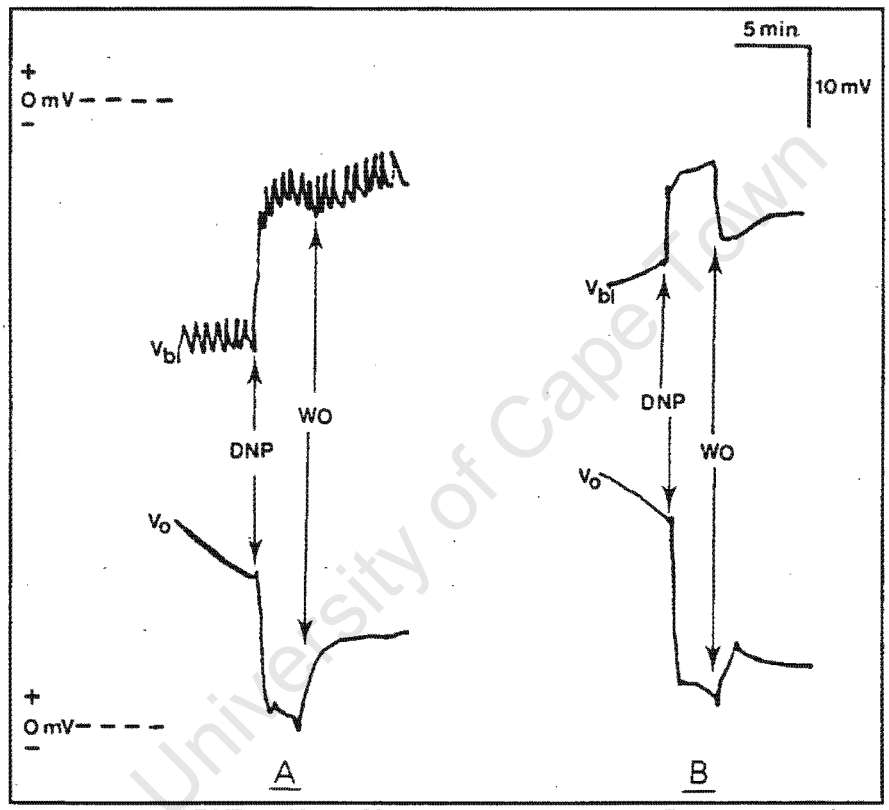

Fig 4.5: Effect of DNP on V_o and V_{bl}. WO=wash out with bath Ringers. A and B are separate experiments.

EFFECT OF
DNP
ON Vo AND CABLE PARAMETERS OF THE MALPIGHIAN TUBULE

CABLE PARAMETERS		N	MEAN	±SD	P<
Vo (mV)	PRE	11	11.62	13.20	0.05
	POST	11	2.70	3.64	
LAMBDA (μ)	PRE	11	268.98	160.80	N.S.
	POST	11	282.31	180.86	
Rtrans (kOhm.cm)	PRE	11	6.22	5.47	N.S.
	POST	11	5.78	4.51	
Rcore (MOhm/cm)	PRE	11	18.37	25.42	N.S.
	POST	11	12.95	14.16	
DIAMETER (μ)	PRE	11	37.44	23.45	N.S.
	POST	11	37.70	24.07	
SCCv (μA/cm)	PRE	11	2.05	1.8	0.05
	POST	11	0.58	1.3	
Rinput (kOhm)	PRE	11	292.37	308.64	N.S.
	POST	11	247.72	153.50	
FRBL (%)	PRE	10	19.25	13.44	N.S.
	POST	10	18.46	20.16	

Table 4.3: Values are means; N.S. - not significant (P>0.05); N - number of tubules. Pre - control; Post - experimental. Cable parameters was measured before and after 2',4'-DNP was introduced into bath. See Table 1 for abbreviations.

	N	Vo	Va	Vbl
Control	10	11.62±13.2	37.24±11.63	-25.2±10.7
DNP	10	2.7±3.64	14.7±5.34	-12±11.43
Washout	10	4.9±3.94	19±8.9	-14.1±11.35

Table 4.4: All values are expressed in millivolts as means±S.D.. Means were all significantly different from each other at P<0.05.

4.3.2 Effects of Chloride-free Ringers

The effects of chloride free Ringers (CFR) on the electrical properties of the Malpighian tubule of *Onymacris plana* are summarized in tables 4.5 and 4.6 and illustrated in figure 4.6 by three experiments which show, simultaneously, the transepithelial (Vo) and basolateral membrane (Vbl) potentials. Figure 4.6 shows that while the effects on Vbl were repetitive and consistent, the effects on Vo did not always show a consistent pattern. Cable parameters were measured before CFR was introduced into the bath and then also shortly before and immediately after CFR was replaced with control bath Ringers (washout). The most common effect of CFR is represented in figure 4.6 **B**; similar traces occurred in 13 of the 21 experiments performed. The intracellular potential was measured in 16 of the 21 experiments. Under control, experimental (CFR) and washout conditions, the mean Vo of the 16 intracellular experiments was not significantly different to the mean Vo of the entire set of 21 experiments ($P<0.0001$).

Under control conditions Vbl and the apical membrane potential (Va) were -19.56 ± 6.9 mV and 34.44±14.54 mV respectively while Vo was 15.2 ± 11.7 mV (N=16). The replacement of bath Ringers with CFR hyperpolarized Vo, Va and Vbl to 22.75±10.4 mV ($P<0.001$), 54.54±14.12 mV ($P<0.00001$) and -35.9±11.22 ($P<0.00001$) respectively (see table 4.6). Upon replacing CFR with control bath Ringers Vo was depolarised and Vbl hyperpolarised by similar amounts to 15.95±11.95 mV and -37.75±8.7 mV respectively while Va underwent no significant change ($P=1$) (see table 4.6).

Table 4.5 summarises the effects of CFR on the cable parameters. Only 16 in a total of 21 experiments summarized in table 4.5 involved intracellular puncture. CFR caused significant increases in both the length constant (lambda:- 302.4±141.3 μm to 361.9±140.8 μm; $P<0.02$) and the transepithelial resistance (Rt) (6.1±4.8kΩ.cm to 7.6 kΩ.cm; $P<0.04$; N=21). CFR significantly decreased the virtual short circuit current (SCCv) from 5.1±3.5 μA/cm to 3.9±2.7 μA/cm; $P<0.05$; N=21). However, the other cable parameters summarized in table 4.5 underwent no significant changes.

THE EFFECT OF CHLORIDE-FREE RINGERS ON Vo AND CABLE PARAMETERS OF THE MALPIGHIAN TUBULE					
CABLE PARAMETERS		N	MEAN	±SD	P<
Vo (mV)	PRE	21	15.2	11.7	0.001
	POST	21	22.8	10.4	
LAMBDA (μ)	PRE	21	302.4	141.3	0.02
	POST	21	361.9	140.8	
Rtrans (kOhm.cm)	PRE	21	6.1	4.8	0.04
	POST	21	7.6	6.9	
Rcore (MOhm/cm)	PRE	21	6.2	3.2	N.S.
	POST	21	6.0	4.9	
DIAMETER (μ)	PRE	21	42.2	28.1	N.S.
	POST	21	43.6	19.9	
SCCv (μA/cm)	PRE	21	5.1	3.5	0.05
	POST	21	3.9	2.7	
Rinput (kOhm)	PRE	21	197.3	94.5	N.S.
	POST	21	213.9	95.9	
FRBL (%)	PRE	16	16.3	12.9	N.S.
	POST	16	17.2	10.2	

Table 4.5: Values are means; N.S. - not significant; N - number of tubules. Pre - control; Post - experimental. Cable parameters was measured before and after Cl-free Ringers replaced control bath Ringers. See Table 1 for abbreviations.

	N	Vo	Va	Vbl
Control	16	14.88±12.45*	34.29±15.08	-19.56±6.9
CL-FREE RINGERS	16	+20.9±11.01*	54.54±14.57‡	-33.6±8.9
WASHOUT	16	+15.95±11.95	54.54±15.5‡	-37.75±8.7

Table 4.6: All values are expressed in millivolts as means±S.D. The * denotes that means are significantly different at P<0.01, + at P<0.006 and ‡ denotes P=1, while all other means are significantly different from each other at P<0.00001. Washout refers to Cl-free Ringers replaced by control bath Ringers.

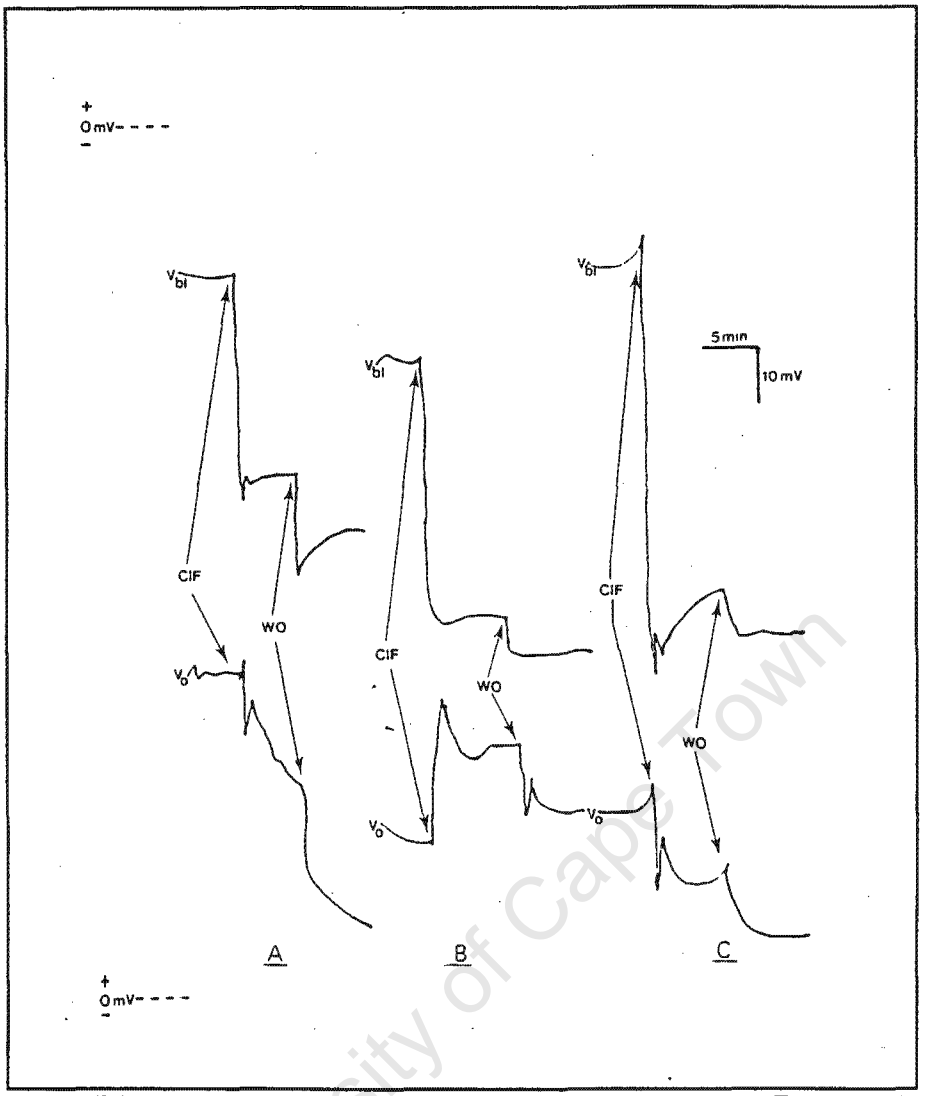

Fig 4.6: Effects of CFR on Vo and Vbl. WO=wash out with bath Ringers. The change in Vo in experiments A, and C are atypical (Vo depolarized by CFR), whereas B is a typical example, i.e. normally both Vo and Vbl were hyperpolarized by CFR.

4.3.4 Effect of high K^+ Ringers (130 mM)

The effect of increasing the bathing medium's concentration of potassium from 20 mM to 130 mM on Vo, Vbl and Va of 21, isolated, perfused Malpighian tubules is summarized in table 4.8 and two typical examples are illustrated in figure 4.7. Under control conditions Vo, Vbl and Va were 8.1±3.9 mV, -26.4±9.6 mV and 34.6±9.3 mV respectively. When the bath Ringers was changed to the Ringers containing a high concentration of potassium (HiK) Vo hyperpolarized to 16.5±7.1 mV ($P<0.00001$) while both Vbl and Va depolarized to -8.1±3.8 mV ($P<0.00001$) and 24.62±8.2 mV

(P<0.0001) respectively. The effects of HiK were immediate. Upon the replacement of HiK with control bath Ringers recovery of Vo, Vbl and Va were partial. Both Va and Vbl only partially recovered to 28.2±7.8 mV (P<0.00002) and -17.3±7.4 mV (P<0.06: not significantly different) respectively. Upon replacing HiK with control bath Ringers Vo was partially depolarised to remain at an elevated voltage above the initial control value at 10.9±6.4 mV (P<0.00001) (see fig. 4.7).

Table 4.7 summarizes the parallel HiK induced changes of the cable parameters. Increasing the bath potassium significantly increased SCCv from a control value of 1.6±1.6 μA/cm to 3.5±2.7 μA/cm (P<0.05). However, this was the only cable parameter that produced a statistically significant change in response to HiK.

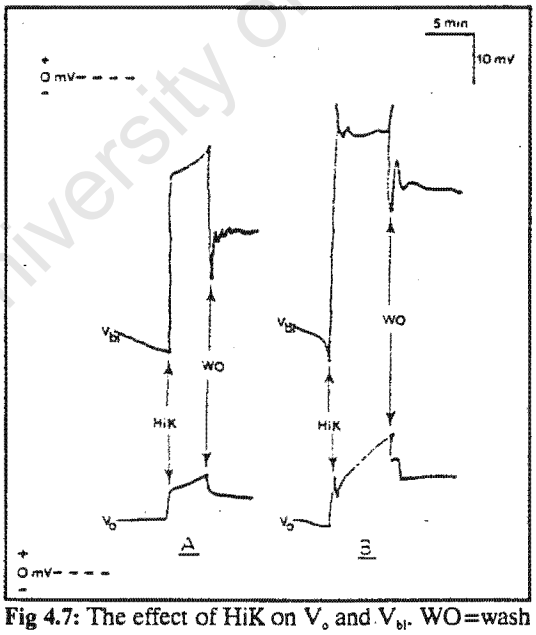

Fig 4.7: The effect of HiK on V_o and V_{bl}. WO=wash out with bath Ringers. A and B represent 2 experiments.

THE EFFECT OF HIGH K^+ ON Vo AND CABLE PARAMETERS OF THE MALPIGHIAN TUBULE					
CABLE PARAMETERS		N	MEAN	±SD	P<
Vo (mV)	PRE	21	8.1	3.9	0.000001
	POST	21	16.5	7.1	
LAMBDA (μ)	PRE	21	381.04	159.31	N.S.
	POST	21	458.46	442.12	
Rtrans (kOhm.cm)	PRE	21	6.23	5.66	N.S.
	POST	21	5.49	4.92	
Rcore (MOhm/cm)	PRE	21	5.66	3.98	N.S.
	POST	21	4.92	3.35	
DIAMETER (μ)	PRE	21	45.95	20.53	N.S.
	POST	21	64.41	65.63	
SCCv (μA/cm)	PRE	21	1.6	1.6	0.05
	POST	21	3.5	2.7	
Rinput (kOhm)	PRE	21	195.51	99.96	N.S.
	POST	21	171.05	100.33	
FRBL (%)	PRE	21	15.58	12.12	N.S.
	POST	21	13.82	10.49	

Table 4.7: Values are means; N.S. - not significant; N - number of tubules. Bath potassium was increased from 20 mM to 130 mM. See table 1 for abbreviations.

	N	Vo	Va	Vbl
Control	21	8.1±3.9*	34.6±9.3+	-26.4±9.6*
HIGH K^+	21	16.5±7.1*	24.6±8.2+	-8.1±3.8*
Washout	21	10.9±6.4	28.2±7.8	-17.3±7.4

Table 4.8: All values are expressed in millivolts as means±S.D.. Means denoted with * and + were significantly different at P<0.00001 and P<0.0001, respectively.

4.3.3 Effect of $BaCl_2$

Table 4.10 summarises the effects on Vo, Vbl and Va. Figure 4.8 illustrates the effects of $BaCl_2$ on the transepithelial (Vo) and basolateral membrane (Vbl) voltages in two representative and isolated perfused Malpighian tubules. The parallel effects on the cable parameters are summarized in table 4.9. Under control conditions the average Vo, Vbl and Va in 5 different tubules were 13.1±12.7 mV, -21.2±6.9 mV and 34.4±18.3 mV respectively. The effects of 1 mM $BaCl_2$ were immediate. Vo was depolarized to 10.64±12.9 mV ($P<0.01$) while both Vbl and Va were hyperpolarized to -32.8±7.7 mV ($P<0.03$) and 43.4±16.9 mV ($P<0.08$; not significantly different from control). Upon replacing the $BaCl_2$ with control bath Ringers both the means of Vo and Va did not significantly change. Vbl, however, was sightly hyperpolarized to -34.5±7.0 mV ($P<0.01$) (see table 4.10 for summary).

In parallel to the $BaCl_2$ voltage induced changes, the transepithelial resistance (Rt) increased from 2.64±1.6 kΩ.cm to 3.14±1.8 kΩ.cm ($P<0.01$; $N=5$) (see table 4.9).

The fractional resistance of the basolateral membrane (FRBL%), in response to $BaCl_2$ and in parallel to the above voltage changes, significantly increased from 12.83±4.3% to 36.47±33.5 % ($P<0.02$; $N=5$). The FRBL% effects were supported by increases in voltage jumps across the basolateral membrane in response to luminal current injection (1.16±1.0 mV to 3.48±1.5 mV; $N=5$; $P<0.05$) (see fig.4.7).

Cable analysis revealed that in the presence of $BaCl_2$ the virtual short circuit current was decreased from 6.14±4.2 μA/cm to 3.0±2.1 μA/cm ($P<0.05$; $N=5$). The input resistance, Ri, which describes the proximal resistance of the tubule to current injection, increased from 142.6±62.1 kΩ to 173.8±72.2 kΩ ($P<0.02$) in response to $BaCl_2$. An increase in Ri indicated that the tubule as an electrical cable had become more narrow. The core resistance, Rc, describes the axial resistance of the tubule. An increase in Rc also

indicated a decrease in the diameter of the tubule. Rc increased from 10.2±12.2 MΩ/cm to 12.0±12.0 MΩ/cm (P<0.06). The mean electrically calculated diameter decreased from 37.1±15.6 μ to 32.8±14.12 μ; however, this change was not statistically different (see table 4.9). The other cable parameters which did not change significantly are summarized in table 4.9.

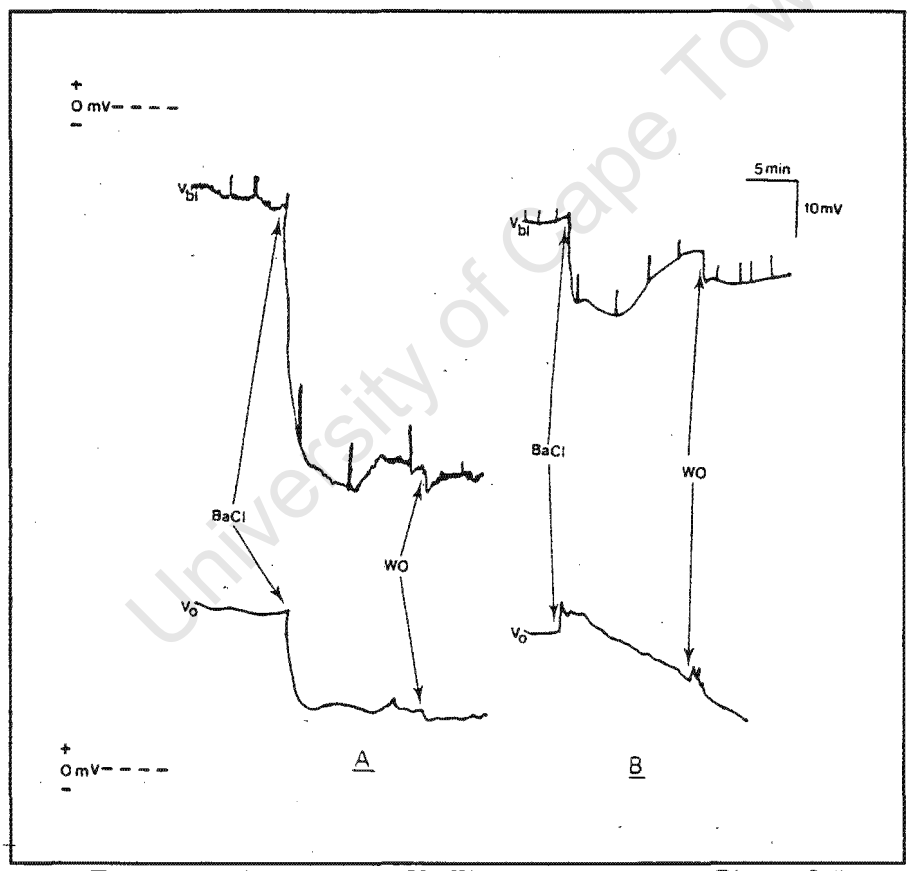

Fig 4.8: The effect of BaCl on V_o and V_{bl}. WO=wash out with bath Ringers. Spikes on V_{bl} trace is due to luminal current injection. A and B are separate experiments.

THE EFFECT OF BARIUM CHLORIDE ON Vo AND CABLE PARAMETERS OF THE MALPIGHIAN TUBULE					
CABLE PARAMETERS		N	MEAN	±SD	P<
Vo (mV)	PRE	5	13.18	12.7	0.01
	POST	5	10.64	12.9	
LAMBDA (μ)	PRE	5	205.32	92.66	N.S.
	POST	5	191.58	76.50	
Rtrans (kOhm.cm)	PRE	5	2.64	1.57	0.01
	POST	5	3.14	1.82	
Rcore (MOhm/cm)	PRE	5	10.24	12.19	0.06
	POST	5	11.98	12.00	
DIAMETER (μ)	PRE	5	37.10	15.56	N.S.
	POST	5	32.80	14.12	
SCCv (μA/cm)	PRE	5	6.14	4.2	0.05
	POST	5	3.0	2.1	
Rinput (kOhm)	PRE	5	142.60	62.05	0.02
	POST	5	173.78	72.23	
FRBL (%)	PRE	5	12.83	4.27	0.02
	POST	5	36.63	33.47	

Table 4.9: Values are means; N.S. - not significant; N - number of tubules. Pre - control; Post - experimental. Cable parameters was measured before and after 2 mM $BaCl_2$ was introduced into bath. See table 1 for abbreviations.

	N	Vo	Va	Vbl
Control	5	$^{+}$13.18±12.7	34.38±6.2*	$^{+}$-21.2±6.9
$BaCl_2$	5	$^{+}$10.64±13.0*	43.4±16.9*	$^{+}$-32.8±7.7^{+}
Washout	5	10.1±11.7*	44.6±15.9*	-34.5±7.0^{+}

Table 4.10: All Values are expressed in millivolts as means±S.D.. Means that are marked with * are not significantly different from each other. All other values are significantly different at $P<0.01^{+}$ and $P<0.03^{+}$.

4.3.5 Effects of Diuretic Homogenate (CCH)

The effect of CCH on the transepithelial (Vo) and basolateral membrane potential (Vbl) is illustrated in figure 4.9 by 3 separate experiments and summarised, with parallel effects on the apical membrane (Va), in table 4.12. Under control conditions Vo, Vbl and Va were 18.6±9.1 mV, -18.2±5.0 mV and 36.8±11.9 mV respectively (N=9). Upon the addition of CCH to the bath Ringers Vo and Va were significantly depolarized to 14.7±8.4 mV ($P<0.003$) and 34.7±11.9 mV ($P<0.03$), respectively, while Vbl did not under go any significant change at -20.0±5.9 mV (see table 4.12). Vo recovered spontaneously to 20.6±12.8 mV (see fig. 4.9 A and B) and sometimes surpassed the control Vo upon recovery (fig. 4.9 C). The CCH induced change in Vo was measured where maximum depolarization had occurred and again when Vo had recovered. After the recovery of Vo, replacement with control bath Ringers had no effect on Vo or Vbl. Vo, Vbl and Va, measured after the spontaneous recovery had occurred, were not significantly different from control values ($P>0.05$).

The parallel changes in the cable parameters are summarised in table 4.11. Only 9 in a total of 14 experiments involved intracellular puncture. None of the cable parameters underwent statistically significant changes in response to treatment with CCH. However, the mean value of RT, Rc, Ri and SCCv decreased while the mean value of lambda, the lumen diameter and FRBl% increased.

THE EFFECT OF CCH ON Vo AND CABLE PARAMETERS OF THE MALPIGHIAN TUBULE					
CABLE PARAMETERS		N	MEAN	±SD	P<
Vo (mV)	PRE	14	15.97	7.54	0.001
	POST	14	13.34	7.74	
LAMBDA (μ)	PRE	14	223.26	126.28	N.S.
	POST	14	225.67	132.67	
Rtrans (kOhm.cm)	PRE	14	6.27	3.21	N.S.
	POST	14	5.34	2.00	
Rcore (MOhm/cm)	PRE	14	19.63	14.56	N.S.
	POST	14	16.22	12.34	
DIAMETER (μ)	PRE	14	27.15	11.63	N.S.
	POST	14	28.26	12.76	
SCCv (μA/cm)	PRE	14	2.02	1.5	N.S.
	POST	14	1.9	1.5	
Rinput (kOhm)	PRE	14	275.64	166.72	N.S.
	POST	14	261.09	94.23	
FRBL (%)	PRE	9	11.36	7.98	N.S.
	POST	9	13.79	10.33	

Table 4.11: Values are means; N.S. - not significant; N - number of tubules. Pre - control; Post - experimental. Cable parameters was measured before and after CCH was introduced into bath. See Table 1 for abbreviations.

	N	Vo	Va	Vbl
Control	9	18.6±9.1	36.8±11.9	-18.2±5.0*
CCH	9	14.7±8.4	34.7±11.9	-20.0±5.9*
Washout	9	20.6±12.8	40.1±15.8	-19.6±5.5*

Table 4.12: All values were expressed in millivolts as means±S.D.. All means not denoted with an * were significantly different (P<0.05).

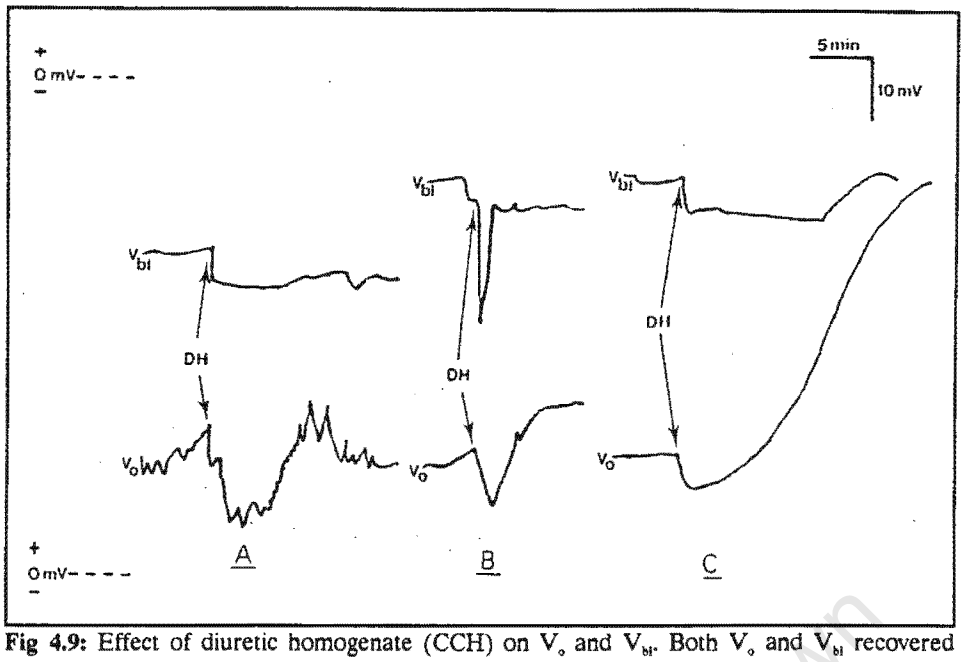

Fig 4.9: Effect of diuretic homogenate (CCH) on V_o and V_{bl}. Both V_o and V_{bl} recovered spontaneously. A, B and C are separate experiments.

4.3.6 Cyclic-AMP

The effects of 1 mM c-AMP on Vo, Vbl and Va in 7 tubules are summarised in table 4.14. Under control conditions Vo, Vbl and Va were 21.4±9.3 mV, -18.4±4.4 mV and 39.9±10.1 mV respectively. The effects of c-AMP were gradual. After the replacing bath Ringers with Ringers containing c-AMP, Vo depolarized and Vbl hyperpolarized to 13.0±9.9 mV ($P<0.01$) and -26.3±5.3 mV ($P<0.005$), respectively, while Va underwent no significant change at 39.3±10.1 mV ($P=0.4$).

The effects of c-AMP were not readily reversible. Upon replacing c-AMP bath Ringers with control bath Ringers Vo ($P=0.5$), Vbl ($P=0.5$) and Va ($P=0.9$) did not change significantly from their experimental condition and both Vo ($P<0.02$) and Vbl ($P<0.05$) remained significantly different from their initial control values (see table 4.14).

Table 4.13 summarizes the effects of c-AMP on the cable parameters. Only 7 in a total of 10 experiments involved intracellular puncture. The pre- and post-experimental means in all of the cable parameters were not significantly different from each other ($P>0.05$).

THE EFFECT (SHORT TERM) OF
CYCLIC AMP
ON Vo AND CABLE PARAMETERS OF THE MALPIGHIAN TUBULE

CABLE PARAMETERS		N	MEAN	±SD	P<
Vo (mV)	PRE	10	18.63	10.84	0.03
	POST	10	12.85	8.80	
LAMBDA (μ)	PRE	10	221.84	147.42	N.S.
	POST	10	231.64	215.11	
Rtrans (kOhm.cm)	PRE	10	4.17	2.46	N.S.
	POST	10	3.92	2.53	
Rcore (MOhm/cm)	PRE	10	25.40	49.94	N.S.
	POST	10	23.64	38.94	
DIAMETER (μ)	PRE	10	32.07	16.28	N.S.
	POST	10	34.38	25.37	
SCCv (μA/cm)	PRE	10	6.0	4.2	N.S.
	POST	10	5.0	3.5	
Rinput (kOhm)	PRE	10	262.71	251.63	N.S.
	POST	10	256.95	228.06	
FRBL (%)	PRE	7	16.88	9.77	N.S.
	POST	7	18.16	12.12	

Table 4.13 Values are means; N.S. - not significant; N - number of tubules. Pre - control; Post - experimental. Cable parameters was measured before and after c-AMP Ringers was introduced into bath. See table 1 for abbreviations.

	N	Vo	Va	Vbl
Control	7	21.4±9.3*	39.9±10.1	-18.4±4.4+
Cyclic-AMP	7	13.0±9.9*	39.3±10.1	-26.3±5.3+
Washout	7	15.14±9.5	40.0±10.5	-24.9±6.9

Table 4.14: All values were expressed in millivolts as means±S.D.. Only values denoted with a * and + were significantly different from each other at P<0.01 and P<0.005 respectively.

The table below summarises the electrical changes across the basolateral membrane in response to either changing the ionic environment in the bathing medium, or to treatments with various drugs:

A SUMMARY OF EFFECTS ON THE BASOLATERAL MEMBRANE POTENTIAL				
BATH RINGERS	N	CONTROL	EXPERIMENT	STATISTICS
HiK	21	-26.4±9.6	-8.1±3.8	P<0.00001
DNP	10	-25.2±10.7	-12±11.43	P<0.005
CFR	16	-19.6±6.9	-33.6±8.9	P<0.00001
cAMP	7	-18.4±4.4	-26.3±5.3	P<0.02
CCH	9	-18.2±5.0	-20.0±5.9	N.S.
$BaCl_2$	5	-21.2±6.9	-32.8±7.7	0.01

Table 4.15: Control and experimental values are expressed as means in millivolts; N is the number of tubules; N.S.,not significant; paired t-tests were used; HiK - 130 mM potassium Ringers; DNP - dinitrophenol; CFR - chloride free Ringers; Cyclic AMP; CCH - diuretic homogenate; $BaCl_2$ - Barium chloride (2 mM).

CHAPTER 5

DISCUSSION

5.1 The tubule's dimensions

Although the dimensions of the Malpighian tubule of *Onymacris plana* allowed for easy mounting of the tubule between the two sets of pipettes, at most times the yellow pigment of the tubule's cells prevented the optical measurement of the diameter of the lumen. The external appearance of the tubule was beaded and the tubule had an external diameter of 138 μm (range: 110-184 μm). Also, no relationship was found between the external diameter of the tubule and the electrically determined lumen diameter.

5.2 Equilibration time

Control studies (see fig. 4.2) showed that Vo and the cable parameters of the *Onymacris plana* tubule were subject to some drift during the first 30 minutes of perfusion but remained stable thereafter. Therefore in most experimental manoeuvres, for example, the addition of a channel blocker to the bathing solution, were carried out at about 30 minutes after perfusion had started.

Often Vo showed superimposed, regular or irregular oscillations. These oscillations were exactly synchronised with contractions of the muscle network surrounding the tubule. Thus the oscillations are in fact muscle action potentials which are superimposed on, but unrelated to the magnitude of Vo.

5.3 Low and high basolateral potential

The basal cell membrane potential was measured as the potential difference between an intracellular microelectrode and a reference electrode in the bath. An example of a

typical impalement potential profile is shown in fig. 4.3. Initially two types of intracellular potentials could be identified: namely, a low potential (-9.6 mV) and a high potential (-23 mV) (see section 4.3.1.1).

A few possibilities existed in interpreting these results. Firstly, the probability that a muscle cell had been impaled could be excluded as it was easy to identify an impaled muscle cell since the intracellular potential oscillated, showing repetitive action potentials which were never steady, and always tended to drift towards zero. Also these potential oscillations could be correlated with contractions of the tubule muscle band by optically observing the contracting tubule while the potential changed.

Secondly, the low potential could have been caused by shunting from ineffective sealing of the cell membrane to the glass wall of the microelectrode. However, gross membrane damage was unlikely as the low potentials were often stable for a time course of two hours or more. Also, membrane damage due to impalement or vibrations was easily distinguishable; during such cases Vbl was seen to drift quite rapidly to close to zero.

Thirdly, the Malpighian tubule of *Onymacris plana* is complicated by the existence of two cell types. Fortunately, the type II cells only make up about 5% of the tubule cells and are much smaller than the primary cells (Nicolson and Isaacson, 1987). Thus the possibility that a different cell type had been penetrated is unlikely.

By chance during one impalement in which a low potential was recorded, gentle tapping of the micromanipulator led to the observation of the second larger and stable intracellular potential. Thereafter, as soon as the low potential stage was encountered, gently tapping or advancement of the micromanipulator was performed resulting in the second larger, stable potential. Further advancement of the microelectrode resulted in the impalement of the lumen and the measurement of the luminal potential, which was the same as the measurement via the perfusion pipet (Vo).

The most plausible explanation of the above was reported by O'Donnell et. al. (1985): they reported that the basal surface of the cells of the Malpighian tubules of *Rhodnius* had a complex array of long basal projections which are parallel to the cell surface under the basement membrane. They also showed that in *Rhodnius* low basal membrane potentials are seen when the microelectrode tip is located in a long projection and that further advancement of the microelectrode resulted in stable and higher potentials. These morphological and experimental findings suggest an explanation for the otherwise puzzlingly low initial intracellular potentials.

5.4 Control Potentials

In the perfused, unstimulated Malpighian tubules of *Onymacris plana*, the cell interior is approximately -21.1 ± 6.8 mV relative to the bathing solution (Vbl) and the transtubular potential (Vo) is 18.5 ± 8.8 mV (lumen positive). The accepted equation for a single layer cellular epithelium is Vo=Va+Vbl; by substituting the above values into this equation we arrive at the following potential profile: Va = 39.6 ± 10.6 mV negative to the lumen; Vo = 18.5 mV (positive with respect to the bath); Vbl = -21.1 mV (negative with respect to the bath). Control basolateral potentials in unperfused tubules were larger at -31 mV while Vo was much more variable at a mean 13.3 mV (range -15 mV to 51 mV) (Nicolson and Isaacson, 1987). Comparisons between insects are difficult at this stage as intracellular measurements in perfused Malpighian tubules of insects have so far only been measured in two other insect species, the yellow fever mosquito (Sawyer, et. al., 1985; Petzel, et. al., 1987; Pannabecker, et. al., 1992) and *Formica polyctena* (Weltens et. al., 1992; Leyssens et. al., 1992). In the yellow fever mosquito the basolateral potential was found to be about -65 mV (i.e. negative with respect to the haemolymph).

5.5 The fractional resistance

Cell punctures along the length of the tubule gave similar values of FRBL%. This was carried out in accord with Frömter (1986) and it showed that there were no significant

cell-to-cell shunts.

The fractional resistance of the basolateral membrane (expressed as a percentage: FRBL%) was determined from the voltage deflection in Vo and Vbl produced by a transepithelial current pulse. Since the sum of the fractional resistances of the apical and basolateral membranes is unity, the fractional resistance of the apical membrane can be calculated from the equation 3.1 (also see appendix C: equation 11).

A fractional resistance of the basolateral membrane of 14% was obtained for the Malpighian tubule of *Onymacris plana*, indicating that under control conditions the conductance of the basolateral membrane is much greater than that of the apical membrane. These observations differ from other reports of FRBL% (Petzel et. al., 1987) in that under control conditions in the yellow fever mosquito a fractional basolateral resistance of 63% was obtained. Thus, in contrast to the Malpighian tubules of the plant eating beetle, *Onymacris plana*, the blood sucking, yellow fever mosquito has a higher conductance across the apical membrane than the basolateral membrane. However, it must be borne in mind that the mosquito tubules secrete a Na^+ rich fluid compared to the beetle's K^+ rich fluid.

The fractional resistance of the basolateral membrane showed a significant increase from 12% (control) to 36% ($p=0.02$) in response to $BaCl_2$ (a K^+ channel blocker). This observation endorsed the view that the basolateral membrane of *Onymacris plana* contains numerous K^+ channels and is highly permeable to K^+. Barium chloride, however, was the only ionic channel blocker, stimulant or ionic permutation that produced a significant change in the FRBL%. It is very likely that significant smaller changes in FRBL% were masked by the recording background noise (noise range: ± 1.0 mV). However, the noise levels varied from day to day so that there were experiments where current induced changes to Vbl of a magnitude of 0.5 mV were easily measured.

5.6 The equivalent electrical circuit

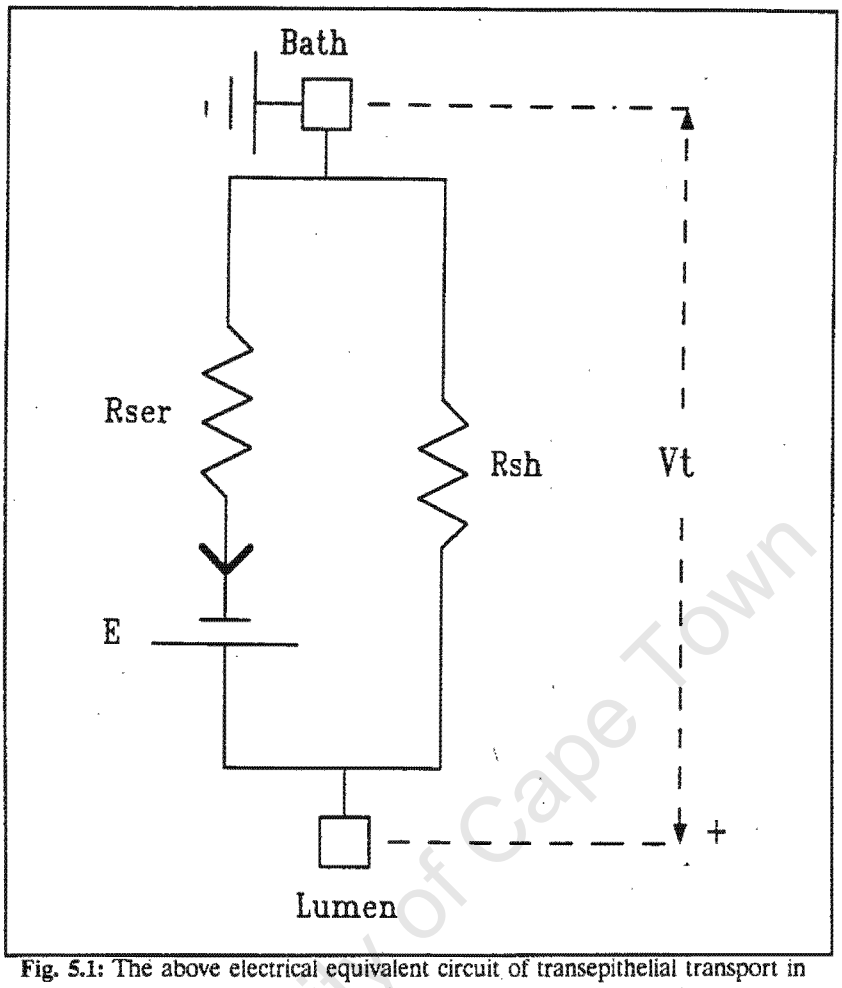

Fig. 5.1: The above electrical equivalent circuit of transepithelial transport in the Malpighian tubules of *Onymacris plana* considers the epithelium a black box across which the transepithelial voltage and resistance are measured. E represents the emf of the transcellular pathway, Rser is the resistance of the transcellular pathway, and Rsh is the resistance of the shunt pathway. Vt is the transepithelial voltage.

The simple equivalent electrical circuit illustrated in figure 5.1 was firstly proposed by Ussing (1951) and applied by Isaacson and colleagues (1989) to the Malpighian tubules of *Onymacris plana*. This equivalent electrical circuit has three components: a battery (E) representing the electromotive force of the active transport mechanism, a series resistance (Rser) encountered by ions within the active transport pathway and Rsh representing the transepithelial leak pathways both transcellular and paracellular for all other ions. Thus Rt, as measured by cable analysis, represents the parallel combination of Rser and Rsh. Vo and SCC can therefore also be expressed in terms of the following equations:

$$Vo = E[\frac{R_{sh}}{R_{sh} + R_{ser}}] \quad (5.1)$$

$$SCC = \frac{E}{R_{ser}} \quad (5.2)$$

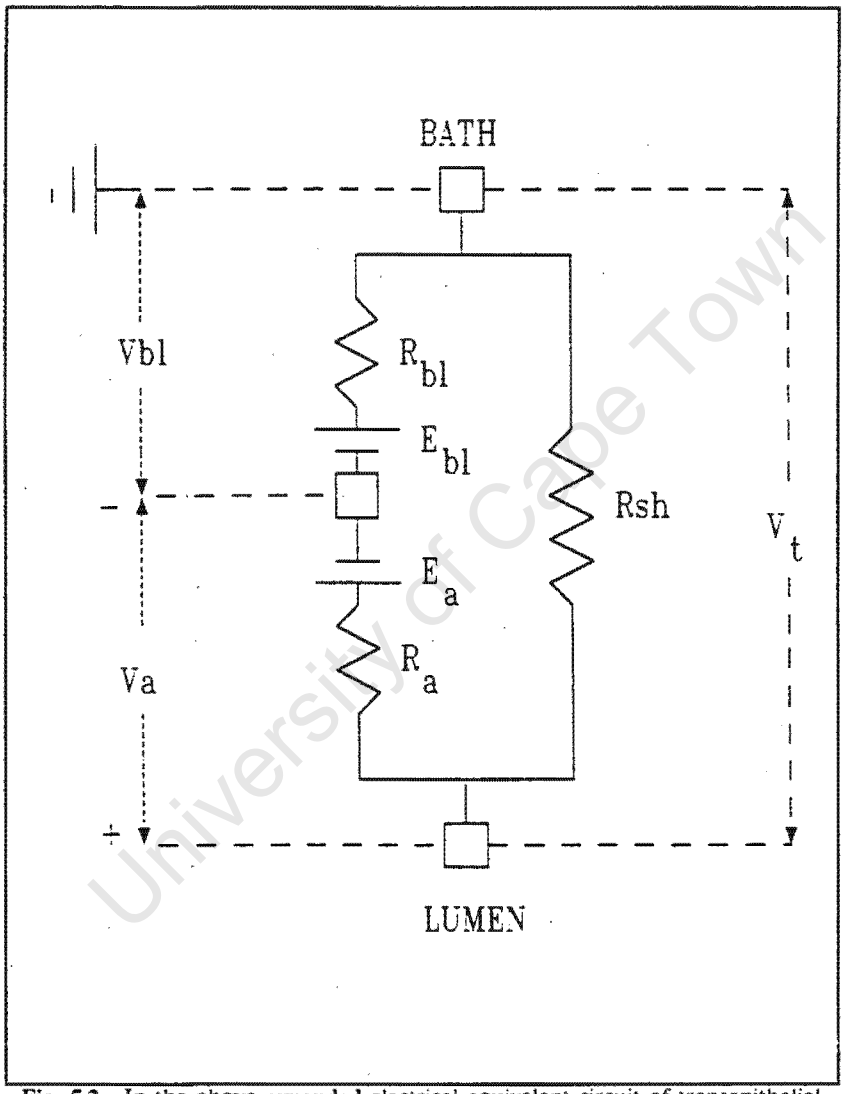

Fig. 5.2: In the above **expanded** electrical equivalent circuit of transepithelial transport in the Malpighian tubules of *Onymacris plana* the transcellular pathway is further divided into emf's (Ea and Ebl) and the resistances (Ra and Rbl) of the apical (a) and basolateral (Bl) membranes. Vt is the transepithelial voltage, while measurements of the voltages across the apical and basolateral membranes, Va and Vbl, were made with intracellular microelectrodes.

The equivalent electrical circuit in figure 5.2 illustrates an expansion of the circuit in figure 5.1. This equivalent electrical circuit is appropriate when measurements of the

apical and basolateral membrane voltages, Va and Vbl respectively, are made with intracellular microelectrodes simultaneously with the measurement of the transepithelial potential (Vo). In the expanded equivalent electrical circuit (fig. 5.2) the transcellular pathway is further divided into the EMF's (E) and resistances (R) of the apical (a) and basolateral (bl) membranes. In this circuit, Rt as measured by cable analysis, represents the parallel combination Ra, Rbl and Rsh. The transepithelial current pulses used in the measurement of Rt give rise to the voltage changes across the epithelium of the tubule at the site of the impalement of the microelectrode (ΔVtx; see appendix C for equation) and across the basolateral membrane (ΔVbl) which are proportionate to their respective resistances. Therefore the fractional resistance of the basolateral membrane can be expressed as follows:

$$FR_{bl} = \frac{\Delta V_{bl}}{\Delta V_{tx}} = \frac{\Delta V_{bl}}{\Delta V_a + \Delta V_{bl}} = \frac{R_a}{R_a + R_{bl}} \qquad (5.3)$$

Vo and SCC (equations 5.1 and 5.2) can now be expressed in the expanded form in equations 5.4 and 5.5:

$$Vo = E[\frac{R_{shunt}}{R_{shunt} + R_a + R_{bl}}] \qquad (5.4)$$

$$SCC = \frac{E}{R_a + R_{bl}} \qquad (5.5)$$

Since only Vo and Rt are measured across the epithelium (fig. 5.2), quantitation of the circuit components is not possible unless one of the values of Rser, E or Rsh can be determined. Although accurate determination of these values is beyond the scope of this study, the components of the expanded equivalent electrical circuit provide valuable insights into the mechanisms of transepithelial transport.

5.7 Validation of cable analysis

The validity of cable analysis on the Malpighian tubule was tested by two different manoeuvres. Initially the ohmic behaviour of the Malpighian tubule was tested. A linear relationship was found between Vo and Io (injected current) that varied from -230 to +230 nA, with a mean input resistance (Appendix C: equation 6) of 241.3 kOhms (see fig. 5.3). The linear relationship between Vo and Io indicated that the forward and backward ionic transepithelial currents did not differ from each other.This is unlike the situation in frog skin and many other epithelia where changes ("breaks") in the slope of an I-V plot frequently occurs (Helman and Fisher, 1977); Helman and Fisher suggested that these changes in the slope are due to differences between the transepithelial resistance to forward and backward ionic transepithelial currents. Accordingly, in the present study all subsequent current pulses injected into the lumen of the tubule were of but one polarity (positive).

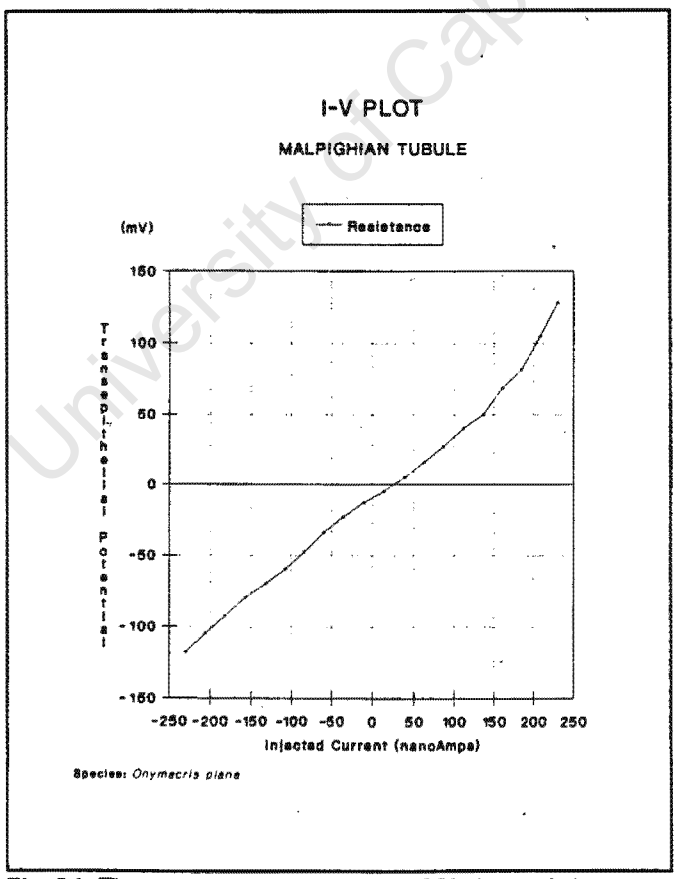

Fig. 5.3: The above graph represents an I-V plot carried out on a (non-stimulated) isolated perfused Malpighian tubule of *Onymacris plana*.

As a second test of validity, cable analysis was used to evaluate the lumen diameter electrically (from the measured value of Rc and the known value of the perfusate resistivity; appendix C: equation 5). Attempts were then made to compare this with the optically determined lumen diameter. However, as pointed out earlier, the lumen of the Malpighian tubule of *Onymacris plana* is not only of highly irregular contour, but very frequently is impossible to visualize. Also, the extensive microvilli of the apical membranes are excluded from the optical lumen diameter measurement (seen as a thick margin of the lumen) whereas in the cable measurements these would diminish the lumen (Rcore) conductance.

Furthermore, no consistent relationship was found between the calculated luminal diameter and the external diameter.

Nevertheless, some strong confirmation of the validity of cable analysis can be seen in the following discussion.

5.8 The effect of tubule contractions on cable analysis

In this study, a change in the size of the lumen diameter, due to the contractions of the surrounding muscle band, influenced the value of the cable derived tubule lumen diameter as well affecting the cable derived values of Vo, Ri, λ, SCC and Rc (see table 4.2). To attempt to understand these changes one should perhaps, firstly, try to comprehend the mechanisms which give rise to these values.

The core resistance, Rc, describes the axial resistance of the tubule i.e. the resistance offered by the luminal contents of the tubule to the flow of current. An increase in Rc indicated that the tubule, as an electrical cable, had become thinner. During contractions Rc increased dramatically from 5.51 to 35.4 MOhm/cm. Rc is also used to obtain the electrically derived luminal diameter (appendix C: equation 5), i.e. Rc is a measure of the resistance to luminal current flow and is inversely proportional to the luminal diameter. Therefore it is not surprising that with an increase in Rc the luminal diameter decreased

from a mean of 36.6μ to 16μ (see table 4.2).

Whenever the tubule contracted Vo increased by ± 6 mV and then returned to base line levels during relaxation. It is difficult to present explanations for the changes in Vo based on ionic fluxes across the Malpighian tubule's epithelium because these changes were uncomplicated by changes in the intrinsic resistance of the tubule wall or in pump activity. i.e. Rtrans and SCCv were not significantly affected by the contraction of the muscle band surrounding the tubule (see table 4.2). A possible explanation is that the muscle network that surrounds the tubule contracts, then squeezes on the tubule and mechanically increases the shunt resistance - in terms of the equivalent circuit of either figure 5.1 or 5.2 this would necessarily increase Vt.

The input resistance (Ri) increased by approximately 50%. This is largely due to the increase in the proximal voltage jump in response to current injection (for formulae see appendix C, 6). The voltage jump, in response to current injection, is primarily effected by Rc (average = 15 MOhm/cm) and secondly by Rt (average = 6.21 kOhm.cm). Thus the increase in Ri was as a result of the increase in Rc and not in Rt, the latter not changing during contractions.

Although Rt remained unchanged the value of the length constant fell, being inversely proportional to Rc. It is of interest to note that although many of the cable parameters changed dramatically SCCv remained quite constant while SCC (μA/cm^2), which is a function of both the active transport and the luminal surface area, decreased significantly during the contraction phase of the experiment. These findings further justify reporting SCCv (μA/cm) rather than SCC (μA/cm^2) as a measure of relative transport across the tubule epithelium in this study (see chapter 4).

Therefore the fall in the electrically calculated value of the lumen diameter accompanying contraction confirms the validity of the use of cable equations. Furthermore, changes in Rc together with the absence of change in SCCv and Rt are consistent with this.

5.9 Comparing Vo with VL

During the entire period of all the perfusion experiments performed during this study, Vo (which is the voltage measured at the proximal end of the tubule) was larger than Vl (which is the voltage measured at the distal end of the tubule). This phenomenon has been reported before (Helman et. al., 1971) and plausible reasons have been provided (Isaacson, et. al., 1989). However, there is a need for these reasons to be reiterated. Firstly, it must be borne in mind that the electrode measuring Vo is placed differently to the electrode measuring Vl. The electrode measuring Vo is the perfusion pipette and measures the potential directly between the lumen and the bath. Secondly, the electrode measuring Vl is placed distal to the insulated portion of the far end of the tubule within the collecting pipette. Thus the Vl recording electrode measures the true Vt minus a potential source of smaller magnitude within the collecting pipette, but of opposite polarity to that within the proximal part of the tubule. The terminal, electrically active, portion of the tubule within the collecting pipette acts as an opposing battery to the electrically active segment of tubule outside the pipette, and therefore the measured potential, Vl, is the summation of these two potentials, i.e. Vt minus the transtubular potential of the tubule distal to the insulated portion of the far end of the perfused tubule. The difference between the recorded Vo and Vl is irrelevant, however, to cable analysis, in which only Vo and the current induced voltage jumps at the proximal and distal ends of the tubule enter into the calculations needed for cable analysis.

5.10 Malpighian Tubules: Potentials and cable parameters

It has been known for some time (Phillips, 1981) that the transport of water across the cells of the Malpighian tubule is linked to the active transport of ions. However, the precise mechanism by which this process occurs has still to be fully worked out and therefore a knowledge of the ionic and electrical gradients across Malpighian tubules is fundamental to an understanding of how these ions and water are transported across the basal and apical membranes. In this study the expanded equivalent electrical circuit is used to attempt to explain the electrical responses of the tubule to various manoeuvres.

5.10.1 The effects of Dinitrophenol (DNP): The drug 2,4-dinitrophenol uncouples oxidative phosphorylation strongly impeding the production of ATP; it also stimulates the hydrolysis of ATP (Conn and Stumpft, 1972). DNP has also been shown to abolish secretion in Malpighian tubules (Pilcher, 1970). Therefore, as a measure of the active transport contribution towards the generation of the transepithelial potential (Vo), DNP was added to the bathing medium. DNP consistently depolarised Vo by an average of 76%, Va by 60% and Vbl by 52% (see table 4.4). These results are consistent with the view that DNP inhibition of the electrogenic pumps within the cell resulted in the apical and basolateral membrane potentials dropping to their ionic diffusion potentials in accordance with the Goldman equation. If the electrogenic pumps are situated only on the apical membrane the data are consistent with the view that the magnitude of Vbl is coupled (by "cross-talk") to the active transport of K^+ across the apical membrane (Ea in fig. 5.2).

In the Malpighian tubules of the Mosquito *Aedes aegypti* (Pannabecker et. al., 1992) DNP caused Vo, Va and Vbl to drop to values close to zero. They also obtained increases in the transepithelial resistance (Rt) (11.4±1.6 KΩ.cm to 16.8±2.2 KΩ.cm), while the FRBL% decreased from 68% to 43%. Using this data they estimated the shunt resistance. However, in the present study Rt and FRBL% underwent no significant changes (see table 4.3) and the membrane potentials did not drop to values close to zero; therefore estimation of the shunt resistance was not possible. The fact that Rt and the FRBL% did not change and that both Va and Vbl did not fall to zero suggest that DNP did not affect the conductive component of the apical or/and the basolateral membrane. The effects of DNP support the hypothesis that the active transport of K^+, and therefore Ea, is the major contributor towards Vt. After the DNP Ringers was replaced with normal bath Ringers, Vt and Vbl failed to recover completely (see fig. 4.5). This was probably due to the cells of the tubule being saturated with DNP and the limited rinsing of the bath with control Ringers so as not to disturb the impaled intracellular electrode. However, Nicolson and Isaacson (1987) reported the complete recovery of transepithelial potential in unperfused tubules (N=4) treated with DNP. Their experimental technique allowed for far more vigorous rinsing of the bath and thus for a more complete removal of DNP, which allowed for a fuller recovery of the transepithelial potential.

5.10.2 The effects of Chloride-free Ringers: The literature (O'Donnell and Maddrell, 1984) suggests that chloride crosses the basolateral membrane against an electrical gradient by means of a cation-anion co-transport mechanism and passively crosses the apical membrane into the lumen in response to a favourable electrical gradient despite an unfavourable chemical gradient. If chloride channels exist in the basolateral membrane and chloride is removed from the bath, then chloride would move down its chemical and electrical gradients from the intracellular compartment into the haemolymph; one would assume (Nernst equation) that the basolateral potential (Vbl) would then decrease; this in turn would increase transepithelial potential (Vo=Va+Vbl).

However, in the present study the introduction of chloride free Ringers (CFR) into the bath caused significant hyperpolarization in Vo, Va and Vbl (see table 4.6), increasing the length constant ($P<0.02$) and the transtubular resistance ($P<0.04$), while causing a drop in the SCCv ($P<0.05$)(see table 4.5).

CFR always rapidly hyperpolarised Vbl with an average of 16 mV and the resultant changes in Vo must be ascribed to changes at both the apical and the basolateral membranes (Vo=Va+Vbl), i.e. if Vo increased from 14.9 mV to 20.9 mV and Vbl hyperpolarised from -19.6 mV to -33.6 mV, then Va was hyperpolarised from 34.3 mV to 54.5 mV [(+21)=(+54)+(-33)].

The hypolarization of Vbl clearly cannot be ascribed to the presence of Cl^--channels in the basolateral membrane (as the polarity of change in Vbl is opposite to that which would be expected), but rather supports the hypothesis that there is a K^+-Cl^- co-transport mechanism operating at the basolateral membrane i.e. on the removal of chloride from the bath, the co-transported K^+ ceases while K^+ continues to be actively pumped across the apical membrane; this would result in the depletion of intracellular K^+. However, the co-transport system clearly does not represent the only means whereby K^+ is transported across the basolateral membrane, as the presence of K^+-channels have been demonstrated (Nicolson and Isaacson, 1990) and strongly endorsed by this study (see $BaCl_2$ and high K^+ sections). Nevertheless, the intracellular supply of K^+ via the

basolateral membrane would be somewhat curtailed by the cessation of K^+-Cl^--co-transport and therefore a (gradual) decrease in the active transport of K^+ across the apical membrane could theoretically be expected. This is supported by the traces of Vo and Vbl which illustrates (fig.4.6 B) that both Vo and Vbl initially increase rapidly in response to CFR, almost spike-like, after which Vo decreases exponentially while Vbl remains constant; this implies that the changes occurring in Vo after CFR are a reflection of changes occurring at the apical membrane. The initial hyperpolarization of Vo and Vbl on the introduction of CFR into the bathing medium probably results because Cl^- ceases to passively cross the apical membrane, while K^+ continues to be pumped across the apical membrane (at a slower and slower rate, however). The SCCv data (see table 4.5), which indicates the transcellular ion transport through the active pathway, showed a decrease of 23.5% ($P<0.05$), which strengthens the latter view.

Any change in Vbl is reflected in Va, and vice versa ("cross talk"), i.e. if Vo hyperpolarises, then so will Va, especially if Ra is much greater than Rbl. It can be seen from figure 5.2 that if Vbl hyperpolarises from -19 mV to -33 mV, then a potential drop is set up across Ra (by virtue of the current running through the circuit via Rsh) - the nett effect would thus be to increase Va, making the lumen more positive. The magnitude of this "cross-talk" depends on the relative magnitudes of Ra and Rbl; if Ra is much greater than Rbl, the effect on Va is large. Similarly, a change in Ea would result in a corresponding change in Vbl.

Nicolson and Isaacson (1987) reported the effects of low-Cl^- bath Ringers (control Cl^- =149 mM; low Cl^-=16.5 mM) on nonstimulated tubules. They found the transepithelial potential to hyperpolarize by 13.8±2.0 mV while Vbl and Va depolarized by 21.4±3.6 mV and ±7 mV respectively. They also found that thiocyanate sodium (10 mM), used to block Cl^- transport across cell membranes in some epithelia, reduced the depolarization of Vbl by 41% (N=3); these effects were reversible. These data seem to indicate the presence of Cl^- channels in the basolateral membrane. A possible explanation for this discrepancy is that in the present study Cl^- was totally excluded from the bathing medium and, if Cl^--channels exist in the basolateral membrane, the absence

of Cl^- in CFR may have changed the transport characteristics of the Cl^--channel as well as the co-transport mechanism, i.e. causing the basolateral membrane's Cl^- channels and co-transport mechanism to cease to function. Support for this view comes from the effects of replacing CFR with control bath Ringers (152 mM Cl^-)(washout: see table 4.6). On washout Va remained unchanged, while Vo depolarized and Vbl hyperpolarized by similar amounts, viz. 4.95 mV and 4.2 mV respectively; thus the change in Vo is a reflection of the change at the basolateral membrane (see table 4.6 and fig. 4.6). The hyperpolarization of Vbl on washout suggests that CFR resulted in changes that were, at least temporarily, not reversible. The postulation of the closure of Cl^--channels in response to CFR is therefore a new one, the mechanism of which is obscure.

According to the expanded electrical equivalent circuit (fig. 5.2) the increased transepithelial resistance and the decreased SCCv support the theory that if chloride is removed from the bath, the resistance of transcellular pathways, Ra and Rbl, will increase as the resistance of these pathways depend largely on the availability of transportable ions.

5.10.3 The effect of High K^+ Ringers: The literature strongly supports the view that in Malpighian tubules active K^+ secretion into the lumen is thought to be primarily responsible for fluid secretion (Maddrell, 1977; Phillips, 1981). Nicolson and Isaacson (1990), using the patch clamp technique, clearly demonstrated the presence of potassium channels in the basal membrane of *Onymacris plana's* Malpighian tubules. In *Onymacris plana* Malpighian tubules (unstimulated) the concentration of K^+ was 187±6 mM in the secreted fluid while the bathing medium contained 25 mM of K^+. Using the patch clamp technique Nicolson and Isaacson (1990) calculated the intracellular K^+ activity to be in the region of 158 mM. These data necessitate the postulation of an active mechanism for the secretion of K^+.

In the present study the Malpighian tubule was perfused with a perfusate containing 130 mM K^+ and bathed in a Ringers containing 15 mM K^+ (control). Treatment with a 130 mM K^+ bathing Ringers (HiK) resulted a sharp increase in the transepithelial potential

(Vo). Measurements with intracellular microelectrodes indicated an initial and rapid depolarization of the basolateral membrane following the elevation of bath potassium concentration (130 mM) (see fig. 4.7). In unperfused tubules depolarization of the basolateral membrane in response to elevated potassium (in the bath) was also reported by Nicolson and Isaacson (1987). From the postulated equivalent circuit (fig 5.2) it is evident that the polarities of the Thèvenin equivalent EMF's (i.e. Ea and Ebl) oppose each other, as well as Va and Vbl. Therefore the nett increase in Vo occurred because the magnitude of the depolarization of Va was less than the magnitude of the depolarization of Vbl (Vt=Va+Vbl)(see table 4.8). The HiK reduced the electrochemical gradient across the basolateral membrane and this caused its depolarization (Nernst equation).

HiK also caused a parallel increase in SCCv (by 54%) while Rt and FRBL% did not significantly change (see table 4.7). The increase in SCCv indicates an increase in the transepithelial active transport of ions (in this case, K^+). The absence of change in Rt or FRBL% suggests that no or minimal change occurred in Ra, Rbl and/or Rshunt.

Therefore, during HiK exposure entry of K^+ across the basolateral membrane occurs chiefly by means of a passive process down an electrical gradient. On the other hand the lumen across the apical membrane is positive (Va=24.6 mV: from Vt=Va+Vbl) relative to the cell interior and the concentration of potassium in the lumen (perfusate = 120 mM K^+) is probably similar to that inside the cell. Therefore, potassium must move against a considerable electrical gradient. This necessitates postulation of an active potassium transport mechanism across the apical membrane. The most likely candidate for this role appears to be the apical vacuolar-type H^+-ATPase which actively pumps H^+ into the lumen and potassium/H^+ antiport which uses the H^+ gradient (lumen to cell) to drive K^+ secretion; this then makes up the components of the K^+ secretion mechanism (Bertram et. al., 1991).

5.10.4 The effect of $BaCl_2$: Barium chloride is a well known K^+ channel blocker. The addition of $BaCl_2$ to the bathing medium provided a convenient means of studying the

role of K^+-channels in the basolateral membrane. The addition of $BaCl_2$ resulted in the rapid depolarization of Vt (see fig. 4.8) along with simultaneous hyperpolarization of Va and Vbl (see tables 4.9 and 4.10). These results were endorsed by Weltens et. al. (1992) in the species *Formica polyctena* where Ba also caused the hyperpolarization of both Va and Vbl. The FRBL% significantly ($p<0.02$) increased (by 183%) in response to $BaCl_2$, while it decreased in response to high K^+ Ringers (bath). The results of FRBL% were also supported by results obtained by Weltens et. al. (1992). These observations confirm the presence of K^+ specific channels in the basolateral membrane. These observations also supports the postulated equivalent circuit diagram: (i) $BaCl_2$ induces an increase in Rbl by blocking the basolateral membrane K^+ channel while intracellular K^+ is being transported across the apical membrane. As K^+ is the primary cation that is transported across the epithelium the interior of the cell would become more negative with respect to the bathing medium (i.e. Vbl would increase). With the concentration of intracellular K^+ dwindling, both the chemical and electrical gradients from the bathing medium across the basolateral membrane would increase, thus contributing to the increase of the basolateral membrane's EMF. (ii) With $BaCl_2$ impeding the entry of K^+ across the basolateral membrane together with the transport of K^+ across the apical membrane, the intracellular concentration of K^+ decreases, culminating in less K^+ transported across the apical membrane; the K^+ chemical gradient (lumen to cell) would decrease and therefore the apical membrane's EMF decreases. (iii) As Vt is the sum of Va and Vbl, it is easy to see why Vt depolarises.

5.10.5 The effect of CCH: The crude homogenate of the corpora cardiaca (CCH) is reported to result in marked stimulation of secretion rates (60-70 nl/min) when added to isolated *Onymacris plana* tubules (Nicolson and Hanrahan, 1986). More recently, Isaacson et. al. (1989) reported a spectrum of Vo responses to CCH and suggested that these varied effects may be due, at least in part, to the influence of biogenic amines released during the disruption of tissue or to the presence of an anti-diuretic factor. A much stronger CCH effect was reported in isolated, unperfused tubules of *Onymacris plana* in which the transepithelial potential decreased by -12.6 ± 5.5 mV ($P<0.001$) (Nicolson and Isaacson, 1987). The present study supported the latter report (see tables 4.11 and 4.12)

in which the majority of responses resulted in a decrease in Vo ($P<0.001$). However, there were occasions when either no response or a slight increase in Vo was measured. Although CCH significantly decreased Vo no significant effects on the other cable parameters was seen.

CCH had no significant effect on Vbl (see table 4.12 and fig. 4.9). The hyperpolarization of Va occured in parallel with the depolarization of Vo. This indicated that CCH brings about an increase in secretion by affecting mechanisms at the apical membrane. Although no significant changes occurred in any of the cable parameters in this study Isaacson et. al. (1989) found a significant decrease in Rt ($P<0.001$) and Rc ($P<0.01$) accompanied by a parallel increase luminal diameter, as calculated by cable analysis. The mean changes in Rt, Rc and luminal diameter in the present study (see table 4.11), though not significant ($P>0.05$), showed the same trends. The increase in luminal diameter and parallel decrease in Rc are indicative of the CCH induced increased fluid secretion while the fall in Rt implies a fall in Rt and/or Rsh.

The only clear indication to the mechanism by which CCH induces fluid secretion is that it is located at the apical membrane. In terms of the postulated equivalent circuit, the hyperpolarization of Va indicates an increase in Ea; however, it is not clear from the literature or the present study's data whether Ra, Rbl or/and Rsh is responsible for the fall in Rt.

5.10.6 The effect of Cyclic-AMP: Nicolson and Isaacson (1987) reported the dramatic increase of Vo in response to 1 mM cAMP. These effects of cAMP were almost immediate (1-3 minutes) and attained peak values at 24±7 minutes. The present study addressed the short term effects (10-15 minutes) of c-AMP. Cyclic-AMP significantly decreased both Vo and SCCv (see table 4.13).

However, the long term effects (20-30 minutes) of c-AMP (Isaacson, Nicolson and Fisher, 1989) resulted in increases in Vo, SCCv (almost 5-fold) and the luminal diameter with concomitant decreases in Rtrans and Rcore (see table 5.1). The decrease in Rt appears

to indicate that c-AMP increases the transport of ions across the tubule by increasing the permeability of the tubule. Whether the increase in permeability occurs at the level of the apical, the basolateral membrane or both remains to be investigated at a later date. The decrease in Rc indicates a larger lumen diameter which in turn is indicative of increased fluid secretion. These results support the view that c-AMP acts as an intermediate in a chain of events which gives rise to the stimulation of fluid transport.

In terms of the simple equivalent electrical circuit (fig. 5.1), exposure to cAMP (see table 5.1) resulted in SCCv increasing almost fivefold while Vo increased but threefold, a pattern of change which may be interpreted as a fall in Rser. This interpretation is consistent with the fall observed in Rt, the data presenting no cogent reasons to postulate major changes in Rsh or E.

EFFECT (LONG TERM) OF CYCLIC-AMP ON Vo AND CABLE PARAMETERS

CABLE PARAMETERS		N	MEAN	±SD	P<
Vo (mV)	PRE	17	13.7	10.3	0.001
	POST	17	38.1	17.8	
LAMBDA (μ)	PRE	17	294	125	0.05
	POST	17	353	151	
Rtrans (kOhm.cm)	PRE	17	7.77	3.66	0.001
	POST	17	4.76	2.77	
Rcore (MOhm/cm)	PRE	17	13.76	13.14	0.001
	POST	17	7.94	10.27	
DIAMETER (μ)	PRE	17	29.5	11.4	0.005
	POST	17	51.2	31.8	
SCC_v (μA/cm)	PRE	17	2.1	1.8	0.001
	POST	17	9.8	5.2	
Rinput (kOhm)	PRE	17	302	108	0.001
	POST	17	179	106	

Table 5.1: Taken from Isaacson L., S. Nicolson and D. W. Fisher, (1989). The above c-AMP results were obtained in collaborated paper which culminated in the fore mentioned article. N.S. - not significant (P>0.05); N - number of tubules. Pre - control; Post - experimental. Cable parameters was measured before and after c-AMP was introduced into bath. See Table 1 for abbreviations.

5.11 GENERAL CONCLUSION:

The study endorsed the view that the cells of the Malpighian tubules of *Onymacris plana* use the transport of K^+ as a means to drive fluid secretion and further confirmed the view that K^+ secretion was largely, if not entirely, an active process requiring the presence of ATP. This was substantiated by adding DNP to the bathing solution which resulted in the immediate decrease in Vo, Va and Vbl. Furthermore, decreasing the concentration of K^+ in the bath resulted in a decrease in Vo while $BaCl_2$ (a specific channel blocker for K^+), when added to the bath, resulted in a decrease in Vo while both Va and Vbl were hyperpolarized. $BaCl_2$ experiments provided additional evidence that the basolateral membrane was highly conductive to K^+. This was demonstrated by a threefold increase of the FRBL% in response to $BaCl_2$. Increasing the concentration of K^+ in the bath caused a rapid drop in Vbl indicating a high K^+ conductance across the basolateral membrane.

The apical membrane was clearly shown to be much less conductive than the basolateral membrane. This was clearly illustrated in figure 4.4 which shows the large difference between the potential jumps across the apical and basolateral membranes in response to current injection into the lumen. This is contrary to the situation in *Aedes aegypti* where the apical membrane is much more conductive than the basolateral membrane.

The effects of Chloride-free Ringers seems inexplicable in the light of today's knowledge, however, a plausible mechanism provides an attempt to explain the data. Chloride appears to be co-transported with K^+ across the basolateral membrane and is presumably passively transported across the apical membrane. It is for this reason that Cl^- availability in the haemolymph appears to have an indirect role to play in fluid secretion, i.e. if Cl^- is absent from the bathing fluid the K^+-Cl^- co-transport ceases - therefore the intracellular concentration of K^+ decreases - and thus the substrate for the "K^+ apical pump" decreases (i.e. a decrease in Ea) and the apical potential decreases.

CCH had a varied response. However, in this study CCH appears, in some way, to induce a mechanism by which fluid secretion is increased. The fact that Vo but not Vbl was effected,

implies that an apical mechanism was responsible for an increase in fluid secretion.

In the literature most insects appear to have at least 2 diuretic hormones (Spring, 1990). In this study a crude diuretic homogenate (CCH) was used to illicit an electrical response. It was not surprising to obtain a varied response after so many factors had been introduced into the medium bathing the tubule. The effects of purified, isolated diuretic hormones would be of great interest. Initial work in this area has shown that only 2 HPLC fractions bore any significant response, both of which caused diuresis (Nicolson, 1991).

The apical vacuolar-type H^+-ATPase which actively pumps H^+ into the lumen and K^+/H^+ antiport which uses the H^+ gradient (lumen to cell) to drive K^+ secretion into the lumen is the probable mechanism which in turn drives fluid secretion in *Onymacris plana* (Bertram et. al., 1991). Nicolson (unpublished results) has already shown in a closely related species (*Onymacris rugatipennis*) vacuolar-ATPase inhibitor (Bafilomycin A_1) stops fluid secretion, which supports the above postulated mechanism for *Onymacris plana*. The figure below summarises the postulated model for ionic transport in the Malpighian tubule's of *Onymacris plana*.

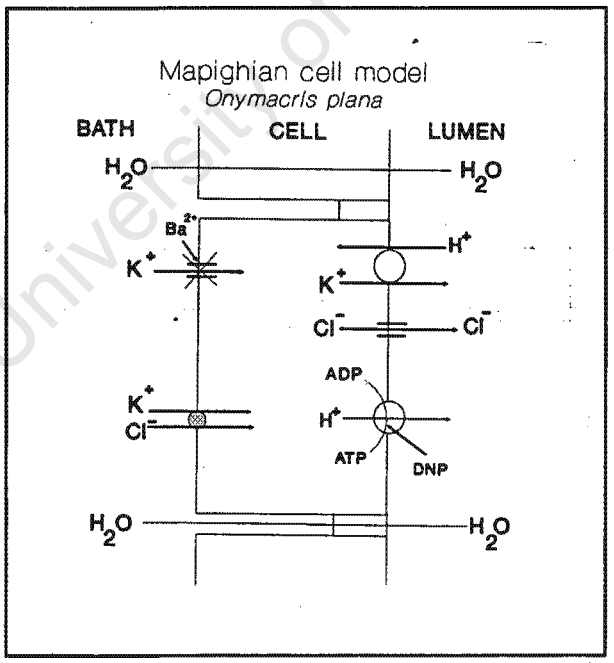

Fig.5.4: Transport model of transepithelial ionic transport in *Onymacris plana*. For further explanation see GENERAL CONCLUSIONS.

* REFERENCES *

* APPENDIXES *

REFERENCES

Aneshansley, D. E., Marler, C. E. and Beyenbach, K. W. (1988): Transepithelial voltage measurements in isolated Malpighian tubules of *Aedes Aegypti*. J. Insect Physiol. 35 (1): 41-52.

Baldrick, P., Hyde, D. and Anstee, J. H. (1988): Microelectrode studies on Malpighian tubule cells of *Locusta migratoria*: Effects of external ions and inhibitors. J. Insect Physiol. 34 (10): 963-975.

Berridge, M. J. and Prince, W. T. (1972): Transepithelial potential changes during stimulation of isolated salivary glands with 5-hydroxytryptamine and cyclic AMP. J. Exp. Biol. 56, 139-153.

Berridge, M. J. and Oschman, J. L. (1969): A structural basis for fluid secretion by Malpighian tubules. Tissue cell. 1: 247-272.

Berridge, M. J. (1977): Insect Malpighian tubules. In Transport of Ions and Water in animals. (Ed. by B. L. Gupta, R. B. Moreton, J. L. Oschman and B. J. Wall). Academic Press, London. 541-569.

Bertram, G., Schleithoff, L., Zimmerman, P. and Wessing, A. (1991): Bafilomycin A_1 is a potent inhibitor of urine formation by Malpighian tubules of *Drosophila hydei*: is a vacuolar-type ATPase involved in ion and fluid secretion? J. Insect Physiol. Vol. 37, No. 3, pp. 201-209.

Burg, M. B., Isaacson, L. C., Grantham, J. and Orloff, J. (1968): Electrical properties of isolated perfused rabbit renal tubules. Am. J. Physiol. 215: 788-794.

Burg, M. B., Grantham, J., Abramow, M. A. and Orloff, J. (1966): Preparation and study of fragments of single rabbit nephrons. Am. J. Physiol. 210: 1293-1298.

Conn E. E. and Stumpf, P. K. (1972): Outlines of Biochemistry, 3rd. ed., John Wiley and Sons, INC., New York, pp. 327-328.

Edney, E. B. (1977): Water balance in land Arthropods. New York: Springer-Verlag.

Frizzel, R. A., Field, M. and Schultz, S. G. (1979): Sodium-coupled chloride transport by epithelial tissues. Am. J. Physiol. 236 (Renal Fluid Electrolyte Physiol. 5): F1-F8.

Frömter, E. (1986): The electrophysiological analysis of tubular transport. Kidney Int. 30: 216-228.

Gee, J. D. (1976): Fluid secretion by the Malpighian tubules of the tsetse fly, *Glossina morsitans*: the effects of ouabain, ethacrynic acid and amiloride. J. Exp. Biol. 65: 323-332.

Greger, R. and Schlatter, E. (1983): Properties of the lumen membrane of the cortical thick ascending limb of Henle's loop of rabbit kidney. Pflügers Arch. 396: 315-324.

Hanrahan, S. A. and Nicolson, S. W. (1987): Ultrastructure of the Malpighian tubules of *Onymacris plana plana Peringuey* (Coleoptera: Tenebrionidae). Int. J. Insect Morphol. & Embryol. 16: 99-119.

Helman, S. I. (1972): Determination of the electrical resistance of the isolated cortical collecting tubule and its possible anatomical location. Yale J. Biol. Med. 45, 339-345.

Helman, S. I. and Thompson, S. M. (1982): Interpretation and use of electrical equivalent circuits in studies of epithelial tissues. Am. J. Physiol. 243 (Renal Fluid Electrolyte Physiol. 12): F519-F531.

Helman, S. I., Grantham, J. J. and Burg, M. B. (1971): Effect of vasopressin on electrical resistance of renal cortical collecting tubules. Am. J. Physiol. 220: 1825-1832.

Helman, S. I and Fisher, R. S. (1977): Microelectrode studies of the active Na transport pathway of frog skin. J. Gen. Physiol. 69: 571-604.

Isaacson, L. C. and Nicolson, S. W. (1989): A reappraisal of the oil gap technique for the measurement of transtubular potentials in insect epithelia. J. Exp. Biol. 141: 429-440.

Isaacson, L. C., Nicolson, S. W. and Fisher, D. W. (1989): Electrophysiological and cable parameters of perfused beetle Malpighian tubules. Am. J. Physiol. 257 (Regulatory

Integrative Comp. Physiol. 26): R1190-R1198.

Kay I., Coast, J. M., Cusinato, O., Wheeler, C. H., Totty, N. F., and Goldworthy, G. J. (1992): Isolation and characterization of a diuretic peptide from *Acheta domesticus*: Evidence for a family of insect diuretic peptides. Biol. chem. Hoppe-Seyler, 372: 505-512.

Lapointe, J-Y., Laprade, R. and Cardinal, J. (1984): Transepithelial and cell membrane electrical resistances of the rabbit proximal convoluted tubule. Am. J. Physiol. 247 (Renal fluid electrolyte physiol. 16): F637-F649.

Leyssens, A., Steels, P., Lohrmann, E., Weltens, R., Van Kerkhove, E.(1992): Intrinsic regulation of K^+ transport in Malpighian tubules (*formica*): Electrophysiological evidence. J. Insect Physiol. Vol. 38, No. 6, pp. 431-446.

Maddrell, S.H.P. and O'Donnell, M. J. (1992): Insect Malpighian tubules: V-ATPase action in ion and fluid transport. J. Exp. Biol. (in press).

Maddrell, S. H. P. (1971): The mechanisms of insect excretory systems. Adv. Insect physiol. 8: 199-331.

Maddrell, S. H. P. (1977): Insect Malpighian tubules. In "Transport of Ions and Water in Animal Tissues" (B. L. Gupta, R. B. Moreton, J. L. Oschman, and B. J. Wall, eds.), pp. 541-569. Academic Press, New York.

Maddrell, S.H.P. and Overton, J. A. (1988): Stimulation of sodium transport and fluid secretion by ouabain in an insect malpighian tubule. J. Exp. Biol. 137, 265-276.

Bradley, T. J. (1985): The excretory system: structure and physiology. In: Comprehensive insect Physiology, Biochemistry and Physiology, edited by G. A. Kerkut and L. I. Gilbert. Oxford, UK: Pergamon, vol. 4 pp. 421-465.

Morgan, P. J. and Mordue, W. (1983): Electrochemical gradients across *Locusta* Malpighian tubules. J. Comp. physiol. 151:175-183.

Nicolson, S. W. and Isaacson, L. C. (1990): Patch clamp of the basal membrane of beetle Malpighian tubules: Direct demonstration of potassium channels. J. Insect Physiol. Vol. 36, No 11, pp. 877-884.

Nicolson, S. W. and Hanrahan, S. A. (1986): Diuresis in a desert beetle? Hormonal control of the Malpighian tubules of *Onymacris plana* (Coleoptera: Tenebrionidae). J. comp. Physiol. B. 156: 407-413.

Nicolson, S. W. (1991): Diuresis or clearance: Is there a physiological role for the "diuretic hormone" of the desert beetle *Onymacris*? J. Insect Physiol. Vol. 37, No 6, pp. 447-452.

Nicolson, S. W. and Isaacson, L. C. (1987): Transepithelial and intracellular potentials in isolated Malpighian tubules of tenebrionid beetle. Am. J. Physiol. 252: F645-F653.

O'Donnell, M. J. and Maddrell, S. H. P. (1984): Secretion by the Malpighian tubules of *Rhodnius prolixus* Stal: Electrical events. J. Exp. Biol. 110: 275-290.

O'Donnell, M. J., Maddrell, S. H. P., Skaer, H. LE. B. and Harrison, J. B. (1985): Elaborations of the basal surface of the cells of the Malpighian tubules of an insect. Tissue and Cell 17 (6): 865-881.

O'Donnell, M. J. and Machin, J. (1991): Ion activities and electrochemical gradients in the mealworm rectal complex. J. Exp. Biol. 1555: 375-402.

Pannabeker, T. L., Aneshansley, D. J. and Beyenbach, K. W. (1992): Unique electrophysiological effects of dinitrophenol in Malpighian tubules. Am. J. Physiol. (in press).

Petzel, D. H., Hagedorn, H. H. and Beyenbach, K. W. (1985): Preliminary isolation of mosquito natriuretic factor. Am. J. Physiol. 249: R379-R386.

Petzel, D. H., Berg, M. M. and Bayenbach, K. W.(1987): Hormone-controlled cAMP-mediated fluid secretion in yellow-fever mosquito. Am. J. Physiol. 253 (Regulatory Integrative Comp. Physiol. 22): R701-R711.

Phillips, J. E. (1981): Comparative physiology of insect renal function. Am. J. Physiol. 241 (Renal fluid electrolyte physiol. 10): R241-R257.

Phillips, J. E. (1983): Endocrinology of Insects: Endocrine control of salt and water balance: Excretion. Chpt.2, 411-425.

Pilcher, D. E. M. (1970): The influence of diuretic hormone on the process of urine secretion by the Malpighian tubules of *Carausius morosus*. J. Exp. Biol. 53: 465-484.

Purves, R. D. (1981): Microelectrode methods for intracellular recording and ionophoresis. Academic Press INC. (London) LTD. 24-28 Oval Rd., London NW1.

Ramsay, J. A. (1954): Active transport of water by the Malpighian tubules of the stick insect, *Dixippus morosus* (Orthoptera, Phasmidae). J. Exp. Biol. 31: 104-113.

Sawyer, D. B. and Bayenbach, K. W. (1985): Dibutyryl-cAMP increases basolateral sodium conductance of mosquito Malpighian tubules. Am. J. Physiol. 248 (Regulatory Integrative Comp. Physiol. 17): R339-R345.

Spring, J. F. (1990): Endocrine regulation of diuresis in insects. J. Insect Physiol. 36 (1): 13-22.

Stobbart, R. H. and Shaw, J. (1974): Salt and water balance: Excretion. In *The Physiology of Insecta* 2nd ed., Vol. V. M. Rockstein (Ed.). Academic Press, New York, pp. 361-446.

Taylor, R. E. (1963): Cable theory: In: Physical Techniques in Biological Research, edited by Nastuk W. L., New York, Academic Press, vol 6/B: 219-262.

Ussing, H. H. and K. Zerahn (1951): Active transport of sodium as the source of electric current in the short-circuited isolated frog skin. Acta Phys. Scandinav. 23: 110-127.

Weltens, R., Leyssens, A., Zhang, S.L., Lohrmann, E., Steels, P., Van Kerkhove, E. (1992): Unmasking of the Apical Electrogenic H Pump in isolated Malpighian tubules (*Formica polyctena*) by the use of Barium. Cell Physiol Biochem; 2: 101-116.

Wessing, A. and Eichelberg, D. (1969): Elektronoptische untersuchungen an den nierentubuli (Malpighian gefasse) von *Drosophilia melanogaster*. 1. Regionale gliederung der tubuli. Z. Zellforsch. Mikro. Anat. 101: 285-322.

Wigglesworth, V. B. and Salpeter, M. (1962): Histology of the Malpighian tubules in *Rhodnius prolixus* Stål (Hemiptera). J. Insect Physiol. 8: 299-307.

Williams, J. C. JR. and Beyenbach, K. W. (1984): Differential effects of secretagogues on the electrophysiology of the Malpighian tubules of the yellow fever mosquito. J. Comp. Physiol. B. 154: 301-309.

Wright, J. M. and Beyenbach K. W. (1987): Chloride channels in apical membranes of mosquito Malpighian tubules. Fed. Proc. (Abstract) 46:347.

* APPENDIXES *

APPENDIX A

Apple program:

The following Apple specific computer program was designed by L.C. Isaacson and modified by D.W. Fisher. The main features of the program were the following:

1. The program monitored the potential differences (in millivolts) in Vo, Vl and VBL, and also determined the current injected (in nanoAmps) (Io).

2. Enabled the user to monitor and input current (in nanoAmps) injection via the A/D Mountain card and also measured the current clamp duration time (approximately 600 ms ; see chapter 2 and appendix B).

3. The program was able to carry out a series of current clamps, and provided the options for these data to be plotted and printed as an I-V plot.

4. The program recorded the changes in Vo, VL, VBL and Io which resulted from current injection.

5. Given the perfusate's specific resistivity (measured with a conductivity meter - Zoology department, UCT) the program would calculate the transtubular resistance (Rt), the core resistance (Rc), the input resistance (Ri), the short circuit current (SCCv) and the calculated luminal diameter, immediately after each single current clamp.

6. At the end of a single or multiple current clamp the options of printing, saving or returning to the main menu could be selected.

APPLE II PROGRAM PRINTOUT:

```
10  REM  ...CABLI..
20  REM  ..TUBULE CURR.CLAMP...
30  REM  ..FOR CABLE PARAMETRS,
40  REM ..& INTRACELL. PD.
50  REM .MOUNTAINCARD A/D-D/A
60  REM   ... IN SLOT 2 ..
70  REM .ADDR=49280+SLOT NO.*16
80  REM ...+ CHANNEL NO.
90  REM ..D/A NEEDS 2V OUTPUT
100 REM ..VO=PROX.TUB.(PIA) PD
110 REM ..VL=DISTAL TUB.PD
120 REM  ..VI=INTRACELL.PD
130 REM  ..I=CLAMP CURRENT
140 REM  ..VO -8 TO 120 MV
150 REM ..VL -8 T0 120 MV
160 REM ..VI -100 TO 28 MV
170 CLEAR : HOME
180 SLOT =  4 :  REM .. CLOCK
190 ON ERR  GOTO 1060
200 FOR I = 770 TO 790: READ J: POKE I,J: NEXT
210 DATA  173,48,192,136,208,5,206,l,3,240,9,202,208,
      245,174,0,3,76,2,3,96
220 REM  ..SLOT 2=D/A
230 REM ..CLAMP SWITCHED ON/OFF
240 REM   .BY ANNUNCIATOR 3
250 POKE   -16289,0: REM  ..OFF
260 HP  =  1 : PN$  =  "CABLI " :  GOSUB  4920
270 D$  =  " " :    REM  CTRL  D
280 C$  =  " " :    REM  . .CTRL-C
290 Q$  =  " " :    REM  . . . CTRL-Q
300 CC = 0
310 DIM N(80),VO(80),VL(80),VI(80),I(80)
320 REM  ======INITIALISE===
330 IF  PEEK (800) <  > 0 GOTO 380
340 POKE 800,2: POKE 801,28: REM ...TL
```

```
350  POKE 803,120: REM  O.D
360  POKE 804,24: POKE 805,21: REM ...RE
370  POKE 806,0: POKE 807,100: REM ...PS
380  AD = 49312: POKE 49312,128
390  IF CC = 0 GOTO 1060: REM ...MENU
400  IF NN > 20 GOTO 1060
410  HOME:N = 0:NN = 0:N1 = 0
420  REM --------A/D INPUT---
430  IF N < 3 GOTO 490
440  SA  =  AG  +  NN  *  Q2
450  IF N = 3 THEN  GOSUB 1390 : T1$  =  T$
460  POKE  -16290,1
470  POKE  49312, SA
480  FOR T = 1 TO 120: NEXT
490  N = N + 1
500  FOR C = 0 TO 3
510  X = PEEK (49312 + C)
520  X = PEEK (49312 + C)
530  IF C = 0 THEN VO(N) = X
540  IF C = 1 THEN VI(N) = X
550  IF C = 2 THEN VL(N) = X
560  IF C = 3 THEN I(N) = X
570  NEXT C
580  IF N <  > (3 + N1) GOTO 490
590  GOSUB 1390:T2$ = T$
600  POKE  - 16289,0
610  POKE 49312,128
620  POKE 768,P: POKE 769,D: CALL 770
630  IF NN <  > 1 THEN  PRINT : PRINT :  GOTO  710
640  T1 =  VAL(MID$(T1$,13,6))
650  T2 =  VAL(MID$(T2$,13,6))
660  DT =  INT ((T2 - T1) * 1000)
670  REM      --------VDU------
680  PRINT : PRINT
690  DT = INT (DT)
700  PRINT  DT ; "  MSEC  CLAMP "
710  PRINT  "CLAMP  " ; NN ; " : "
720  HTAB 6
730  PRINT TAB(9);"VO";TAB (18);"VL";TAB(27);"VI";
       TAB(35); "I"
740  REM  ===CONVERT  A/D====
750  FOR T = (N1 + 1) TO N
760  VO(T) = -INT((VO(T)-240)*5)/10
770  VI(T) = -INT((VI(T)-56)*2.5)/10
780  VL(T) = -INT((VL(T)-240)*5)/10
780  I(T) = INT(I(T)-128)*100/64)
800  REM----------------------
810  REM  BV=BATH MV JUMP/100 NA
820  BV = .85
```

```
830  MI =  INT (.5 + (BV * I(T) / 10)) / 10
840  VL = VL(T) - MI
850  VL(T) = VL
860  VO = VO(T)
870  VI = VI(T) - MI
880  VI(T) = VI
890  PRINT TAB(9);VO;TAB(18);VL;TAB(27);VI;TAB(35);I(T)
900  NEXT
910  NI  =  N
920  REM   ===INTERCLAMP LAG===
930  FOR T = 1 TO 2: NEXT
940  NN = NN + 1
950  IF NN > 1 AND SC = 1 GOTO 980
960  P = 90 - NN  * 3
970  IF NN > 20 THEN POKE AD,128: GOTO 1060
980  GOTO 430
990  HTAB 1: VTAB 23
1000  PRINT  "MENU   0R  LENGTH  CONST. ( M/L ) ? : " ;
1010  GET Z$
1020  IF Z$  <   >  "M " AND  Z$  <  > "L" GOTO  1010
1030  IF Z$ = "M" GOTO  1060
1040  IF Z$  = "L" GOTO  3650
1050  REM  --------MENU-----
1060  POKE - 16289,0
1070  POKE 49312,128
1080  HOME:CC = 0:SC = 0:FL = 0
1090  HTAB 8
1100  PRINT "TUBULE CURRENT CLAMP"
1110  HTAB 8
1120  PRINT  " ------------------"
1130  PRINT : PRINT "SELECT:"
1140  HTAB 9: VTAB 4
1150  PRINT "1) SAVE I/V FILE"
1160  HTAB 9: VTAB 6
1170  PRINT  "2) LOAD I/V  FILE"
1180  HTAB 9: VTAB 8
1190  PRINT "3) LIST  I/V  DATA"
1200  HTAB 9: VTAB 10
1210  PRINT  "4) CURRENT CLAMP"
1220  HTAB 9: VTAB 12
1230  PRINT  " 5) I/V PLOT"
1240  HTAB 9: VTAB 14
1250  PRINT  "6) A/D MONITOR"
1260  HTAB 9: VTAB 16
1270  PRINT "7) LENGTH CONSTANT"
1280  HTA8 9: VTAB 18
1290  PRINT  " 8) EXIT"
1300  HTAB 9: VTAB 20
1310  PRINT  " 9) INPUT  PARAMETERS"
```

```
1320  HTAB 30: VTAB 23
1330  PRINT  "WHICH ?";
1340  GET A$: IF VAL (A$) < 1 OR VAL (A$) > 9 GOTO 1340
1350  A = VAL (A$): HOME
1360  ON A GOTO 1470,1900,2090,2320,2620,3150,3420,1370,4960
1370  HOME : END
1380  REM ---TIMER SUBROUTINE--
1390  PRINT D$ ;"NOMON C,I,O":VTAB PEEK (37): CALL - 868
1400  PRINT D$ ; " IN#" ; SLOT
1410  PRINT  D$; "PR#" ; SLOT
1420  INPUT  "    " ; T$
1430  PRINT  D$ ; "IN#O"
1440  PRINT  D$ ; "PR#O
1450  RETURN
1460  REM  ----SAVE TO DISC---
1470  HOME
1480  IF N = 0 GOTO 1060
1490  INPUT "FILE NAME?" ;F$
1500  GOSUB 1390 : REM GET TIME
1510  GOSUB 1710: REM  FIND DATE
1520  PRINT  D$ ; "OPEN" ; F$
1530  PRINT   D$ ; "DELETE" ; F$
1540  PRINT  D$ ; "OPEN" ; F$
1550  PRINT  D$; "WRITE" ;F$
1560  PRINT F$
1570  PRINT T1$
1580  PRINT N
1590  FOR R = 1 TO N
1600  PRINT VO(R)
1610  PRINT VL(R)
1620  PRINT VI(R)
1630  PRINT  I(R)
1640  NEXT R
1650  PRINT D$ ; "CLOSE " ; F$
1660  PRINT : PRINT
1670  PRINT  "FILE  ** " ; F$ ; " ** NOW  ON  DISC"
1680  FOR T = 1 TO 2000: NEXT
1690  GOTO 1060: REM TO MENU
1700  REM      ------------DATE---
1710  MTH$=LEFT$(T$,2):DAY$=MID$(T$,4,2):MTH=VAL (MTH$)
1720  IF MTH = 1 THEN MTH$ = "JAN"
1730  IF MTH = 2 THEN MTH$ = "FEB"
1740  IF MTH = 3 THEN MTH$ = "MAR"
1750  IF MTH = 4 THEN MTH$ = "APR"
1760  IF MTH = 5 THEN MTH$ = "MAY"
1770  IF MTH = 6 THEH MTH$ = "JUN"
1780  IF MTH = 7 THEN MTH$ = "JUL"
1790  IF MTH = 8 THEN MTH$ = "AUG"
1800  IF MTH = 9 THEN MTH$ = "SEP"
```

```
1810  IF MTH = 10 THEN MTH$ = "OCT"
1820  IF MTH = ll THEN MTH$ = "NOV"
1830  IF MTH = l2 THEN MTH$ = "DEC"
1840  G$ = DAY$  +  " "  +  MTH$  +  " " +  "1990"
1850  H$ =  MID$ (T$,7,5)
1860  TI$ = G$ + " " + H$ + " " + "HRS"
1870  T2$ = H$ + " " + "HRS"
1880  RETURN
1890  REM  -- --LOAD DISC FILE--
1900  HOME
1910  INPUT  "FILE NAME ?" ;F$
1920  PRINT D$;"NOMON C,I,O"
1930  PRINT D$ ;"OPEN " ; F$
1940  PRINT D$ ="READ" ;F$
1950  INPUT F$: INPUT TI$: INPUT N
1960  PRINT : PRINT
1970  PRINT F$
1980  PRINT T1$
1990  PRINT
2000  FOR R = l T0 N
2010  INPUT VO(R): INPUT VL(R): INPUT VI(R)
2020  NEXT R
2030  PRINT D$ ; " CLOSE " ; F$
2040  HTAB l: VTAB 22
2050  PRINT "FILE  ** " ; F$ ; "  **  LOADED "
2060  FOR T = l TO 1500: NEXT
2070  GOTO 1060
2080  REM  ----------LIST---
2090  HOME :PP = 0
2100  PRINT  "FILE NAME : " ; F$
2110  GOSUB 1710
2120  PRINT  "DATE : " ;G$
2130  PRINT  "TIME : " ; T2$
2140  VTAB 7: HTAB 6
2150  PRINT "V-PROX";SPC(3);"V-DIST";SPC(5);"VI";SPC(7);"I"
2160  FOR R = 3 TO N STEP 3
2170  HTAB 9: PRINT VO(R);
2180  HTAB 18: PRINT VL(R);
2190  HTAB 27:PRINT VI(R);
2200  HTAB 35: PRINT I(R)
2210  NEXT
2220  PRINT:PRINT"================================="
2230  PR#0
2240  IF PP = 1 THEN PP = 0: GOTO 1060
2250  HTAB l
2260  PRINT "PRINT-OUT OR MENU (P/M )  ? " ;
2270  GET A$ : F  A$ <  >  "P" AND A$  <   >  "M"  GOTO 2270
2280  IF A$  =  "M " GOTO 1060
2290  PP = l
```

```
2300  PR# 1: PRINT : GOTO 2100
2310  REM  =========CLAMP=========
2320  HOME
2330  IF N = 0 GOTO 2410
2340  HTAB 4: VTAB 9
2350  PRINT "THIS COMMAND CLEARS ALL DATA ! "
2360  PRINT
2370  HTAB 3: VTAB 15
2380  PRINT "SURE YOU WISH TO DO THIS (Y/N) ?" ;
2390  GET A$ : IF A$ <  > "Y" AND A$ <  > "N" THEN GOTO 2390
2400  IF  A$  =  "N"  GOTO  1060
2410  HOME
2420  CLEAR : DIM VO(80),VL(80),VI(80),I(80)
2430  D = 30
2440  HTAB 12: VTAB l
2450  PRINT  "CURRENT CLAMP"
2460  HTAB 12: VTAB 2
2470  PRINT  " ----------"
2480  HTAB l: VTAB 4
2490  PRINT " SELECT : "
2500  HTAB 8: VTAB 7
2510  PRINT "l) LENGTH CONSTANT"
2520  HTAB 8: VTAB 9
2530  PRINT " 2) I/V RELATIONSHIP"
2540  HTAB l: VTAB 20
2550  PRINT  " WHICH ?";
2560  GET A$:A =  VAL (A$): IF A < l OR A > 2 GOTO 2560
2570  SLOT = 4 : D$ =  " "
2580  IF A = l GOTO 2940
2590  AG = 32:Q2 = 10:CC = l
2600  GOTO 410
2610  REM ======PLOT VO/I=====
2620  HOME
2630  REM ..VO=-8 TQ 120 MV
2640  REM ..I=-200 TO 200 N-AMP
2650  HGR :FV = 10:FH = 12
2660  HPLOT 120,0 TO 120,150
2670  HPLOT 0,120 TO 240,120
2680  FOR L - 150 TO 0 STEP - FV
2690  HPLOT 117,L TO 123,L
2700  NEXT L
2710  FOR L = 0 TO 250 STEP FH
2720  HPLOT L,117 TO L,123
2730  NEXT L
2740  FOR P = 3 TO N STEP 3
2750  VA = I(P)
2760  X = 120 + VA * 0.6
2770  VB = VO(P)
2780  Y = l20 - VB
```

```
2790  IF Y > 120 THEN Y = 120
2800  IF X < 3 THEN X = 3
2810  IF X > 250 THEN X = 250
2820  IF Y < 3 THEN Y = 3
2830  HPLOT X - 2,Y + 2 TO X + 2, Y - 2
2840  HPLOT X + 2,Y + 2 TO X - 2, Y - 2
2850  NEXT P
2860  HTAB l: VTAB 2l
2870  PRINT  F$ ; "    " ; TI$
2880  PRINT "X=20 N-AMP/DIV; Y=VO(10 MV/DIV)"
2890  PRINT "HARDCOPY OR MENU (H/M)  ?" ;
2900  GET A$ : IF A$ <  > "H"  AND A$ <   > "M" GOTO 2900
2910  IF A$  =  " M " THEN  NEXT : GOTO 1060
2920  GOTO 4830
2930  REM  ===SINGLE CLAMP=====
2940  HOME : HTAB l: VTAB l
2850  CLEAR :D = 30
2960  TL = PEEK (800) * 256 + PEEK (80l)
2970  DR = PEEK (803)
2980  RE = (256 * PEEK (804) + PEEK (805)) / 100
2990  PS = PEEK (806) * 256 +  PEEK (807)
3000  PRINT "'LENGTH CONSTANT, RT & RC . "
3010  HTAB l: VTAB 2
3020  PRINT " ----------------------------"
3030  HTAB l: VTAB 4
3040  PRINT "CURRENT INPUT ASSUMES 10 MEG RESISTOR."
3050  REM ..SO 100 NAMP/VOLT..
3060  HTAB l: VTAB 7
3070  PRINT " CLAMP CURRENT (NANO-AMP)  " ;
3080  INPUT JJ
3090  Q2 JJ / 2:I = JJ
3100  REM ..D/A TRIMPOT AT O.5
3110  AG = 128
3120  SC = l: REM  ..SINGLE CLAMP FLAG
3130  SLOT = 4 : D$  =  " "
3140  HOME : GOTO 430
3150  REM -----A/D MONITOR---------
3160  HOME
3170  HTAB 6: VTAB 5
3180  PRINT "VO";TAB(16);"VL";TAB(26);"VI";TAB(35);"I"
3190  HTAB 9: VTAB 23
3200  PRINT "HIT ANY KEY FOR MENU"
3210  FOR C = 0 TO 3
3220  X = PEEK (49312 + C)
3230  X = PEEK (49312 + C)
3240  IF C = 0 THEN VO = X
3250  IF C = l THEN VI = X
3260  IF C = 2 THEN VL = X
3270  IF C = 3 THEN I = X
```

```
3280  NEXT C
3290  VO =  -  INT ((VO - 240) * 5)  /  10
3300  VI =  -  INT ((VI - 56) * 2.5 )  /  10
3310  VL =  -  INT ((VL - 240) * 5)  /  10
3320  I =  INT ((I - 128) * 100 / 64 )
3330  I1 = 0.5
3340  HTA8 6: VTAB 7
3350  PRINT VO;" ";TAB(16);VL;" ";TAB(26);VI;TAB(35);I;" ";
3360  REM        ---INTERRUPT---
3370  XC =  PEEK ( - 16384)
3380  POKE  - 16368,0
3390  IF XC > 127 THEN  GOTO 1060
3400  GOTO 3210
3410  REM  =====LENGTH CONST====
3420  HOME : PR#0 : FL = 0
3430  HTAB 8
3440  PRINT "LENGTH CONSTANT, RT, &  RC "
3450  HTAB 8
3460  PRINT  " ------------------------------"
3470  VTAB 6
3480  PRINT  " SELECT : "
3480  HTAB 8
3500  PRINT "l) LENGTH CONST.,ETC"
3510  HTAB 8: VTAB 9
3520  PRINT "2) LOAD DISC FILE"
3530  HTAB 8: VTAB 11
3540  PRINT  "3 ) SAVE  TO  DISC"
3550  HTAB 8: VTAB 13
3560  PRINT "4 ) LIST"
3570  HTAB 8: VTAB 15
3580  PRINT " 5 )  MAIN  MENU"
3590  HTAB l: VTAB 20
3600  PRINT " WHICH ? "  ;
3610  GET A$: IF  VAL (A$) < 1 OR VAL (B$) > 5 GOTO 3610
3620  A =  VAL (A$)
3630  ON A GOTO 4960,4310,4090,4470,1060
3640  REM  ====LENGTH CONST,ETC====
3650  HOME
3660  VD = (VO(5) + VO(6)) / 2
3670  VP = (VO(l) + VO(2) + VO(3)) / 3
3680  VO = VD - VP
3690  VF = (VL(5) + VL(6)) / 2
3700  VN = (VL(l)+VL(2)+VL(3))/3
3710  VL = VF  -  VN
3720  IA = (VI(5) + VI(6)) / 2
3730  IB - (VI(l) + VI(2) + VI(3)) / 3
3740  ID =  - 1 * (IB - IA)
3750  IK = (I(5) + I(6)) / 2
3760  IL = (I(l) + I(2) + I(3))
```

```
3770  IM = IK - (IL / 3)
3780  REM  ===FOR LENGTH CONST.===
3790  IF VL = 0 GOTO 4470
3800  X = VO / VL
3810  IF X < = 0 GOTO 4470
3820  CO =  LOG (X + (X * X - 1) ^O.5)
3830  KL = INT (TL / CO)
3840  REM ..SY=SINH(Y),CY=COSH(Y)
3850  Y = TL / KL
3860  SY = EXP (Y) - EXP ( - Y)
3870  CY = EXP (Y) + EXP ( - Y)
3880  REM  ...TY=TANH(Y)
3890  TY = SY / CY
3900  RT = VO * KL * TY / I
3910  RT = RT / 10:RT = INT (RT *1000) / 1000
3920  RC = VO * TY / (I * KL)
3930  RC = RC * 10000:RC = INT (RC * 1000) l 1000
3940  RI = INT (VO * 1000 / I)
3950  REM ..#RES. BASOLAT MEMBR
3960  AX = TL - PS) / KL
3970  VV = (VO * (EXP (AX)+ EXP(-AX))) / EXP (Y)
3980  FR = INT (ID * 100 / VV)
3990  REM ----------
4000  REM  .CD=ELECTRICAL I.D
4010  REM ..FROM LENGTH AND RC
4020  SR = RE * lE - 6: REM  ..MEG/CM
4030  CD = (4 * SR) / (3.1416 * RC))
4040  D2 = SQR (CD):D3 = INT (D2 * 10000)
4050  IS = 10000 *VP / (RT * 3.1416 * D3)
4060  HOME : GOTO 4490
4070  :
4080  REM  ===SAVE TO DISC===
4090  HOME
4100  INPUT "FILE NAME ?"" ;F$
4110  GOSUB 1390: REM GET TIME
4120  GOSUB 1710: REM GET DATE
4130  IF A$  = "P" THEN  FL = l :PR#l:GOTO 4470
4140  D$ =  " "
4150  PRINT D$; "0PEN " ;F$
4160  PRINT D$ ; " DELETE " ; F$
4170  PRINT D$; "OPEN " ; F$
4180  PRINT D$; "WRITE " ;F$
4190  PRINT F$
4200  PRINT TI$
4210  PRINT TL: PRINT DR: PRINT VI
4220  PRINT VO:PRINT VL:PRINT KL
4230  PRINT RT:PRINT RC:PRINT CR
4240  PRINT D3:PRINT SC:PRINT RI
4250  PRINT D$ ; "CLOSE " ; F$
```

```
4260  PRINT :. PRINT
4270  PRINT "FILE  ** " ;F$; "  ** NOW ON DISC"
4280  FOR T = 1 TO 2000: NEXT
4290  GOTO 3420: REM ..TO MENU
4300  REM  =====LOAD DISC FILE===
4310  HOME
4320  INPUT "FILE NAME ?" ;F$
4330  PRINT D$ ; " NOMON  C ,I ,O "
4340  PRINT D$ ; "OPEN " ; F$
4350  PRINT D$ ; "READ " ; F$
4360  INPUT F$: INPUT TI$
4370  INPUT TL: INPUT DR: INPUT VI
4380  INPUT VO: INPUT VL: INPUT KL
4390  INPUT RT: INPUT RC: INPUT RI
4400  INPUT CR: INPUT D3: INPUT SC
4410  PRINT
4420  PRINT D$ ; "CLOSE " ; F$
4430  HTAB  1 : VTAB 22
4440  PRINT " FILE  **  " ; F$ ; " **  LOADED "'
4450  GOTO 3420: REM  ..MENU 2
4460  REM =====LIST=====
4470  HOME
4480  PRINT "FILE NAME :  " ; F$
4480  GOSUB 1710
4500  PRINT "DATE : " ; G$
4510  PRINT "TIME : " ;T2$
4520  PRINT
4530  PRINT "PUNCTURE SITE (MICRONS) : " ; PS
4540  PRINT "TUBULE LENGTH : " ; TL ; " MICRONS. "
4550  PRINT "TUBULE EXT.DIA. (MICRONS) : " ; DR
4560  PRINT "INTRACELL.PD  = ";INT(IB * 100 ) / 100 ; " MV"
4570  PRINT  "CURRENT CLAMP (N-AMPS ) = " ; IHT  ( IM )
4580  PRINT
4590  PRINT "VO =  "; INT (VP * 10) / 10 ; " MV"
4600  PRINT "VL  =  " ; INT  (VN  *  10) / 10 ; " MV"
4610  PRINT "PROX.VOLTAGE JUMP (MV) = ";INT(VO * 10) / 10
4620  PRINT "DISTAL ' '    ' '= "; INT (VL * 10) / 10
4630  PRINT "INTRACELL.PD JUMP ="INT(ID*10)/10;"MV"
4640  PRINT
4650  PRINT  "LENGTH  CONSTANT = "' ;KL ;" MICRONS"
4660  PRINT "TRANSTUBULAR  RESISTANCE = ";RT;"KOHM . CM "
4670  PRINT  "CORE  RESISTANCE  = " ;RC ; "  MEGOHM/CM "
4680  PRINT  " INPUT  RESISTANCE =  "; RI ; " KILOHMS "
4690  PRINT "F.RES.BASOL.MEMBR (%)=" ; INT (FR * 10)/ 10
4700  IF RT = 0 GOTO 4730
4710  PRINT:PRINT "SCC = ";INT((10000*VP)/(RT*3.1416*D3));
          "UAMP/ SQ.CM"
4720  PRINT "VIRTUAL SCC = ";INT(VF*10/RT)/10;" UAMP/CM "
4730  GOTO 4750
```

```
4740  PRINT "CALCULATED CORE RES ST. = " ; CR ;"MEGOHM/CM"
4750  PRINT "CALC. INT.DIA. = " ;D3 ; " MICRONS"
4760  PRINT "-----------------------------------------"
4770  IF FL = 1 THEN FL = 0: PR#0:GOTO 1060
4780  PRINT "PRINTOUT OR MENU (P/M) ?";
4790  GET A$:IF A$ < > "P" AND A$  < > "M" GOTO 4780
4800  IF A$ = "M " GOTO 3420
4810  FL = l: PR# 1: GOTO 4480
4820  REM  ========PLOT-PRINT=====
4830  PR#l
4840  PRINT CHR$ (27); "3" ; CHR$(22)
4850  PRINT CHR$ (9)  "H"
4860  PRINT CHR$ (9) ;"GM"
4870  PRINT CHR$ (9) ; "X"
4880  PR#0
4890  NEXT
4900  GOTO 1060
4910  REM  ================================
4920  ON HP GOTO 4930: RETURN
4930  IF PEEK (103) <  > 1 OR PEEK (104)<  > 64 THEN POKE
        103,l:POKE 104,64:POKE 16384,0:PRINT CHR$ (4)"RUN"PN$
4940  RETURN
4950  REM  ...TUBULE PARAMETERS..
4960  HOME
4970  DR = PEEK (803)
4980  LH = PEEK (800) * 256:LL = PEEK (801)
4990  TL = LH + LL
5000  RH = PEER (804) * 256:RL = PEEK (805)
5010  RE = (RH + RL) / 100
5020  PA = PEEK (806) * 256:PB = PEEK (807)
5030  PS = PA  +  PB
5040  PRINT "PERFUSATE SP.RES.(OHM.CM):";RE
5050  PRINT "TUBULE LENGTH (MICRONS)  :";TL
5060  PRINT "TUBULE EXT.DIA.(MICRONS) : ";DR
5070  PRINT "INTRACELL.SITE (MICRONS) : ";PS
5080  PRINT : PRINT "DO YOU WANT TO  CHANGE "
5090  PRINT "ANY OF THE ABOVE VALUES (Y/N)? " ;
5100  GET V$ : IF V$< > "Y"  AND V$  <   >  "N"  G0T0 5100
5110  PRINT V$
5120  IF V$ = "Y"GOTO 5140
5130  HOME : GOTO 1060
5140  HOME : PRINT "TUBULE LENGTH AND INNER DIA IN MICRONS"
5150  PRINT "PERFUSATE SP . RES IN OHM. CMS . "
5160  PRINT : PRINT "ENTER NEW VALUES, OR HIT RETURN"
5170  PRINT "TO ACCEPT OLD VALUES"
5180  PRINT : PRINT
5190  PRINT "TUBULE LENGTH (" ; TL ;"):";
5200  INPUT TL$
5210  IF TL$ = " " GOTO  5270
```

```
5220  TL = VAL(TL$)
5230  LH =INT (TL / 256)
5240  POKE 800,LH
5250  LL = TL - LH * Z56
5260  POKE 801,LL
5270  PRINT  "TUBULE EXT.DIA.(";DR;"):";
5280  INPUT DR$
5290  IF DR$ = " " GOTO 5320
5300  DR = YAL (DR$)
5310  POKE 803,DR
5320  PRINT "PERFUSATE SP.RES.( "; RE ; "): " ;
5330  INPUT RE$
5340  IF RE$ = " "  GOTO  5390
5350  RE = VAL (RE$)
5360  RH = INT (RE * 100 / 256)
5370  RL = (RE * 100) - RH * 256
5380  POKE 804,RH: POKE 805,RL
5390  PRINT " INTRACELL . SITE ( " ; PS ;"):";
5400  INPUT PS$
5410  IF PS$ =  " " GOTO  5460
5420  PS = VAL (PS$)
5430  PA = INT (PS / 256)
5440  PB = PS - PA * 256
5450  POKE 806,PA:POKE 807,PB
5460  HOME : GOTO 1060
```


PROGRAM COMMENTS:

The following sections from the program were selected to comment on:

1. line 480:

This program line imposed a delay in reading the voltage changes initiated by the current clamp. This enabled the voltages (Vo and Vbl) to be recorded after the current clamp reached steady state. If the voltages were recorded too soon after the initiation of the current clamp, artifactual voltages would be recorded due to

capacitance currents. (see Methods and Materials (section 3.3 - explanation of current clamp).

2. lines 810-870:

Although the voltage jumps resulting from passing current via the perfusion glass pipette can be nullified using the Wheatstone bridge there remains a voltage jump across the agar (3mM KCl) bridge joining the bath to the earth electrode. in order to subtract this artifactual fraction from the recorded VL, the voltage jump across the collecting pipette and the bath was measured immediately after the bridge had been balanced (i.e. before mounting the tubule between the sets of holding pipettes). In line 820 the variable "BV" (bath voltage) represents the measured artifactual voltage jump which is subsequently subtracted from recorded voltage jumps at both the proximal and distal ends of the tubule; the actual value of BV (0.85 mV here) varied slightly from one agar (3mM KCl) bridge to another.

PROGRAM MENUS

Below are a number of menus that are driven by the program described above. Short notes are added to aid the reader in understanding the functioning of the program.

MAIN MENU
TUBULE CURRENT CLAMP

SELECT:

1) SAVE I/V FILE
2) LOAD I/V FILE
3) LIST I/V DATA
4) CURRENT CLAMP
5) I/V PLOT
6) A/D MONITOR
7) LENGTH CONSTANT
8) EXIT
9) INPUT PARAMETERS

WHICH ?

The above menu is the opening menu and is referred to throughout as the "main menu". Options 1, 2, 3 and 5 are straightforward. Option 1 would save a sequence of injected current (I) and response voltages (V) to a file. Option 2 would enable the program operator to load any given set of I/V values that had previously been saved. Option 3 allows the operator to view the I/V data of any one set; the I/V data can be retrieved from a saved file or from memory if a subsequent current clamp had not been performed. Option 4 is selected when the user wishes to current clamp the tubule. Option 6 is used to monitor the current values of Vo, VL, VI and Io (see below for further discussion). Option 7 takes the user directly to the length constant menu (see below). Option 8 is used to exit the program. Option 9 is used immediately after the mounting of the tubule. Various parameters necessary for the calculation of certain equations eg. perfusion resistivity, tubule length, etc., are put into memory. This option is discussed further below.

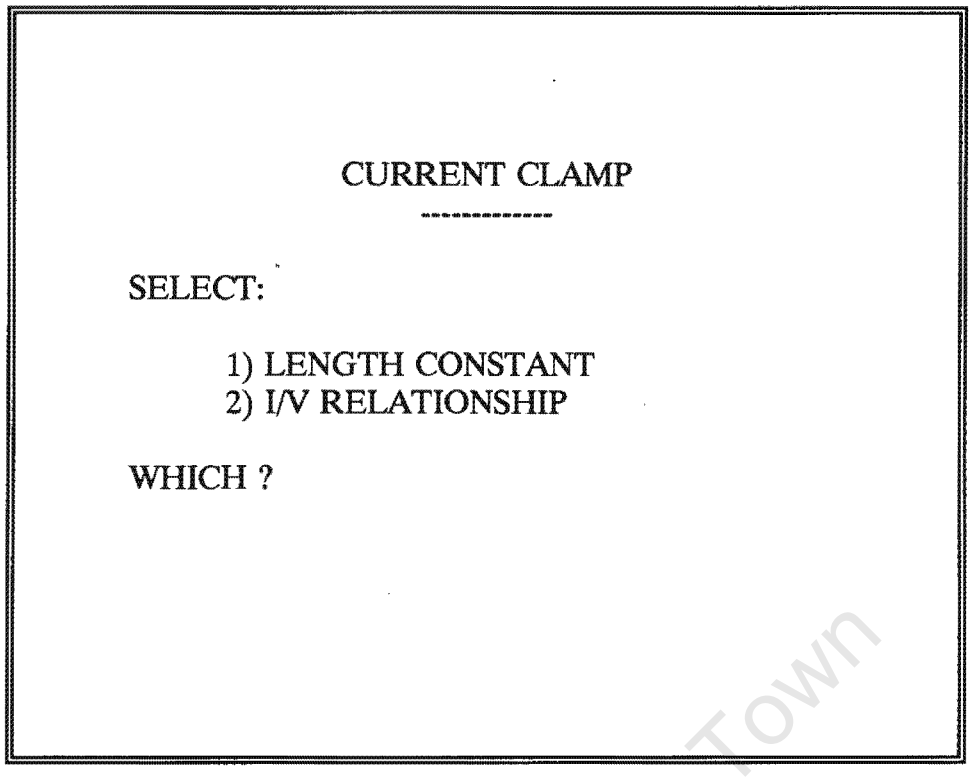

Selection of option 4 ("CURRENT CLAMP") on the main menu would result in the above menu coming up. This menu allows for a choice between performing a single current clamp (option 1), with a view to computing the length constant for the mounted perfused tubule, and performing a series of current clamps with a view to plot a current / voltage relationship (I/V relationship; option 2). If option 1 is selected then the dedicated "length constant menu" below would come up. For more details see program lines 3440 to 3620.

LENGTH CONSTANT, RT & RC

SELECT:

1) LENGTH CONST, ETC.
2) LOAD DISC FILE
3) SAVE TO DISC
4) LIST
5) MAIN MENU

WHICH ?

The above menu comes up on screen when option 1 of the "CURRENT CLAMP" menu is selected. It has 5 options. Option 1 results in a specified current (calibrated in nanoAmps; the program assumes that a 10 Megohm resistor is present so that for every volt a 100 nanoAmps is passed (see appendix B) into the lumen of the mounted perfused tubule and the resulting change in potential across the tubule is captured by the program as a number of variables (see chapter 2). These variables are used to compute the length constant, the transtubular resistance, the core resistance, the short circuit current, the diameter of the lumen and the fractional resistance of the basolateral membrane as a percentage. This procedure is repeated 3 times and the resulting changes are averaged before use in the relevant equations. See program lines 2930 to 3400 and 3640 to 4060.

Option 2 loads from disc a file containing the above mentioned data as well as the date and time at which the data were saved. See program lines 4300 to 4440.

Option 3 saves all the above mentioned variables in file with a specified name. See program lines 4080 to 4290.

Option 4 lists all the above mentioned data in a set format (see figure 1 below) with the option to print the data (hardcopy) or return to the dedicated "LENGTH CONSTANT" menu above. See program lines 4460 to 4760. Option 5 returns the user to the main menu.

Figure 1

FILE NAME: LEN1
DATE: 02 NOV 1990
TIME: 15:05 HRS

PUNCTURE SITE (MICRONS): 150
TUBULE LENGTH: 509 **MICRONS**
TUBULE DIAMETER (MICRONS): 40
INTRACELL. PD. = -25.04 MV
CURRENT CLAMP (N-AMPS) = 198
VO = 15.5
VL = 11.5
PROX. VOLTAGE JUMP : 77.8
DIST. VOLTAGE JUMP : 29.6
INTRACELL. PD JUMP : 2.9

LENGTH CONSTANT = 399 MICRONS
TRANSTUBULAR RESISTANCE = 6.78 KILOHMS
CORE RESISTANCE = 12.761 MEGOHM/CM
INPUT RESISTANCE = 412 KILOHMS
#RES BASOL.MEMBR. (%) = 5

SCC = 1497.92 UAMPS/SQ.CM
VIRTUAL SCC = 15 UAMP/CM
INT. DIA. = 37 MICRONS

PRINTOUT OR MENU (P/M) ?

Upon selection of option 4 of the "LENGTH CONSTANT" menu the above screen appears. At the bottom of the screen a choice of either printing the list, or returning to

the "LENGTH CONSTANT" menu.

In figure 1 the 'puncture site (microns)' is the distance from the proximal end of the tubule to the microelectrode's impalement site. The 'tubule diameter (microns):' denotes the internal tubule diameter i.e. luminal diameter as measured by an ocular micrometer. Vo, Vl, Prox.Voltage Jump, Dist.Voltage Jump and Intracell.Pd Jump are expressed in millivolts. 'VO' represents the transepithelial voltage at the proximal end of tubule. 'VL' represents the transepithelial voltage at the distal end of tubule. 'Prox.voltage jump' represents the voltage jump at the proximal end of the tubule in response to current injection. 'Dist.voltage jump' represents the voltage jump at the distal end of the tubule in response to current injection. 'Intracell. PD jump' represents the voltage jump across the basolateral membrane (measured via the intracellular electrode) in response to current injection.

Using the above values the program computes the cable parameters: length constant, transtubular resistance, core resistance, input resistance, #res basol.membr.(%) (i.e. FRBL%), the SCC, the virtual SCC and the int.dia (the electrically calculated diameter i.e. by cable mathematics).

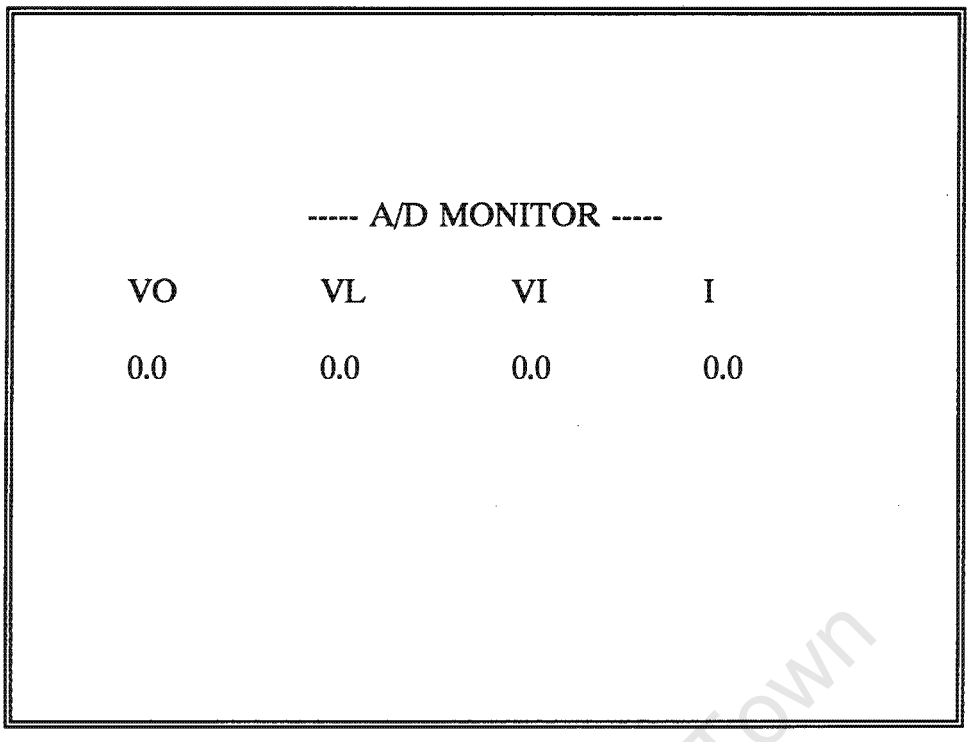

The above screen comes up after selecting main menu's option 6. The screen shows the current values of the proximal transtubular potential (VO), the distal transtubular potential (VL) and the intracellular potential (basolateral membrane potential)(VI) in millivolts, and shows the current (I) in nanoAmps. The A/D monitor was especially useful in setting the offsets (to zero) and amplifier gains before each experiment. Option 6 of the main menu could be selected at any time during the course of the experiment to monitor the above variables. For more details see program lines 3150 to 3400.

TUBULE PARAMETERS

PERFUSATE SP.RES. (OHM.CM): 70
TUBULE LENGTH (MICRONS): 250
TUBULE EXT. DIAMETER (MICRONS): 200
INTRACELLULAR SITE (MICRONS): 80

DO YOU WANT TO CHANGE ANY
OF THE ABOVE VALUES (Y/N) ?

The above menu comes up after selecting option 9 in the main menu. It allows for the viewing of the variables stored in memory with the option of changing any one or more of these. The above variables are used throughout the program with a view to computing the cable equations. For details see program lines 4950 to 5460.

APPENDIX B

The Mountain Card:

The Mountain card specifications are the following: (1) it is specific for the Apple computer; (2) it has 8 bit resolution and has 16 channels (A/D / D/A) available with a conversion time of 9 μsec. This, conveniently, allows for current injection and the resulting changes in voltages to be captured simultaneously. (3) The A/D's input voltage ranges from -5 to +5 volts in 256 steps (8 bit = 2^8 = 256). As the voltages from the Malpighian tubular experimental set-up ranged from -50 mV to +200 mV a preamplifier had to be designed to enable the full resolution of the A/D card's range to be realized, i.e. the voltage range from the tubule preparation (-50 mV to 200 mV) had to be amplified as closely as possible to the -5 to +5 volt range of the A/D card.

Circuit Designs:

A/D PRE-AMP: (see figure B.1.)

An A/D pre-amplifier of the design described below was built for Vo, Vl, Vbl and I (current injection). The above circuits were all housed in a circuit box. The different circuits were all set to their appropriate offsets and gains.

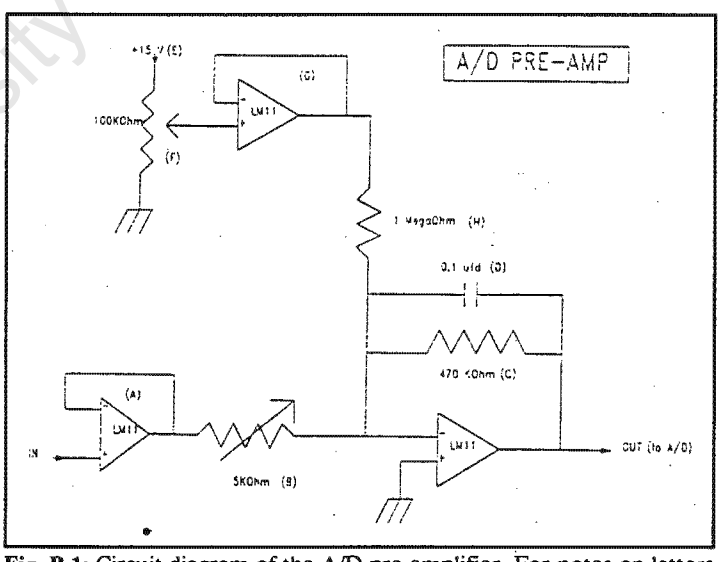

Fig. B.1: Circuit diagram of the A/D pre-amplifier. For notes on letters within brackets, see text.

The input of the preamplifier required a high input resistance; this was achieved by configuring the op-amp (LM11) in a voltage follower format (see 'A'). The op-amps (LM11) operated on a ±15 volt power supply. Measured potentials from the Malpighian

tubules ranged from -50 mV to +200 mV and therefore had to be amplified to obtain the full resolution of the Mountain card. The configuration of the variable resistor (5K) at 'B' and the 470K resistor at 'C' allowed for the amplification to be adjusted. Therefore the signal passed via the voltage follower (A) would be amplified by the following resistor ratio: C/B. This allowed an amplification range from ± x1 to x100 of the signal entering via the voltage follower at 'A'. Most of the 'electrical lead noise' was eliminated by the capacitor at 'D' which acted as a 'low pass' filter.

To utilize the full range of the A/D card a voltage offset was incorporated into the circuit design. The voltage offset circuit consisted of components 'E' to 'G'. A +15 volt source (E) via 100 K variable resistor to earth was used as a variable voltage source. This was connected to a 'voltage follower'(G) and a 1 MegaOhm resistor (H) in series.

D/A output: The D/A output was connected to earth via a variable 100KΩ resistor. The variable resistor was adjusted to give 1 volt out whenever a "100 nAmps" command was given to the Apple Computer. See figure B.2 and B.3. For a further explanation see following section.

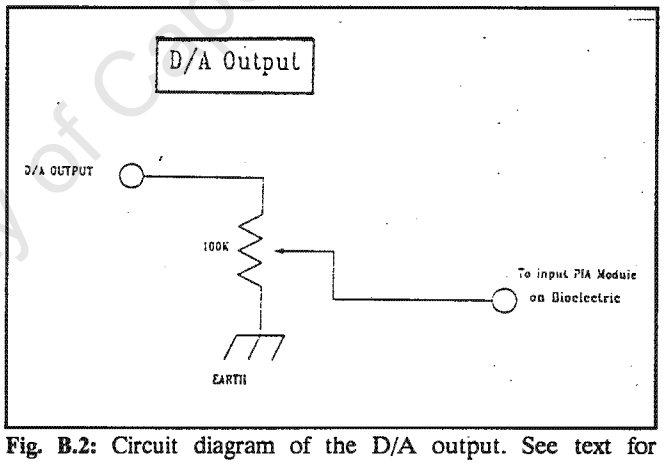

Fig. B.2: Circuit diagram of the D/A output. See text for explanation.

Head-stage pre-amplifier for the Bio-electric

The head-stage provided the biological set-up with a high input impedance so that the recording apparatus did not interfere with biological events. The circuitry was designed to provide for a current injection input as well as a 10 mV calibration switch. For further details refer to figure B.3.

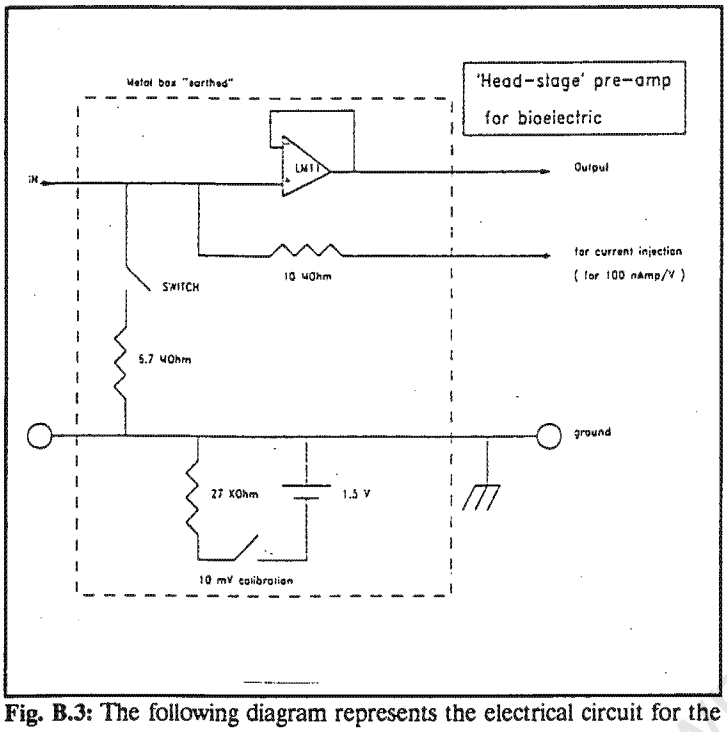

Fig. B.3: The following diagram represents the electrical circuit for the 'head-stage' pre-amplifier of the bio-electric. See text.

Current injection: One volt from the D/A output via the 10 MegaOhm resistor gives (1V / $10x10^6$ Ω = 1 x 10^{-7} Amps) 100 nanoAmps.

A switch was fitted in series to a 6.7 MΩ resistor as part of the circuit designed to test the circuitry of the head-stage before a tubule was perfused. Therefore, whenever the switch was closed the perfusion apparatus was electrically cut off. The 6.7 MΩ resistor was used in place of the resistance of the perfusion apparatus; therefore, when the switch is closed current would pass via the 6.7 MΩ resistor and this would provide the user with an indication that the circuit was operating properly (i.e. passage of a 100 nAmp current would give an output of 67 mV). A 6.7 MΩ resistor was utilized because the resistance of the perfusion apparatus to the flow of current (i.e. during current injection) was similar (±5-10 MΩ). When this resistor was switched into the circuit (i.e. while the perfusion set-up is not plugged into the circuit) it allowed for the approximate setting of the bridge. Whenever the perfusion apparatus is plugged into the head-stage the switch is off and the resistance of the perfusion apparatus is connected to the circuit.

PIA-Bridge circuit:

The following circuit diagram is a facsimile of the bridge circuit diagram illustrated by the manufacturer's manual. The one-turn trimpot which balanced the bridge was replaced with a twenty-turn trimpot. This permitted precise and reproducible balancing of the bridge. For a detailed description of the circuit see figure B.4.

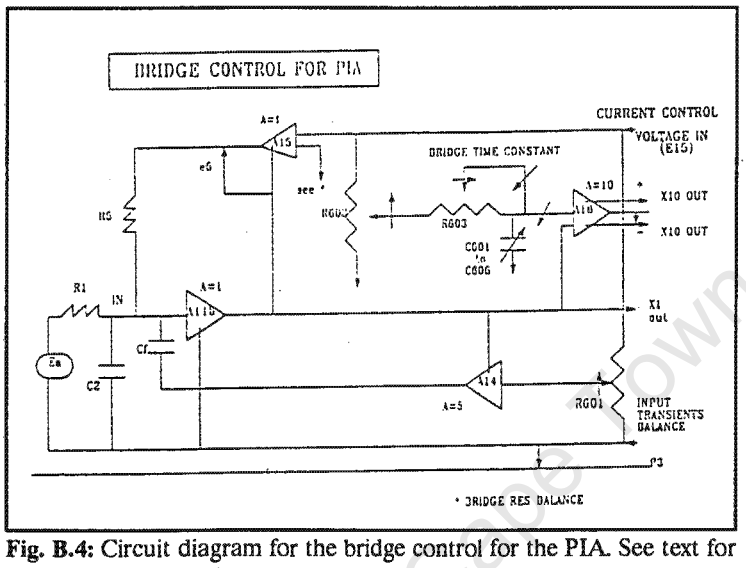

Fig. B.4: Circuit diagram for the bridge control for the PIA. See text for explanation on modification.

APPENDIX C

Cable formulae:

$$\lambda(lengthconstant) = \frac{length}{LN(\frac{dVo}{dVL}) + \sqrt{\frac{(dVo * dVo)}{(dVL * dVL)} - 1}} \quad (1)$$

$$JL = \frac{length}{\lambda} \quad (2)$$

$$R_{trans} = \frac{dVo * \lambda * [EXP(JL) - EXP(-JL)] * 0.1}{[EXP(JL) + EXP(-JL)] * current} \quad (3)$$

$$R_{core} = \frac{dVo * [EXP(JL) - EXP(-JL)] * 10000}{[EXP(JL) + EXP(-JL)] * \lambda * current} \quad (4)$$

$$Diameter_{calc} = \sqrt{\frac{4 * Sp.Res * 100}{\pi * R_{core}}} \quad (5)$$

$$R_{input} = \frac{1000 * dVo}{current} \quad (6)$$

$$SCC(\mu Amps/cm^2) = \frac{Vo * 10000}{R_{trans} * \pi * Diameter_{calc}} \quad (7)$$

$$SCC_{virtal}(\mu Amps/cm) = \frac{Vo}{R_{trans}} \quad (8)$$

$$(jV_t)_x = \frac{jVo * \cosh(\frac{x}{\lambda} - \frac{length}{\lambda})}{\cosh(\frac{length}{\lambda})} \quad (9)$$

$$FRBL\% = \frac{(jVbl)}{(jVt)_x} * 100 \quad (10)$$

$$FRa\% = 100 - FRBL\% \quad (11)$$

Formulae Notes

1. "length" refers to the length of mounted tubule from the Sylgard at the perfusing pipet to the Sylgard of the collecting pipet as measured with an ocular microscope.

2. "dVo" refers to the change in voltage at the proximal end of the tubule in response to current injection.

3. "dVL" refers to the change in voltage at the distal end of the tubule in response to current injection.

4. Equation 2 was used to simplify the equations that followed.

5. "current" refers to amount of current injected into the proximal end of the tubule.

6. In equation 3 R_{trans} was standardised to KOhm.cm by multiplying with a factor of 0.1.

7. In equation 4 R_{core} was standardised to MOhm/cm by multiplying with a factor of 10000.

8. In equation 5 $Diameter_{calc}$ was standardised to microns by multiplying with a factor of 100.

9. In equation 6 R_{input} was standardised to KOhms by multiplying with a factor of 1000.

10. In equation 7 SCC was standardised to uAmps/cm^2 by multiplying with a factor of 10000.

11. Equation 9 was used to calculate the transtubular voltage jump in response to current injection at the point of microelectrode impalement. "x" is the distance from Sylgard in the perfusing pipet to the point of impalement.

APPENDIX D

A typical experimental data sheet:

No	Proc	Time	Vo	I-clmp	jVo	jVl	Lambda	RT	Rcore	DIAc	SCC	SCCv	Riap	Micro	Vtx	jVbl	FRBL
		mins	mV	n-Amps	mV	mV	micron	KOHM.cm	MOHM/cm	micron	uA/cm2	uA/cm	KOHMS	u	mV	mV	%
1	CNTRL	34	22.0	197	40.3	15.1	333.39	6.32	5.69	37.16	298.02	3.48	204.57	108	31.25	5.8	18.56
2	"	34	22.0	197	40.5	14.6	325.15	6.24	5.90	36.50	307.73	3.53	205.58	108	31.02	6.5	20.96
3	"	34	23.3	197	43.8	11.5	271.27	5.82	7.91	31.52	404.34	4.00	222.34	108	30.58	6.3	20.60
4	DH	38	19.0	197	34.5	15.3	375.77	5.90	4.18	43.37	236.44	3.22	175.13	108	28.40	5.6	19.72
5	"	39	18.0	197	35.6	13.5	336.05	5.62	4.98	39.73	256.61	3.20	180.71	108	27.72	5.2	18.76
6	"	39	17.0	197	34.3	14.1	355.26	5.64	4.47	41.93	228.86	3.01	174.11	108	27.46	6.0	21.85
7	DH-CNTRL	45	19.0	197	28.0	11.1	346.32	4.52	3.77	45.66	293.09	4.20	142.13	108	22.13	5.5	24.85
8	"	45	18.8	197	26.6	10.8	352.15	4.35	3.50	47.35	290.85	4.33	135.03	108	21.20	4.1	19.34
9	"	45	19.1	197	26.5	10.3	341.67	4.23	3.63	46.54	308.51	4.51	134.52	108	20.81	5.6	26.92
10	"	47	22.5	197	25.0	8.0	302.34	3.64	3.98	44.45	443.30	6.19	126.90	108	18.46	4.1	22.22
11	"	47	24.0	197	27.8	11.0	345.87	4.48	3.75	45.79	372.21	5.35	141.12	108	21.96	5.5	25.05
12	"	48	25.3	197	26.8	10.6	345.77	4.32	3.61	46.63	399.78	5.86	136.04	108	21.17	5.6	26.46
13	WO-BATH	57	26.6	197	24.3	14.6	497.77	4.91	1.98	62.97	273.93	5.42	123.35	108	22.93	1.3	5.67
14	"	57	27.0	197	26.3	14.8	463.73	5.12	2.38	57.45	292.29	5.28	133.50	108	23.99	2.8	11.67
15	"	57	26.5	197	28.9	14.1	405.90	5.20	3.15	49.90	325.21	5.10	146.70	108	24.71	2.1	8.50
16	"	57	25.8	197	29.1	12.1	358.19	4.81	3.75	45.77	372.91	5.36	147.72	108	23.39	2.5	10.69
21	"	68	20.0	197	34.3	19.5	468.66	6.71	3.06	50.70	187.06	2.98	174.11	108	31.44	1.1	3.50
22	"	68	19.0	197	36.0	19.6	448.61	6.88	3.42	47.95	183.43	2.76	182.74	108	32.31	3.0	9.28
23	"	68	19.9	197	36.4	20.0	452.67	6.99	3.41	47.99	188.86	2.85	184.77	108	32.81	2.4	7.31
24	CL-FREE	86	22.5	197	54.5	28.5	431.70	10.18	5.46	37.92	185.52	2.21	276.65	108	48.02	4.1	8.54
25	"	86	23.8	197	49.8	26.0	431.05	9.29	5.00	39.63	205.69	2.56	252.79	108	43.84	2.3	5.25
26	"	86	22.0	197	52.8	28.1	438.87	9.96	5.17	38.98	180.40	2.21	268.02	108	46.89	2.1	4.48
27	WO-BATH	103	13.0	197	46.6	27.1	480.07	9.24	4.01	44.27	101.18	1.41	236.55	108	43.21	2.3	5.32
28	"	104	14.0	197	64.0	37.0	477.03	12.65	5.56	37.60	93.73	1.11	324.87	108	59.17	3.2	5.41
29	"	104	14.0	197	61.5	35.0	469.17	12.04	5.47	37.89	97.65	1.16	312.18	108	56.41	1.8	3.19
30	HiK	108	24.1	197	50.0	30.6	508.51	10.21	3.95	44.61	168.47	2.36	253.81	108	47.65	1.3	2.73
31	"	108	22.1	197	47.6	30.0	526.92	9.88	3.56	46.97	151.50	2.24	241.62	108	46.13	0.5	1.08
32	"	108	22.5	197	49.3	29.5	495.47	9.93	4.05	44.06	163.63	2.26	250.25	108	46.41	2.4	5.17
33	WO-BATH	111	16.0	197	54.5	31.6	478.53	10.79	4.71	40.84	115.62	1.48	276.65	108	50.46	1.0	1.98
34	"	111	17.0	197	60.1	33.8	463.44	11.69	5.44	37.99	121.84	1.45	305.08	108	54.80	2.4	4.38
35	"	111	14.5	197	48.1	28.5	490.02	9.64	4.01	44.24	108.25	1.50	244.16	108	45.04	2.1	4.66

APPENDIX E

Compositions of perfusate, control and other Ringer solutions

Composition	Control	High K Ringers	Chloride-free Ringers
NaCl	110	20	_
KCl	25	120	-
$MgCl_2$	5	5	-
$MgSO_2$	-	-	5
$CaCl_2$	2	2	-
$CaSO_2$	-	-	2
$KHCO_3$	7	7	7
KH_2PO_4	3	3	3
glycine	10	10	10
proline	10	10	10
serine	10	10	10
histidine	10	10	10
glutamine	10	10	10
glucose	50	50	50
Na isethionate	_	_	125
K gluconate	-	-	15
Total:K^+	25	130	25
Total:Na^+	125	20	125
Total:Cl^-	149	149	-

Table E1: High K Ringers (HiK) was used as a perfusate throughout the study. HiK 130 mM was also used as a bathing medium. The pH was approximately 7. (concentrations in mM/l)

Standard Ringer Solutions for dissecting and bathing Ringers				
Salt	mM	MW	Stock	ml/litre
NaCl	125	58.44	1M	125
KCl	15	74.56	1M	10
$MgCl_2$	5	203.31	1M	5
$CaCl_2$	2	147.02	1M	2
$KHCO_3$	7	100.13	1M	10
KH_2PO_4	3	136.09	1M	5
glucose	100	180.2	1M	100

Table E2: Dissecting Ringers: Distill water was added to the final mixture (i.e. the column most right) to make up 1 liter of disecting Ringers. The pH was approximately 7.

Bathing Ringers: Glucose and amino acid composition				
Substance	mM	MW	g/l	g/500m/s
glucose	50	180.2	9.01	4.505
glycine	10	75.07	0.75	0.375
proline	10	115.13	1.15	0.575
serine	10	105.1	1.05	0.525
histidine	10	155.16	1.55	0.775
glutamine	10	146.15	1.46	0.730

Table E3: Bathing Ringers was made up as in Table E2, but instead of 100 mM glucose, only 50 mM was used. The pH was approximately 7.